Development of Barrel Hadronic Calorimeter for proposed ATHENA experiment

Leszek Kosarzewski

Faculty of Nuclear Sciences and Physical Engineering
Czech Technical University in Prague

WJCF Workshop 11-18.6.2022, Bily Potok

EUROPEAN UNION
European Structural and Investment Funds
Operational Programme Research,
Development and Education

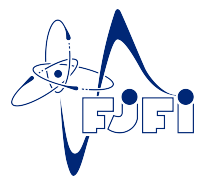

The work was also supported from European Regional Development Fund-Project through International Mobility of Researchers project of the Ministry of Education, Youth and Sports of the Czech Republic, Project No. CZ.02.2.69/0.0/0.0/18_053/0016980

Outline

The Electron-Ion Collider

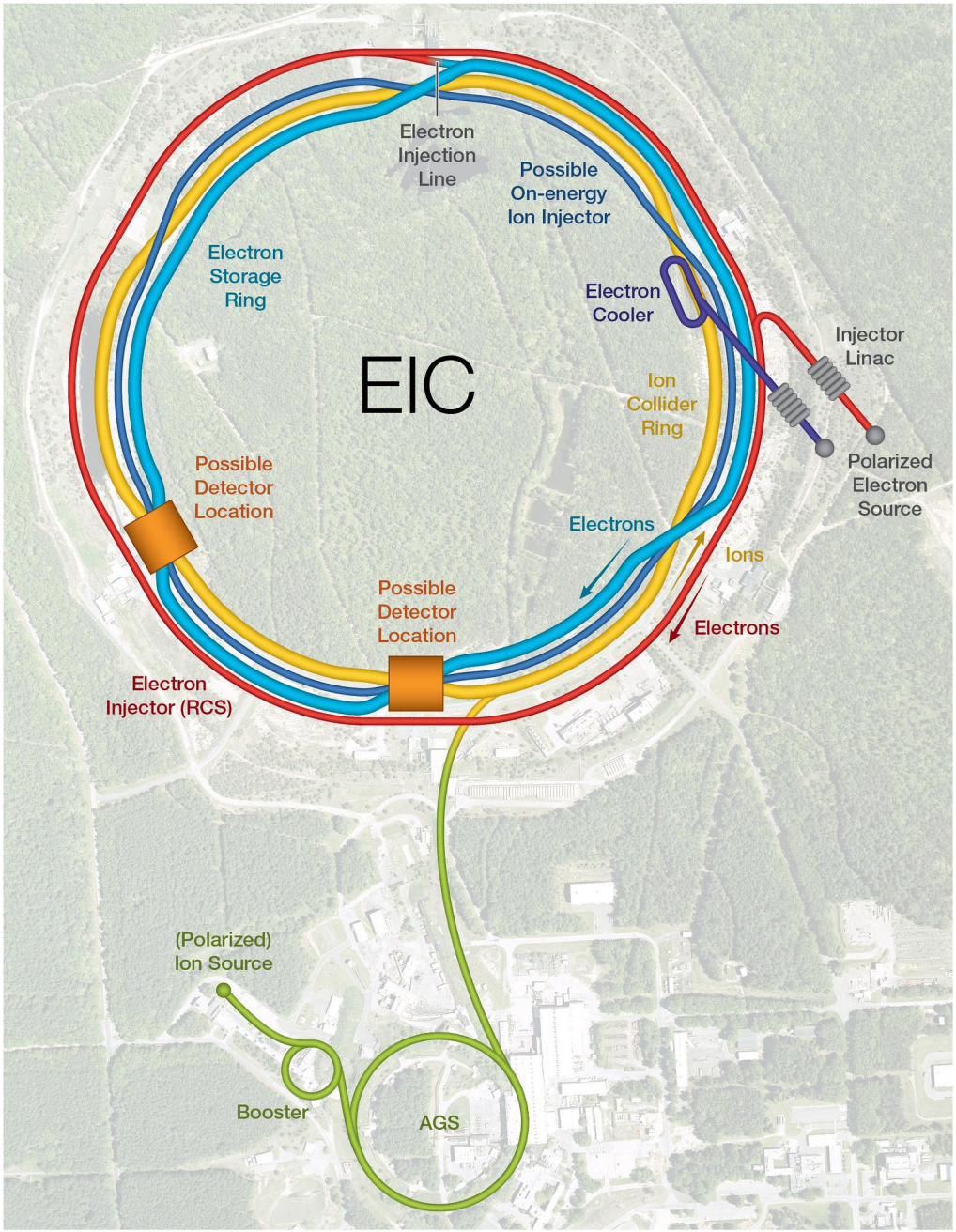

The Electron-Ion Collider (EIC):

- The only electron-ion collider in the world
- To be built at Brookhaven National Laboratory, Upton, NY, USA
- Will make use of existing Relativistic Heavy Ion Collider and add an electron storage ring
- Construction to start in 2024 after RHIC run
- e+p, e+A collisions at $\sqrt{s} = 20 - 140\ \mathrm{GeV}$
- High luminosity: $L = 10^{33} - 10^{34}\ \mathrm{cm}^{-2}\mathrm{s}^{-1}$, 10–100 $\mathrm{fb}^{-1}/\mathrm{year}$

[EIC Yellow Report]

Electron-Ion Collider

Exploring the strongest force in nature

Advanced acceleration and beam-cooling techniques will transform the Relativistic Heavy Ion Collider (RHIC) at Brookhaven National Laboratory into an Electron-Ion Collider (EIC). The EIC will enable a deeper exploration of the mysteries of matter, particularly the role gluons play in generating the essential properties of protons and visible matter.

U.S. DEPARTMENT OF ENERGY | Office of Science

BROOKHAVEN NATIONAL LABORATORY

Inside an EIC collision

By colliding electrons with protons and nuclei, the EIC will produce snapshots of those particles' internal structure — like a CT scanner for atoms. The electron beam will reveal the arrangement of the quarks and gluons that make up the protons and neutrons of nuclei and solve the mystery of proton spin.

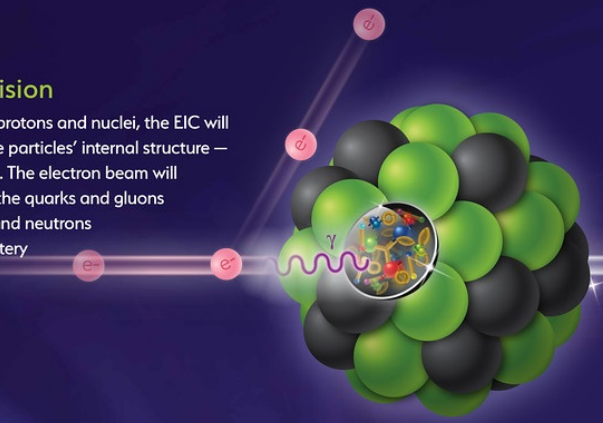

Precision 3-D imaging and search for saturation

The EIC will be the world's first spin-polarized electron-nucleus collider with the flexibility to change the nuclear ion species as well as the beam energies — both crucial for the systematic study of the "glue" postulated to dominate the internal structure of nuclear matter.

Benefits beyond physics

Building the EIC will maintain U.S. leadership in nuclear physics and expand opportunities for scientific discovery and technological advances that could have broad impacts on society. Examples from past or ongoing nuclear physics endeavors include:

- Advanced accelerators for cancer therapy
- Production of radioisotopes for diagnosing, tracking, and treating disease
- New detector technologies for medicine and national security
- Computational tools for managing "big data"

Nucleon structure

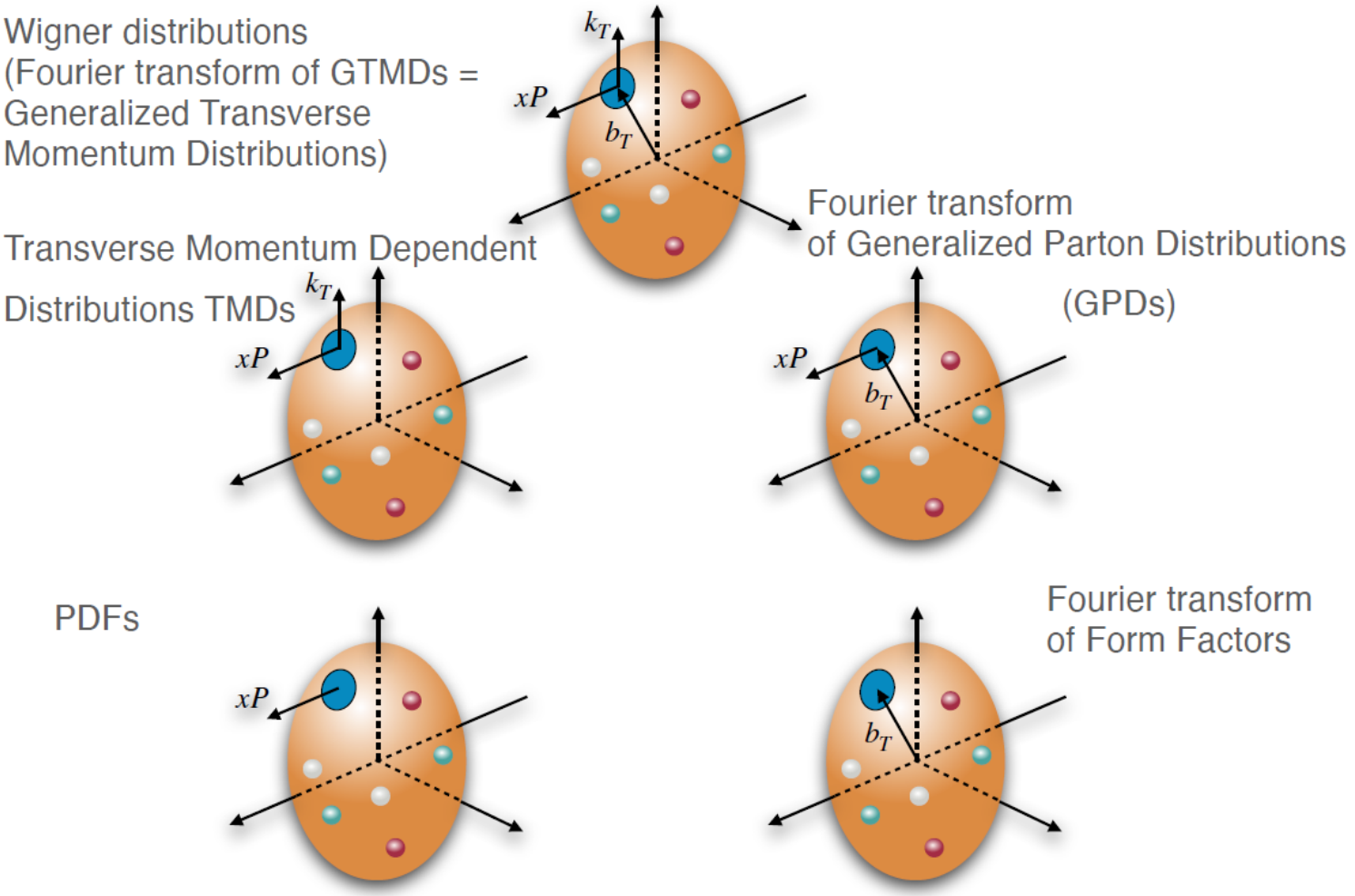

see, e.g., C. Lorcé, B. Pasquini, M. Vanderhaeghen, JHEP 1105 (11)

Taken from A. Prokudin, STAR Collaboration Meeting 2021.9

Parton saturation?

- Parton density can't grow to infinity (it would violate unitarity), so it has to saturate at high energy
- Can parton saturation be observed? EIC will study that.

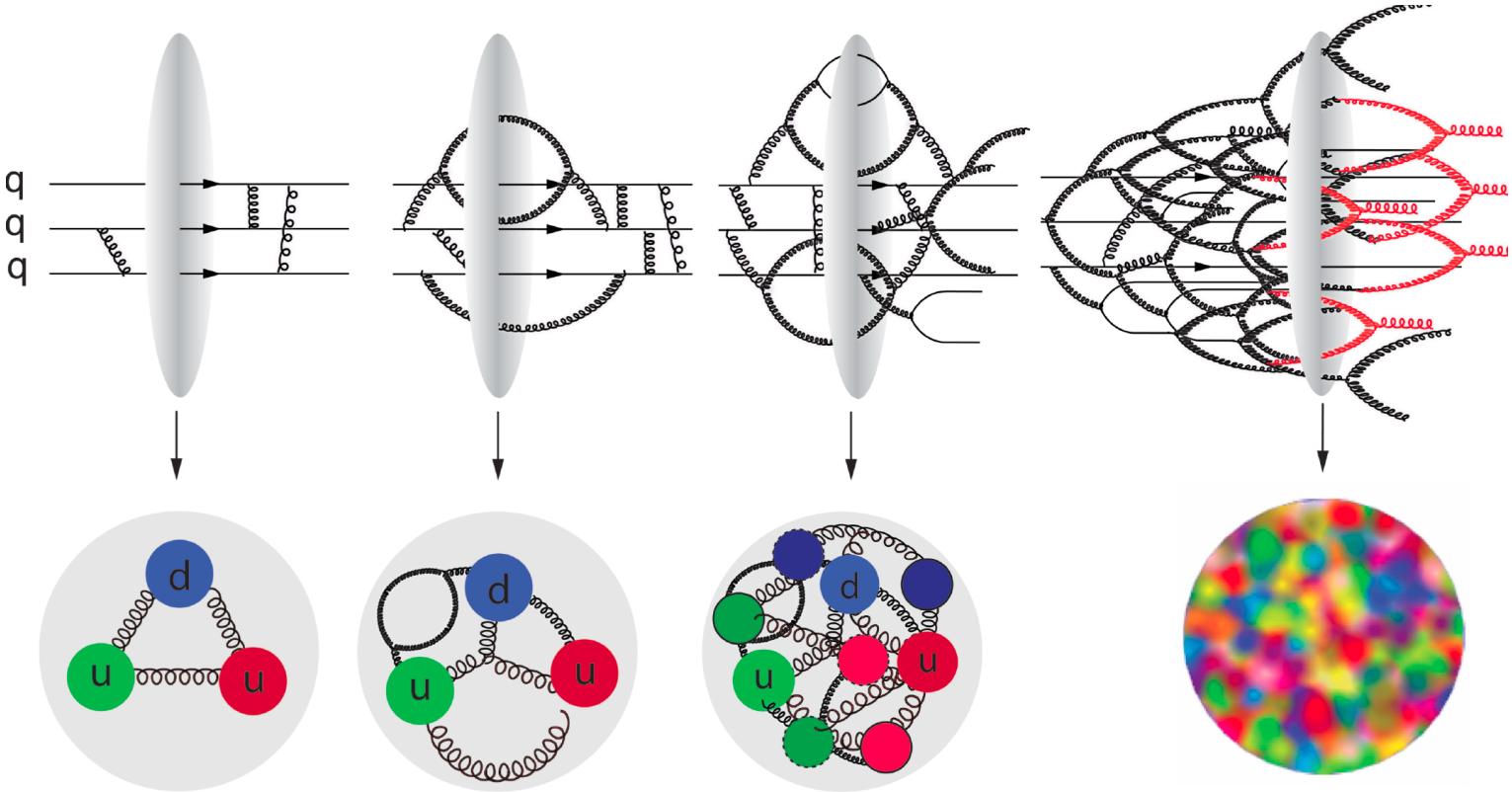

D. Bendova, WJCF Workshop 2022

Parton saturation?

- Parton density can't grow to infinity (it would violate unitarity), so it has to saturate at high energy
- Can parton saturation be observed? EIC will study that.

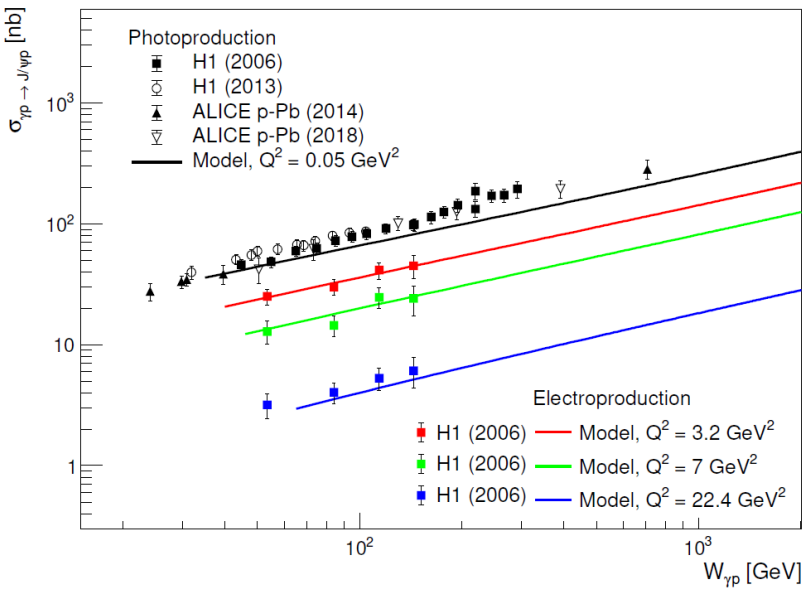

D. Bendova, WJCF Workshop 2022

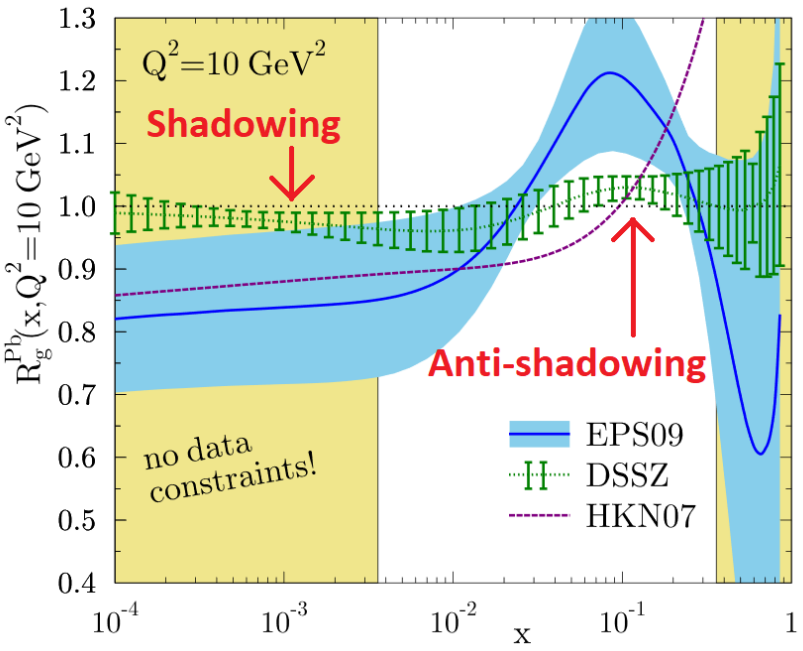

[Nucl.Phys.A 926 24-33(2014)]

- Parton distributions are modified for bound nucleons
  - shadowing
  - anti-shadowing
  - EMC effect (short range nucleon correlations?)
  - Fermi motion

Proposed detectors

3 proposed detector designs for Detector-1:

- to be located at 6 o'clock position (in place of STAR experiment)

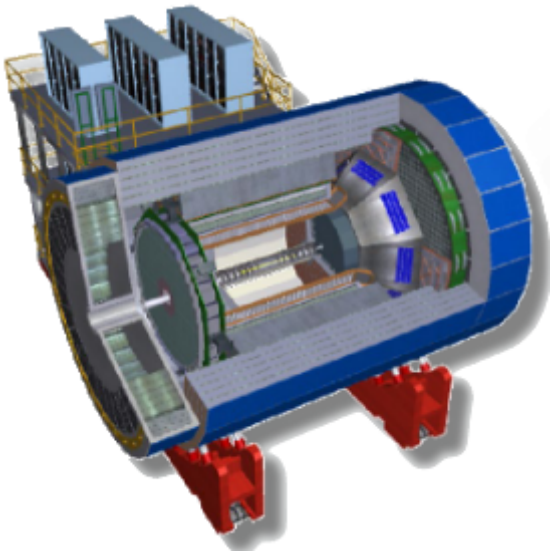

- **A** **T**otally **H**ermetic **E**lectron **N**ucleus **A**pparatus
- General purpose detector inspired by Yellow Report concept.
- Superconducting magnet with variable field up to 3 T
- `https://www.athena-eic.org`

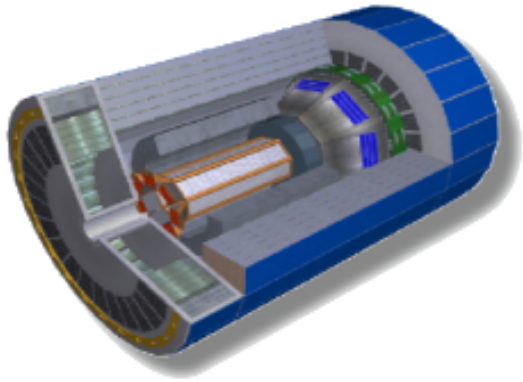

- **Co**mpact Detector for the **E**IC
- Nearly hermetic, general-purpose compact detector
- 2 T magnet (up to 4 T)
- `https://userweb.jlab.org/~hyde/EIC-CORE/`

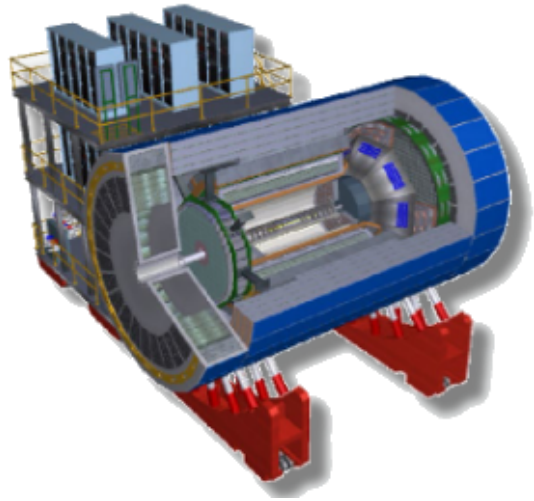

- **E**IC **C**omprehensive **C**hromodynamics **E**xperiment
- General purpose detector
- 1.5 T magnet reused from BaBar and sPHENIX
- `https://www.ecce-eic.org/`
- **Recommended by DPAP**

A Totally Hermetic Electron Nucleus Apparatus

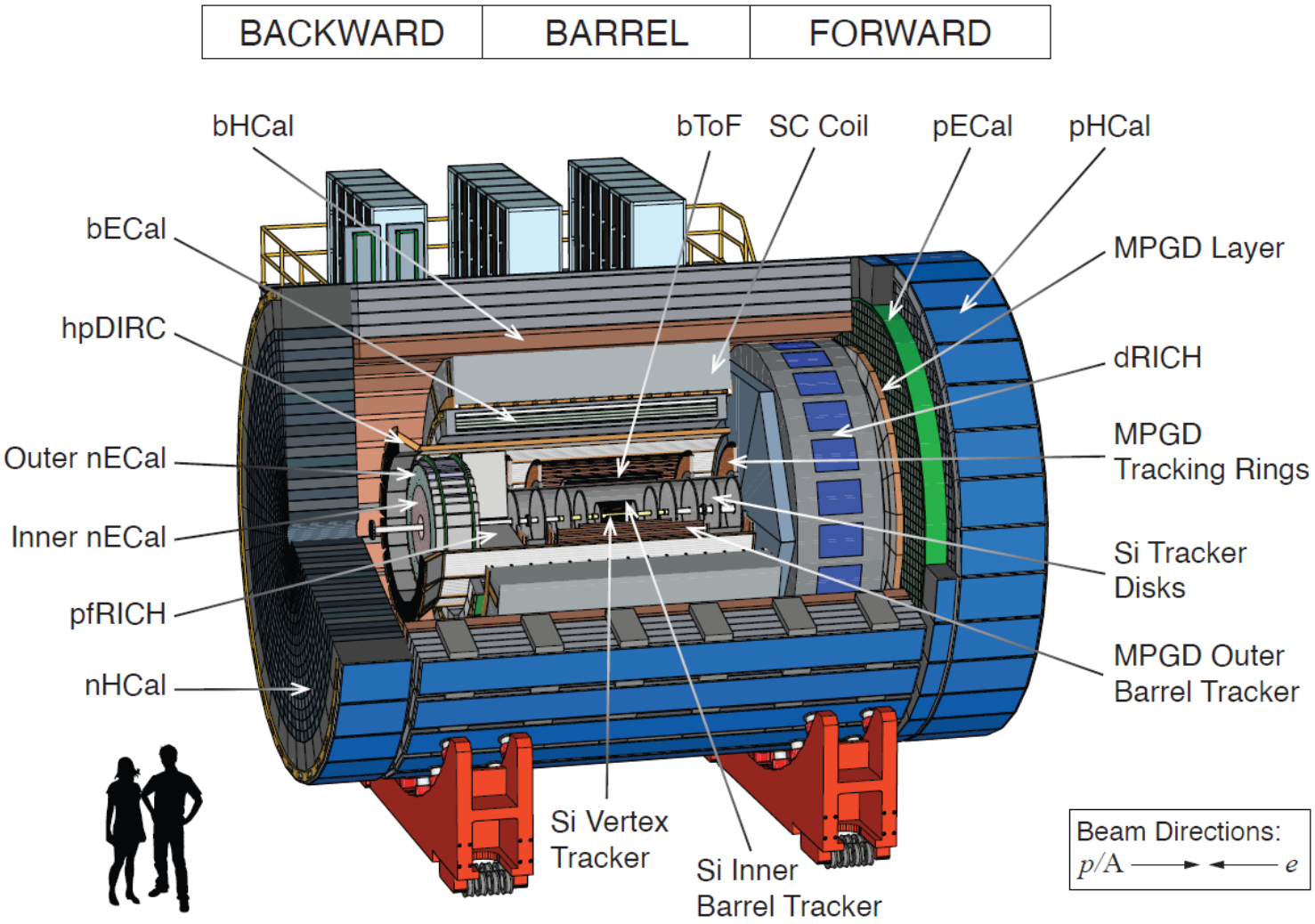

[ATHENA detector proposal]

Table 1.1: Complete list of ATHENA subsystems in the main detector ordered from small to large radii (barrel) and increasing distance from the interaction point (forward and backward regions). The PID range in momentum is quoted for 3σ separation.

	Detector	Purpose	Technology	Acceptance	PID Range (GeV/c)
Forward (h-going)	Si-Tracker Disks	Tracking	6 disks of MAPS	$1.1 < \eta < 3.75$	
	Tracking Rings (MPGD)	Tracking	Planar GEMs with annular shape surrounding the Si-disks	$1.1 < \eta < 2.0$	
	dRICH	PID	Dual RICH with aerogel and gas	$1.2 < \eta < 3.7$	$3 < p < 60$ (K/π) $0.85 < p < 15$ (e/π)
	MPGD Layer	Tracking	Planar μRWell disk	$1.4 < \eta < 3.75$	
	pECal	e/m Calorimetry	W-Powder/SciFi calorimeter	$1.2 < \eta < 4.0$	
	pHCal	Hadron Calorimetry	Fe/Sci sandwich	$1 < \eta < 4.0$	
Barrel	Si Vertex-Tracker	Tracking and Vertexing	3-layer MAPS	$-2.2 < \eta < 2.2$	
	Si Barrel-Tracker	Tracking	2-layer MAPS	$-1.05 < \eta < 1.05$	
	bToF	PID and Tracking	AC-LGAD	$-1.05 < \eta < 1.05$ $p_T > 0.23$ GeV/c @ 3T	$p < 1.3$ (K/π) $p < 0.4$ (e/π)
	Barrel Tracker (MPGD)	Tracking	4 (2+2) layer cylindrical Micromegas	$-1.05 < \eta < 1.05$	
	hpDIRC	PID	DIRC with focusing elements and fine pixel readout	$-1.64 < \eta < 1.25$ $p_T > 0.45$ GeV/c @ 3T	$p < 6.5$ (K/π) $p < 1.2$ (e/π)
	bECal	e/m Calorimetry & Tracking	Hybrid with Astropix imaging layers alternated with Pb/SciFi layers followed by a set of Pb/SciFi layers	$-1.5 < \eta < 1.2$	
	bHCal	Hadron Calorimetry	Fe/Sci sandwich	$-1.0 < \eta < 1.0$	
Backward (e-going)	Si-Tracker Disks	Tracking	5 disks of MAPS	$-1.1 > \eta > -3.8$	
	Tracking Rings (MPGD)	Tracking	Planar GEMs with annular shape surrounding the Si-disks	$-1.1 > \eta > -1.8$	
	pfRICH	PID	Proximity focusing RICH with aerogel	$-1.5 > \eta > -3.8$	$3 < p < 11$ (K/π) $0.85 < p < 3$ (e/π)
	Inner nECal	e/m Calorimetry	$PbWO_4$	$-2.3 > \eta > -4.0$	
	Outer nECal	e/m Calorimetry	SciGlass	$-1.5 > \eta > -2.3$	
	nHCal	Hadron Calorimetry	Fe/Sci sandwich	$-1 > \eta > -4$	

Tracker

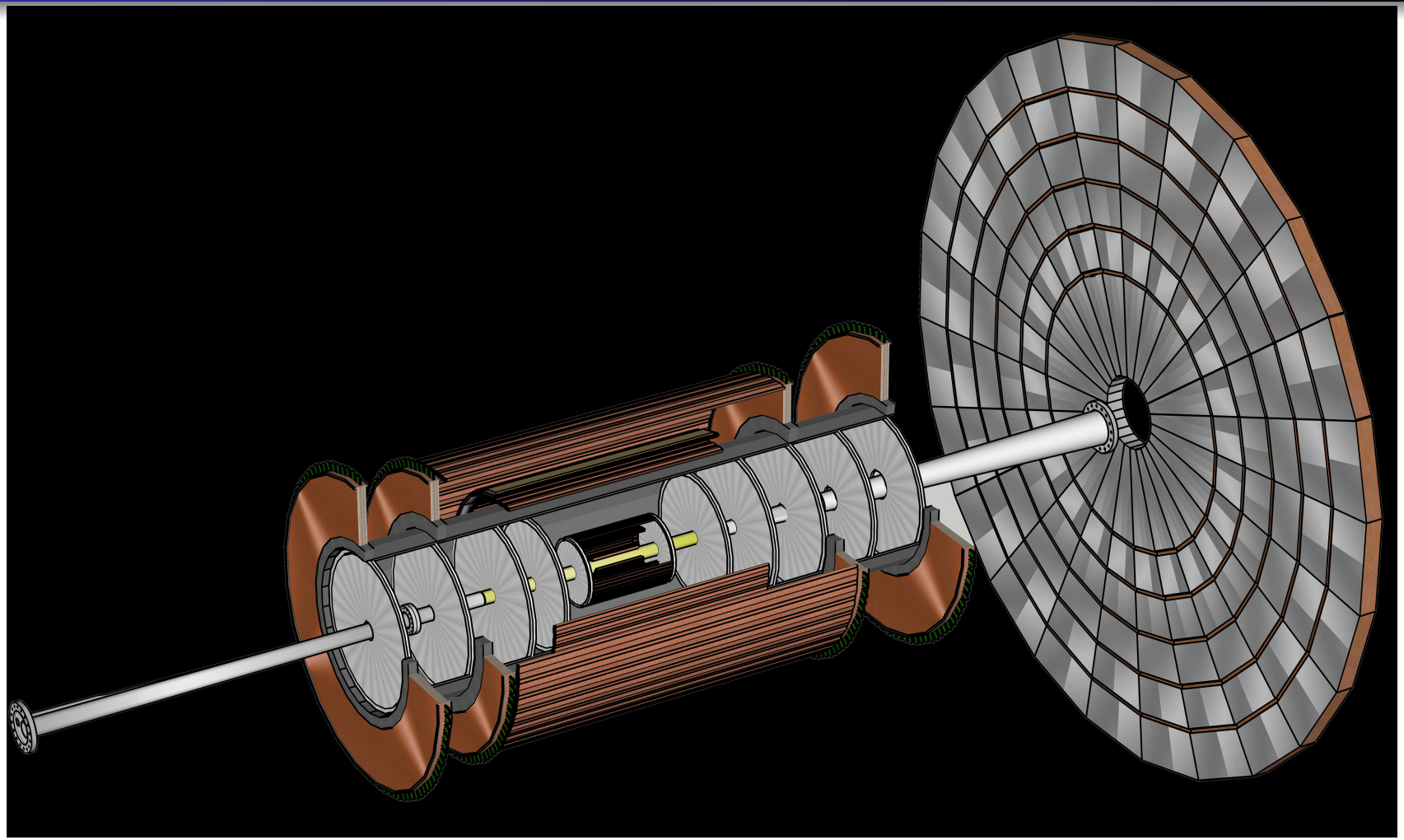

- Silicon sensors:
  - 3 vertex and 2 barrel layers
  - MAPS sensors similar to ALICE ITS3 upgrade
- 4 Micromegas barrel trackers
- GEM disks: 5 *e*-going (backward) and 6 *p*-going (forward)
- Large forward μRWell detector

Tracker performance

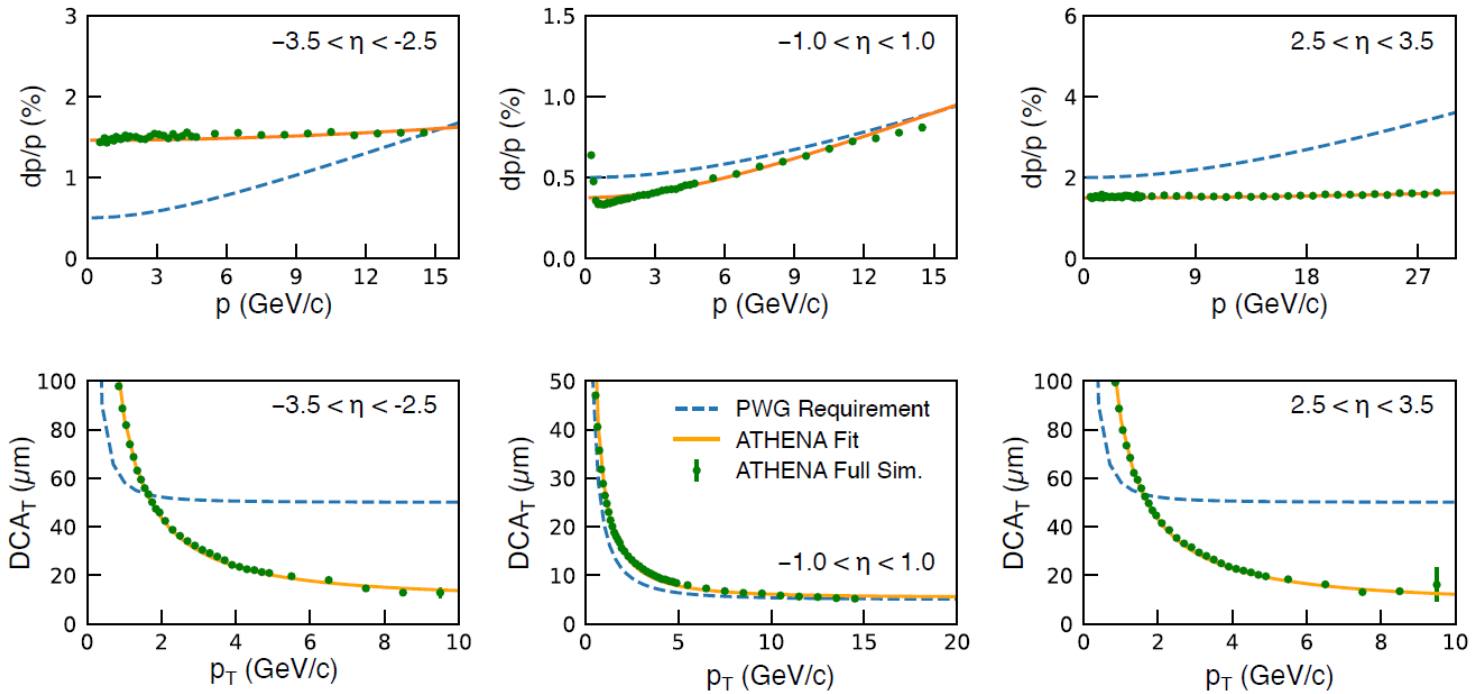

Figure 2.4: ATHENA tracking performance of generated pions compared to the Yellow Report requirements (dashed lines) for selected η bins. Top row: momentum resolutions versus momentum. Bottom row: Transverse DCA performance versus momentum (FullSim).

Table 2.2: Comparison of performance and Yellow Report requirement parameterizations for relative momentum and transverse pointing resolutions as a function of momentum for the ATHENA baseline tracking system.

	Momentum resolution $\sigma(p)/p$		**Transverse pointing resolution** $\sigma(\mathrm{DCA_T})$	
	Performance	Requirements	Performance	Requirements
$-3.5 < \eta < -2.5$	$\sim 0.04\% \times p \oplus 1.5\%$	$\sim 0.1\% \times p \oplus 0.5\%$	$\sim 80/p_T \oplus 10\ \mu m$	$\sim 30/p_T \oplus 50\ \mu m$
$-2.5 < \eta < -1.0$	$\sim 0.01\% \times p \oplus 0.5\%$	$\sim 0.05\% \times p \oplus 0.5\%$	$\sim 50/p_T \oplus 5\ \mu m$	$\sim 30/p_T \oplus 20\ \mu m$
$-1.0 < \eta < 1.0$	$\sim 0.05\% \times p \oplus 0.4\%$	$\sim 0.05\% \times p \oplus 0.5\%$	$\sim 30/p_T \oplus 5\ \mu m$	$\sim 20/p_T \oplus 5\ \mu m$
$1.0 < \eta < 2.5$	$\sim 0.01\% \times p \oplus 0.5\%$	$\sim 0.05\% \times p \oplus 1\%$	$\sim 50/p_T \oplus 5\ \mu m$	$\sim 30/p_T \oplus 20\ \mu m$
$2.5 < \eta < 3.5$	$\sim 0.02\% \times p \oplus 1.5\%$	$\sim 0.1\% \times p \oplus 2\%$	$\sim 80/p_T \oplus 10\ \mu m$	$\sim 30/p_T \oplus 50\ \mu m$

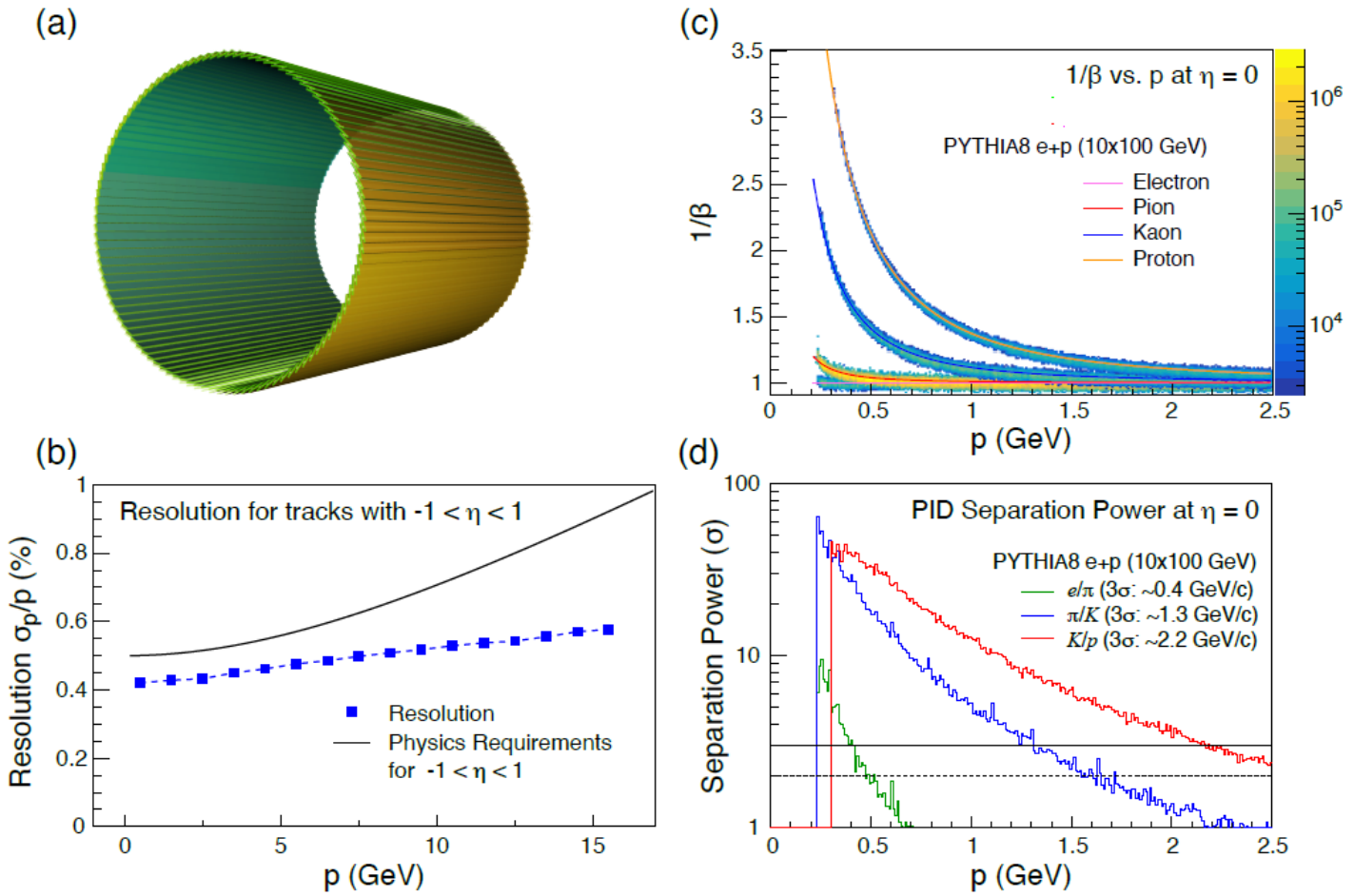

Figure 2.10: a) Configuration of the barrel ToF. b) Anticipated impact from the spatial hit from the ToF system on the tracking performance, with improved baseline performance at higher momenta. c) Shows that ToF more than satisfies the PID requirements in the momentum range below the DIRC kaon threshold (0.47 GeV/c), thereby filling in the PID to 230 MeV/c. d) Separation power in number of σ separation (FullSim).

- AC-coupled LGAD (low-gain avalanche diodes) TOF

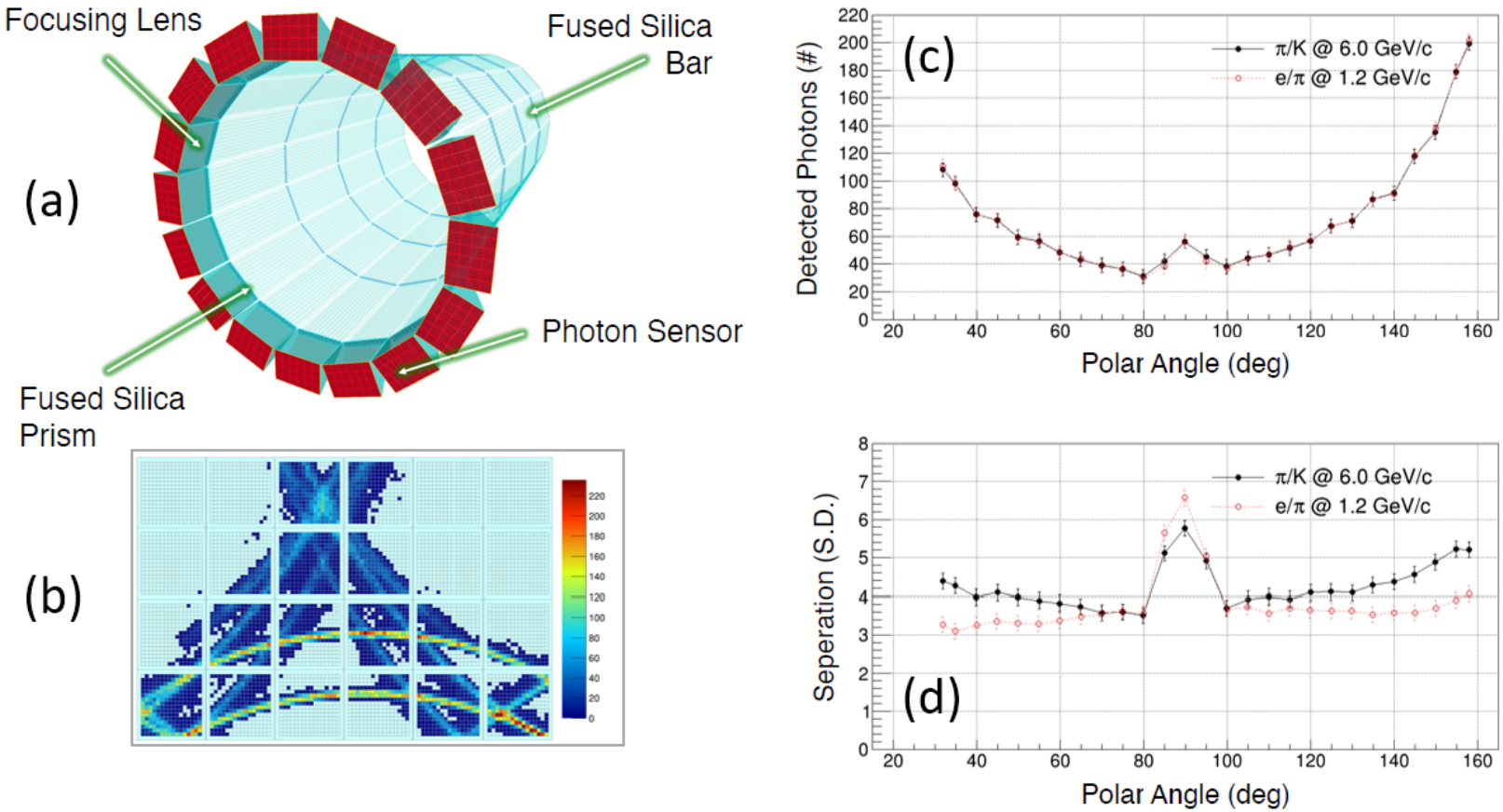

Figure 2.9: a) Configuration of the DIRC. b) Superposition of the distribution of photon hits from 6 GeV/c identical pions. c) Number of detected photoelectrons as a function of polar angle. d) Separation power at the maximum momentum requirement stated in the Yellow Report. Results from a stand-alone GEANT4 simulation.

- high performance DIRC (detection of internally reflected cherenkov light)

Barrel E-M Calorimeter

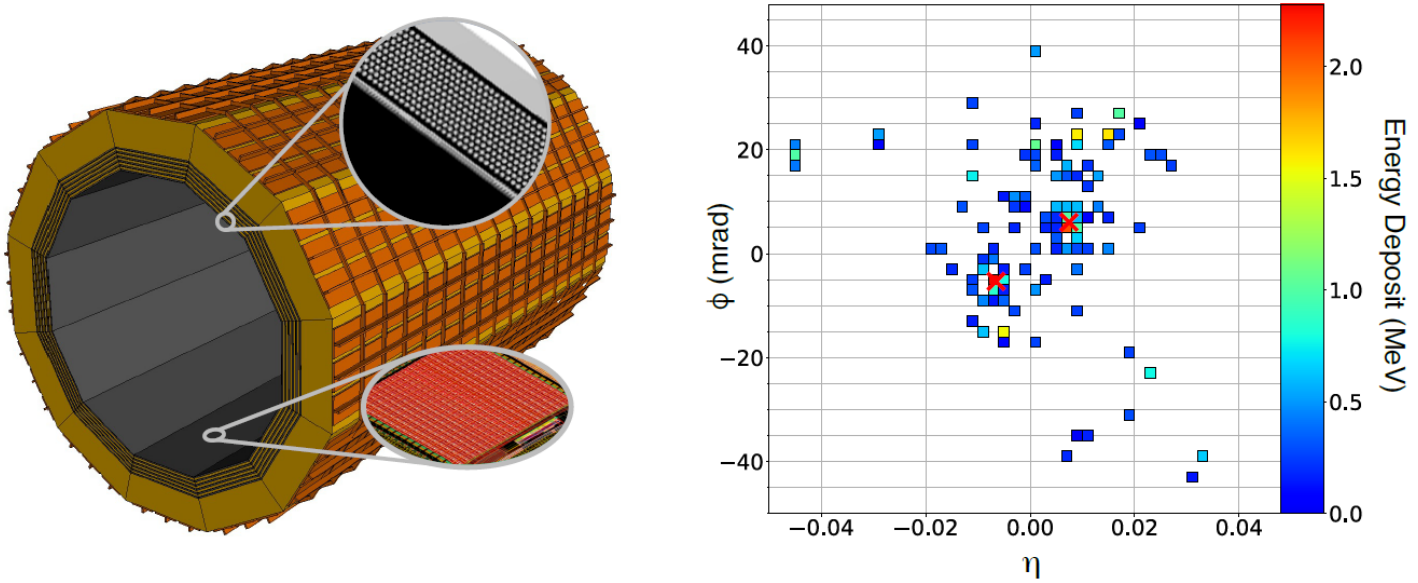

Figure 2.6: Left: The barrel electromagnetic calorimeter as included in detector simulations. The inner radius of the barrel is 103 cm. The first (closest to the beam) 6 layers are imaging layers. The insets show the structure of the Si imaging layers (bottom) and the 1.59 cm thick Pb/SciFi (top). The imaging layers are followed by a thicker Pb/ScFi section, for a total thickness (not including the support structure) of 40 cm. Right: Energy deposited in pixels in the imaging calorimeter demonstrating clean seperation of the two clusters for a 15 GeV π^0. The red crosses mark the reconstructed clusters centers (FullSim).

- Hybrid Pb/SciFi design and imaging with monolithic silicon sensors (AstroPix)
  - 6 layers of silicon sensors
  - 5 layers of Pb/SciFi (1.59 cm) + thick layer of Pb/SciFi
  - Total thickness: $20X_0$
- Outer layer causes 70% of neutrons to shower, which helps identify neutral hadrons
- Hybrid+imaging calorimeter allows use of machine learning techniques for patter recognition of showers in 3D
  - Enables muon identification

Barrel E-M Calorimeter performance

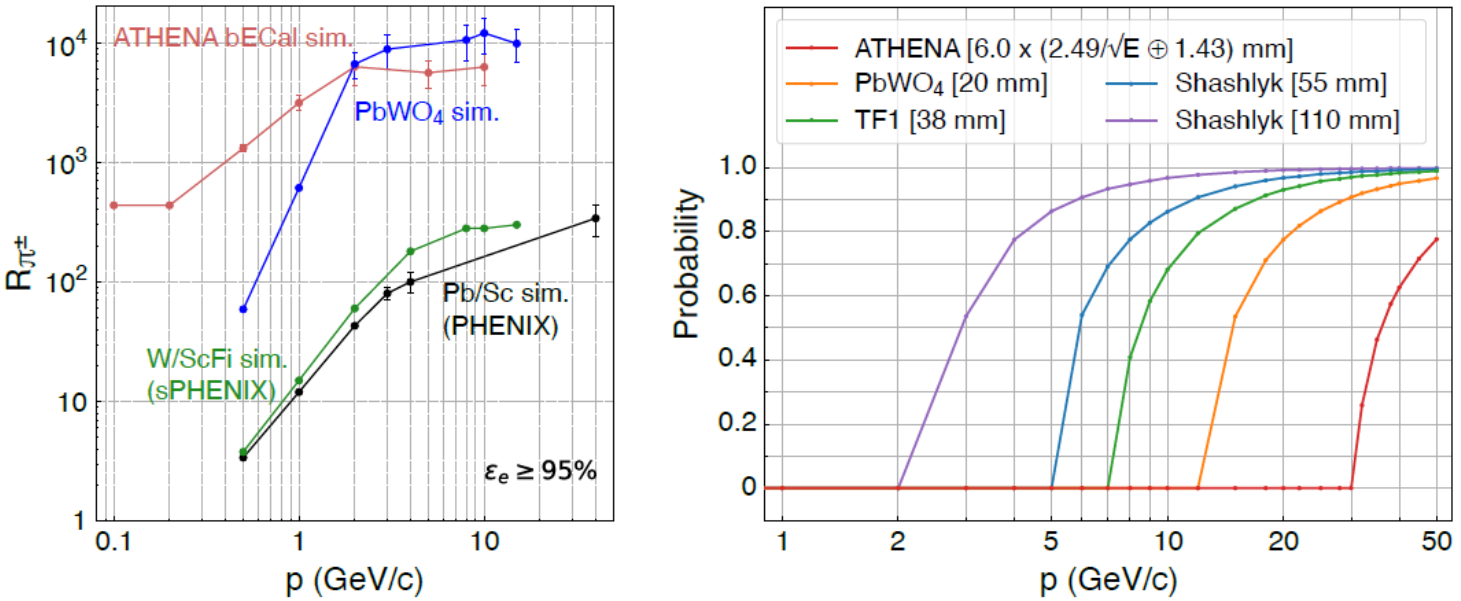

Figure 2.7: Left: The pion rejection power of ATHENA bECal (red solid line) compared with other technologies listed in the EIC Yellow Report. The rejection power of the ATHENA bECal is obtained from the analysis described in the Supplemental Material utilizing the E/p method and pattern matching, while the other rejection powers are determined from the E/p method [3] only. All the curves, including simulations and data, are obtained for the standalone calorimeter, *i.e.*, no other materials are placed in front of the calorimeter and no magnetic field is involved. The effects of material and the magnetic field are discussed further in the supplemental material. Right: The merging probability of the two γs from π^0 decay in the barrel region at r = 1.03 m. For ATHENA bECal, 6σ of its spatial resolution ($2.4/\sqrt{E} \oplus 1.3$ mm) is used to estimate the merging probability, since its pixel size (0.5 mm) is much smaller than the cluster profile. For the other technologies, the cell size is used to estimate the probability [3].

Table 2.3: Expected bECal detector performance.

Energy Resolution	$5.5\%/\sqrt{E} \oplus 1\%^a$
e/π separation	$>$ 99.8% pion rejection with 95% electron efficiency at $p \geq 0.1$ GeV/c^b.
E^{γ}_{min}	< 100 MeV^c
Spatial Resolution	Cluster position resolution for 5 GeV photons at normal incident angle is below $\sigma = 2$ mm (at the surface of the stave $r = 103$ cm) or 0.12°. For comparison, the minimal opening angle of photons from $\pi^0 \to \gamma\gamma$ at 15 GeV is $\sim 1.05°$ (about 19 mm – 37 pixels – of separation at $r = 103$ cm).

[a] Based on the photon simulations with $-0.5 < \eta < 0.5$ and $0 < \phi < 2\pi$. The constant term does not include calibration effects.
[b] Based on simulation for a standalone bECal, see Fig. 2.7 for detailed results.
[c] Based on simulations, 100 MeV photons leave an energy deposit of $\sim$ 15 MeV in SciFi layers and of $\sim$ 1 MeV in the imaging layers. This simulation includes digitization with electronics noise and a noise suppression cut.

Negative E-M calorimeter (nECal)

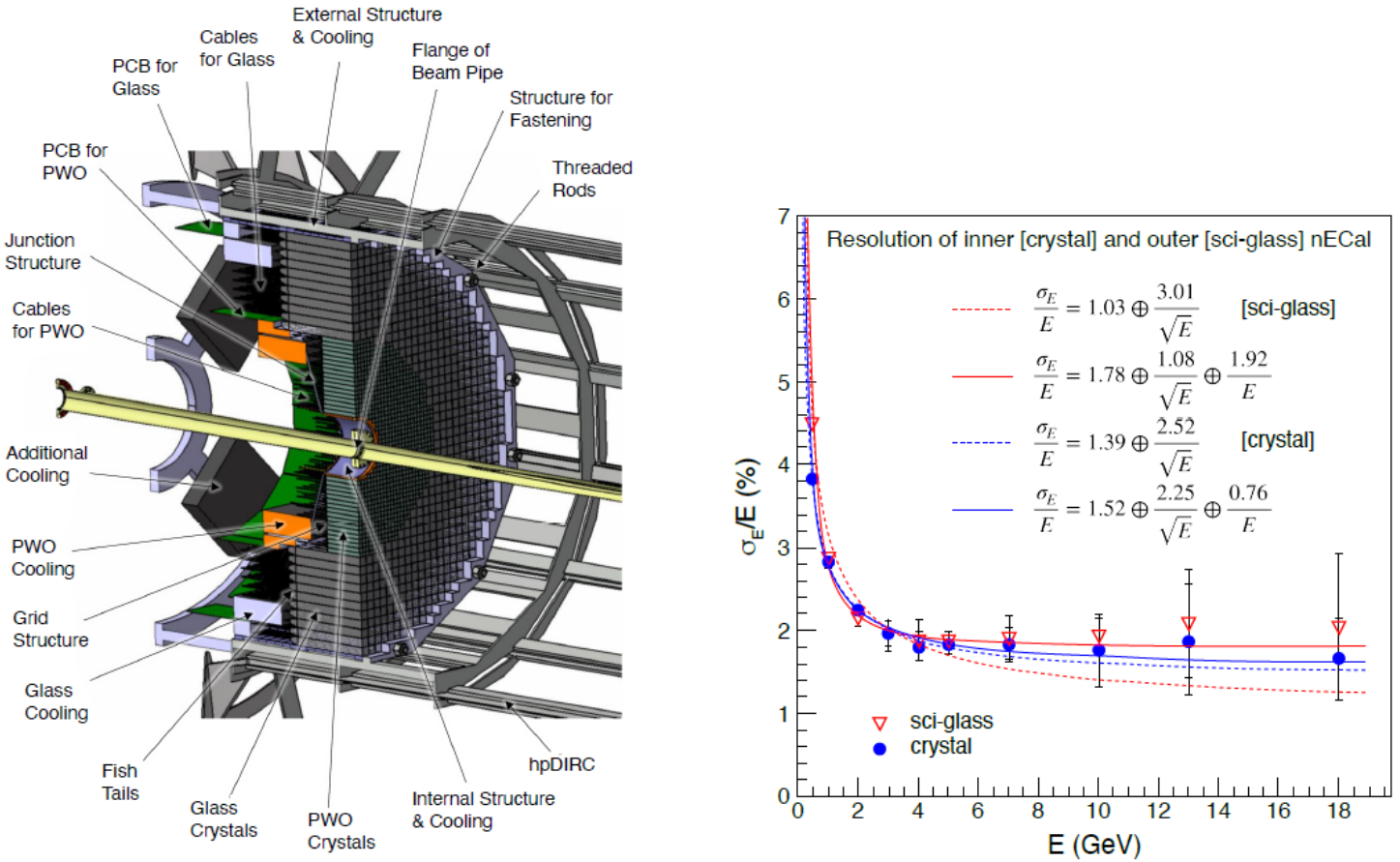

Figure 2.5: Left: The mechanical design of hybrid crystal/glass calorimeter nECal. Right: Expected nECal performance for the stand alone calorimeter, the energy resolution curves for inner $PbWO_4$ ($\sim 22\ X_0$) and outer SciGlass ($\sim 20\ X_0$) regions (FullSim).

- Located in the negative *e*-going (backward) direction
- Inner part: PbWo4 crystals
- Outer part: SciGlass

dRICH (forward)

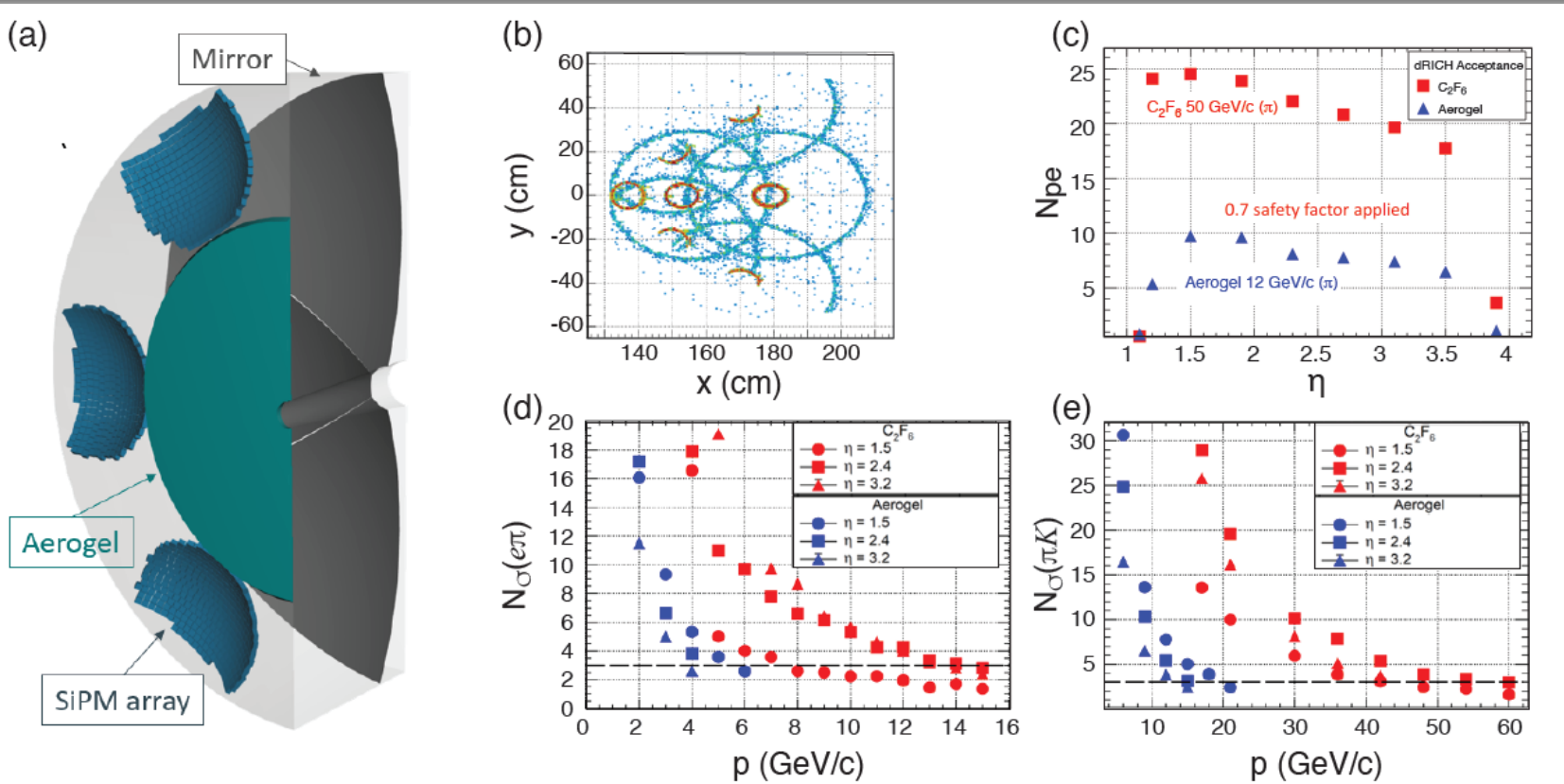

Figure 2.8: Panel a) shows the layout of the dRICH radiators, mirror, and SiPM focal planes. Panel b) shows the superposition of hits from 1000 events with identical primary particles. This effectively captures ring shape (aerogel-large, gas-small), Rayleigh scattering, optical aberration, multiple scattering, tracking resolution, chromaticity, and signal-to-noise effects in one image. Panel c) shows the number of photoelectrons per single ring vs η, and thereby illustrates the acceptance range. Panels d) and e) demonstrate the PID separation for $e\pi$ and πK. The performance meets the Yellow Report specification. Aerogel performance is indicated in blue and C_2F_6 in red (FullSim).

- Dual-radiator RICH at forward rapidity (p-going)
- Good e/π separation

Muon detection - barrel

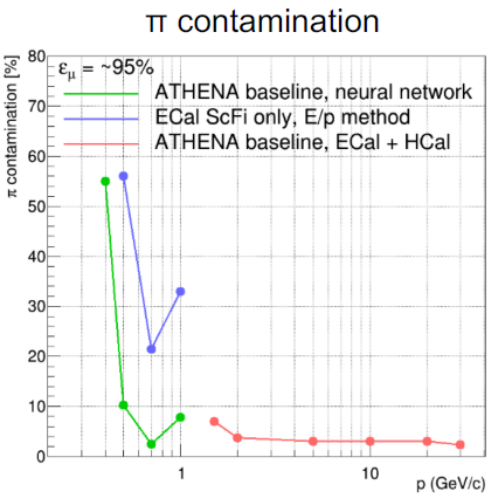

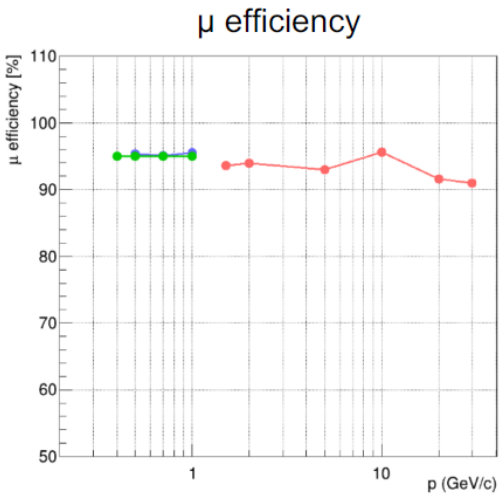

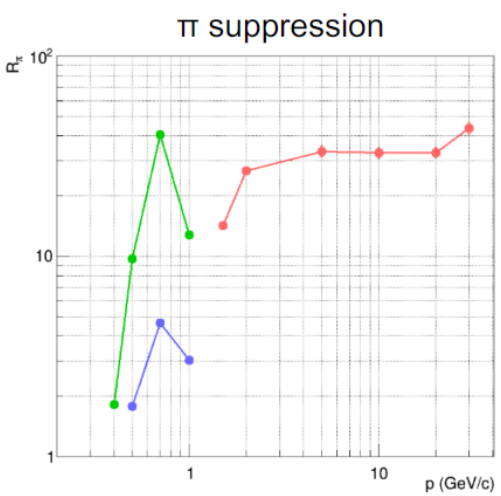

- Information from Barrel E-M and hadronic calorimeters allows to separate μ/π
- Muons with $p > 1.5\,\mathrm{GeV/c}$ reach BHCal
- For $p < 1.5\,\mathrm{GeV/c}$ they curl inside BECal
- Better performance if other PID detectors included

Muon detection - barrel

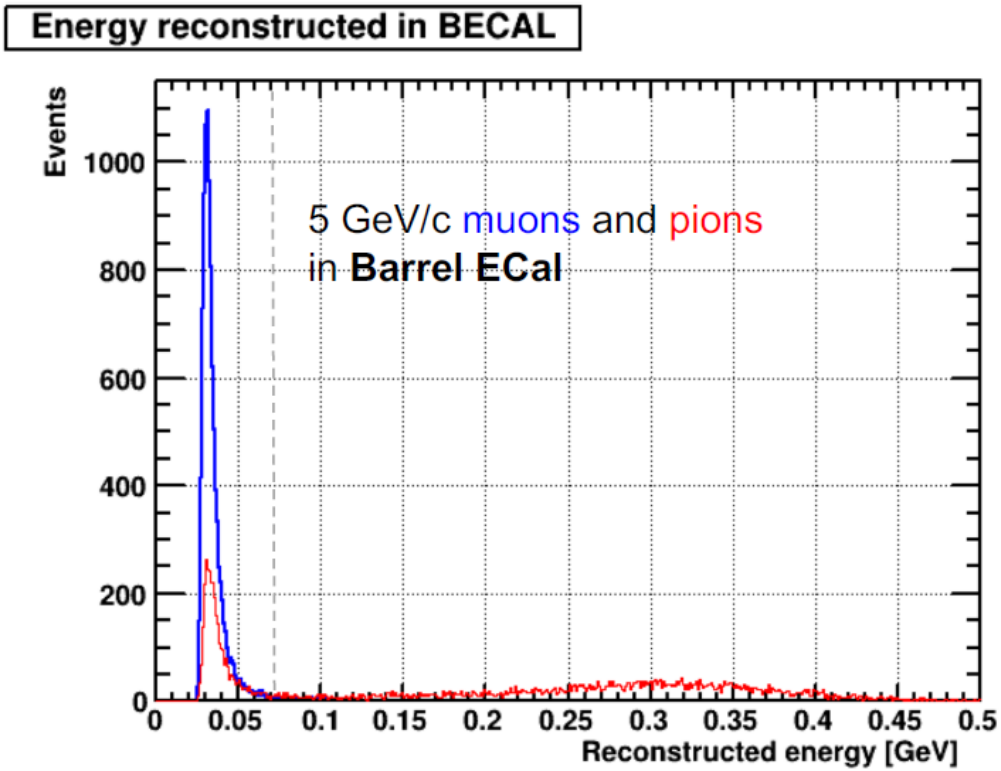

- μ leave MIP signal in BECal
- μ selection:
  - MIP signal in BECal (95% efficiency)
  - hits in each BHCal layers

Muon detection - barrel

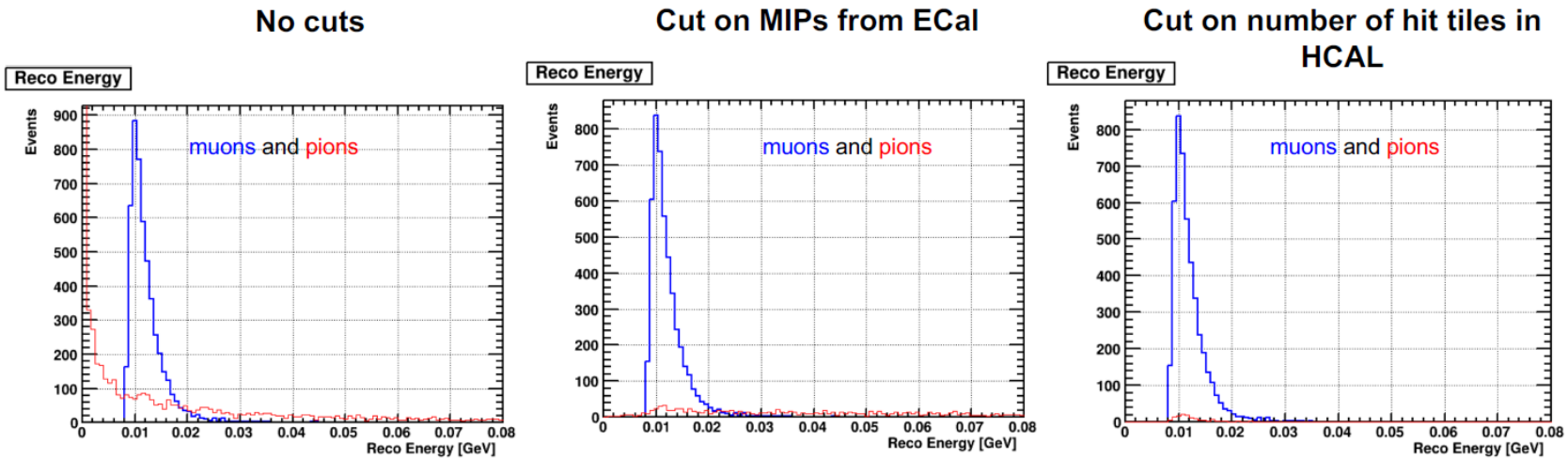

- μ leave MIP signal in BECal
- μ selection:
  - MIP signal in BECal (95% efficiency)
  - hits in each BHCal layers

Muon detection - barrel with ML

Example of **muons** and **pions** at **p = 0.5 GeV/c** at η = (-1,1)
Efficiency: 98.9% ⟶ Rejection Power: 6.6
Efficiency: 95% ⟶ Rejection Power: 9.7

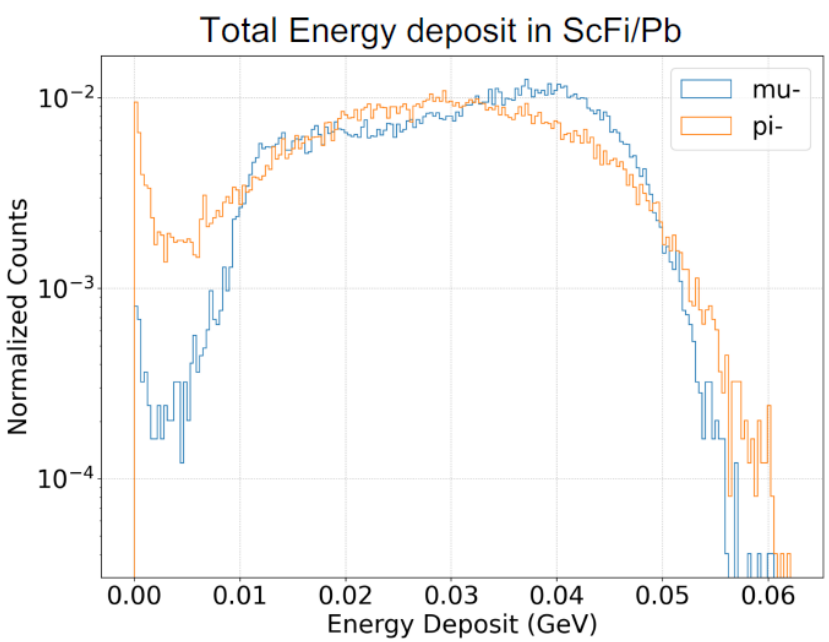

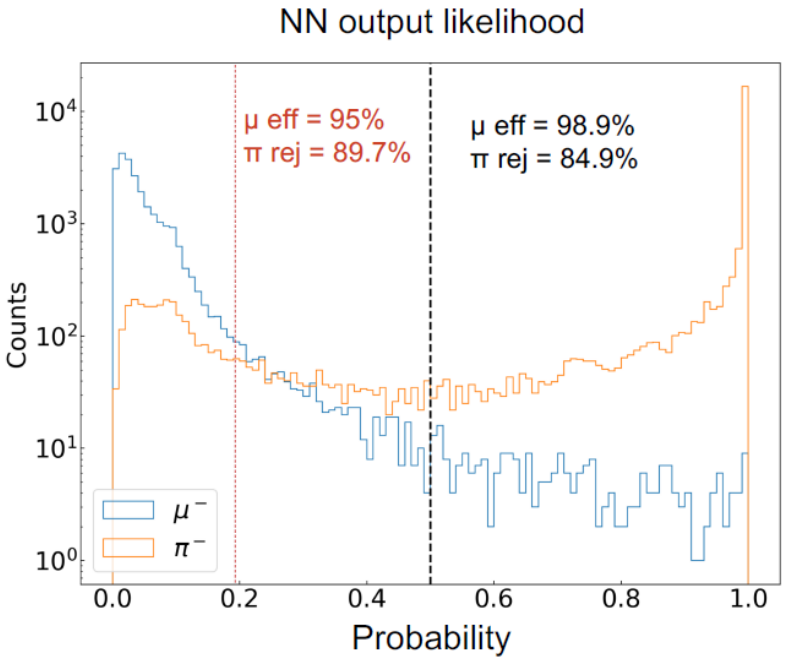

Comparing the two plots demonstrates the power of including the imaging layers:
→ they enhance μ/π separation at low momenta

- Muon identification using information from imaging layers and Pb/SciFi of BECal and machine learning
  - 4 parameters for each hit: η, ϕ, E, R
  - 3 layers convolutional neural network and 3 layers perceptron
  - 95% efficiency

Muon detection - forward (hadron endcap)

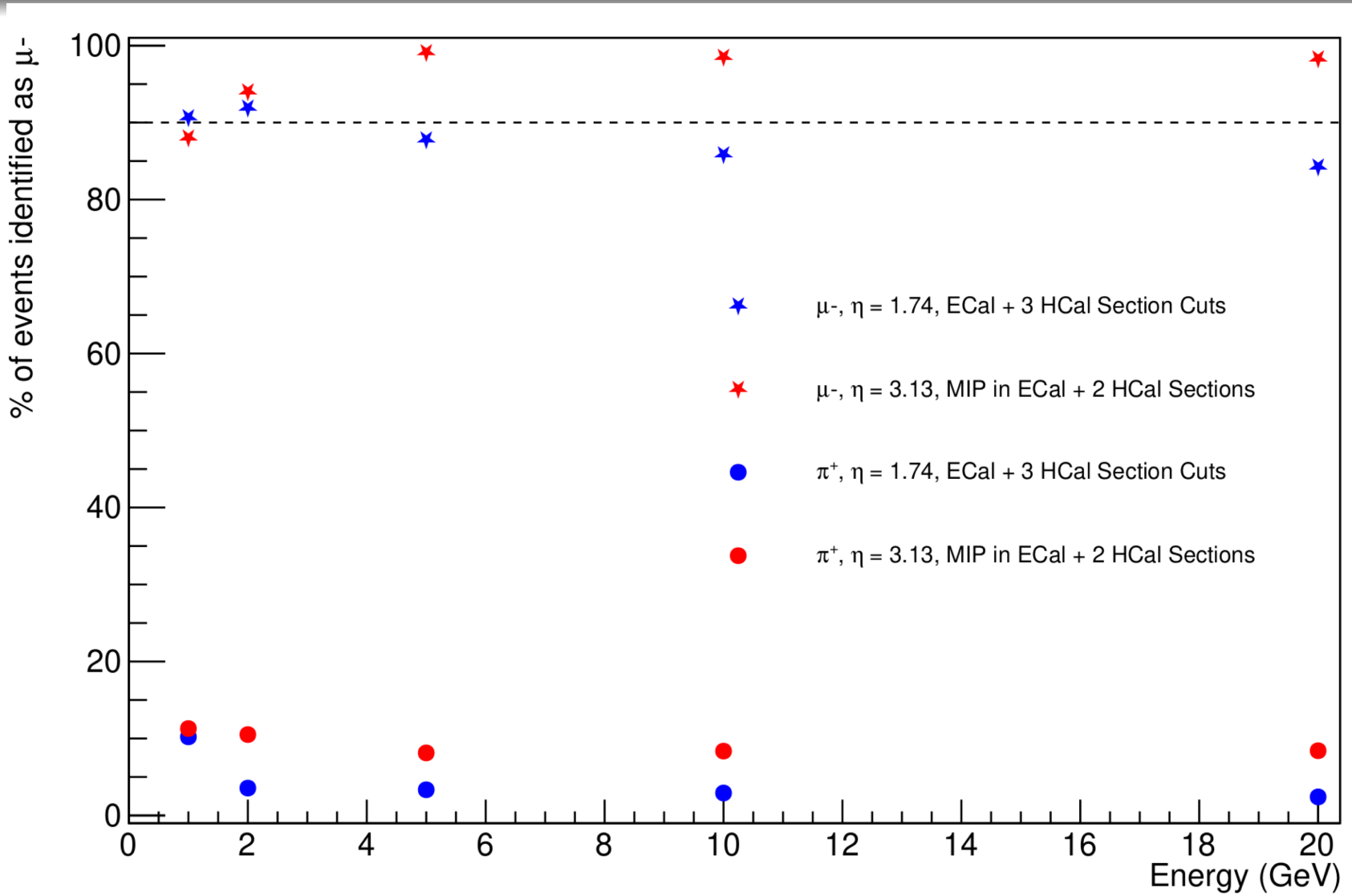

- Muon selection possible with pECal and pHCal information
  - MIP-like signal in pECal
  - Number of hits along the tracks consistent with no shower
- 90% efficiency, only few % pion contamination

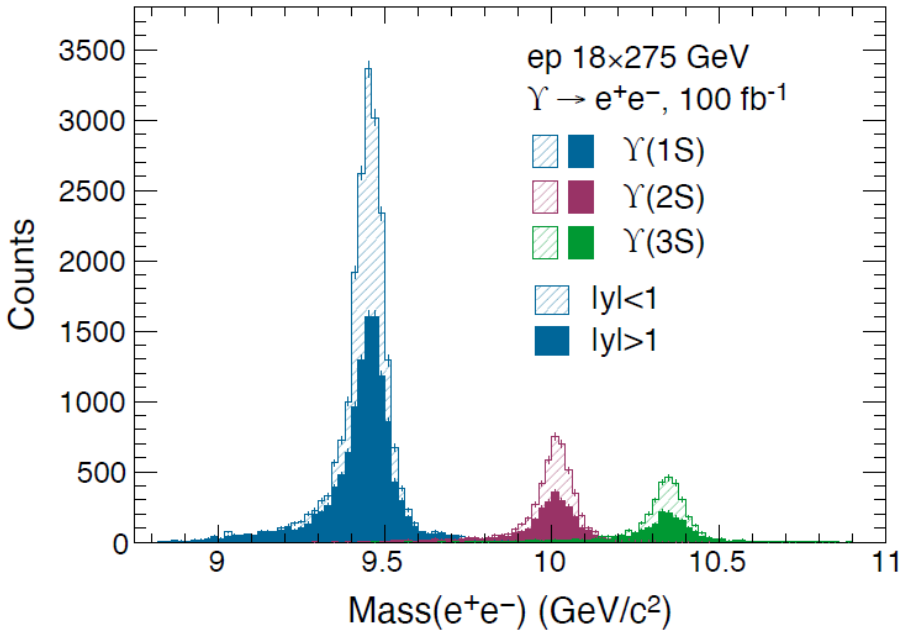

Figure 3.5: The simulated M_{ee} mass spectrum for exclusive production of the three Υ states in 18 $\times$ 275 GeV e+p with 100 fb^{-1} of integrated luminosity, using the cross sections from eSTARlight [58]. Spectra are shown for Υ-production at mid-rapidity ($|y| < 1$) and away from mid-rapidity ($|y| > 1$) (FullSim).

- Upsilon states well separated in the dielectron channel
- Low bremsstrahlung tails thanks to low-mass trackers and beampipe

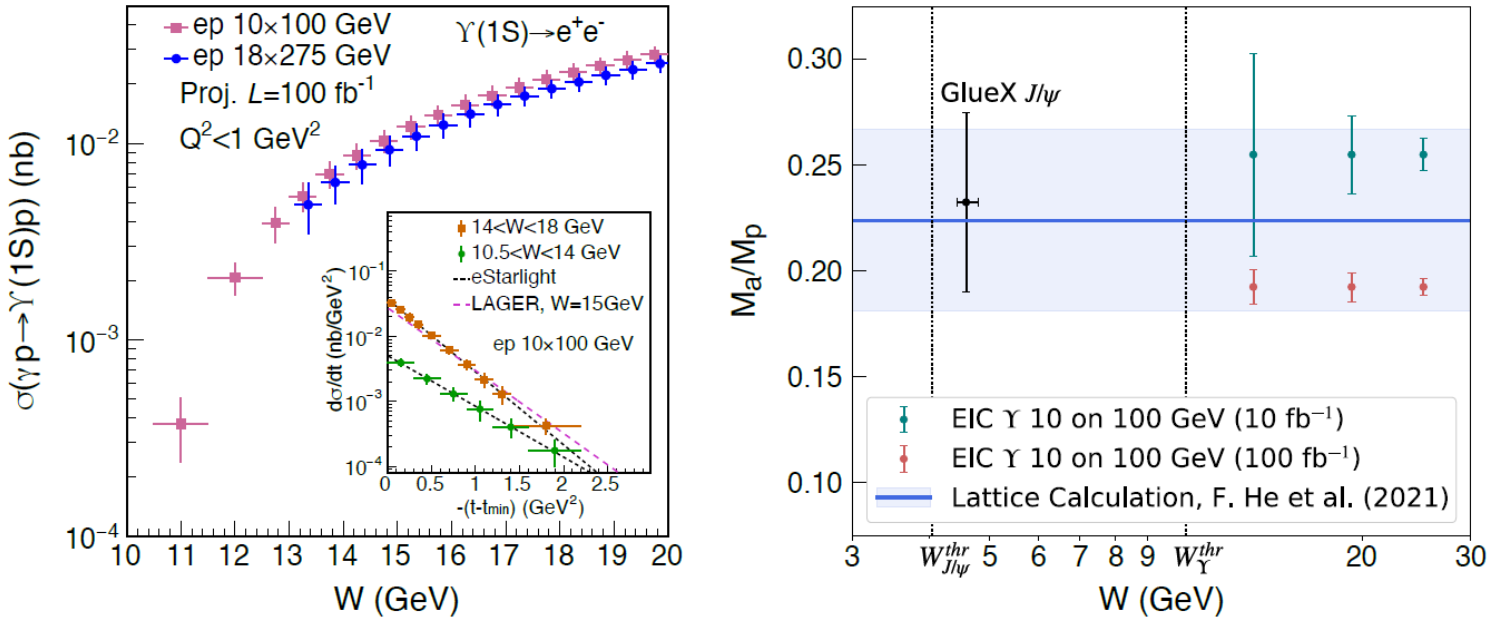

Figure 3.19: Left: The projected uncertainty of total and differential (insert panel) cross section of $\Upsilon(1S)$ near threshold for photo-production and electro-production ($Q^2 < 1$ GeV^2) in e+p collisions via the di-electron decay channel. Two model predictions [58, 101] of the near threshold differential $d\sigma/dt$ are also shown (FullSim). Right: The trace anomaly contribution to the proton mass in Ji's decomposition according to [104, 105] and references therein. Green and red points correspond to 10 fb^{-1} and 100 fb^{-1} integrated luminosity, respectively, and are offset from each other. The band is the result of a recent lattice QCD calculation [106] (FullSim).

- Needs measurement of electron and/or proton momentum
- Projections both for 10 fb^{-1} and 100 fb^{-1}

EIC Comprehensive Chromodynamics Experiment

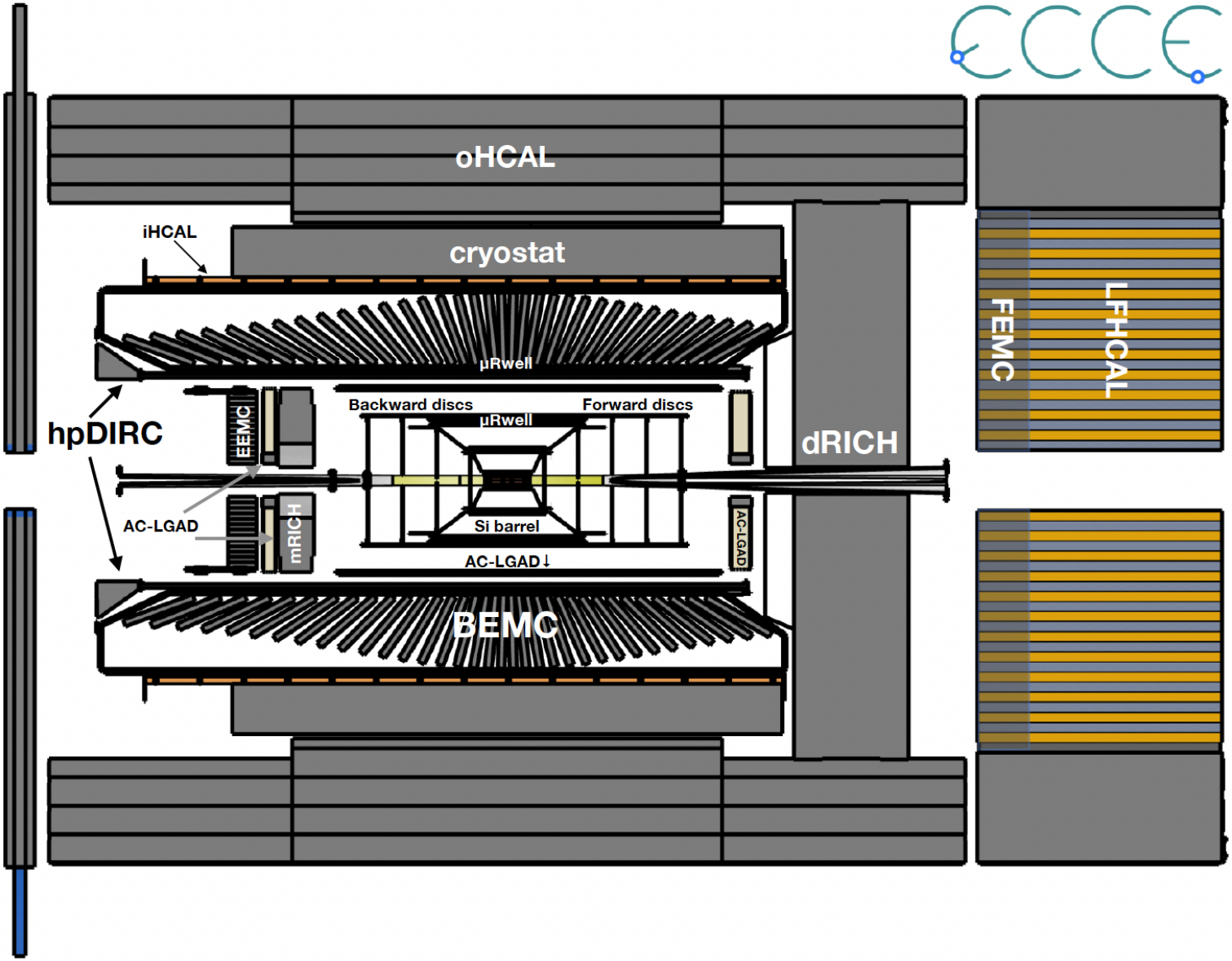

[ECCE detector proposal]

ECCE - subdetectors

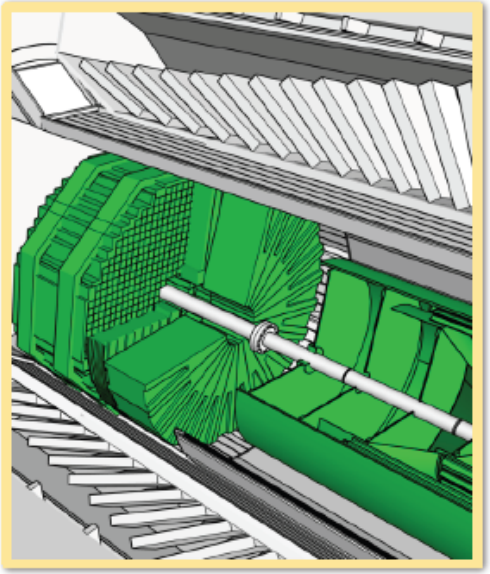

Backward Endcap

Tracking:
- ITS3 MAPS Si discs (x4)
- AC-LGAD

PID:
- mRICH
- AC-LGAD TOF
- $PbWO_4$ EM Calorimeter (EEMC)

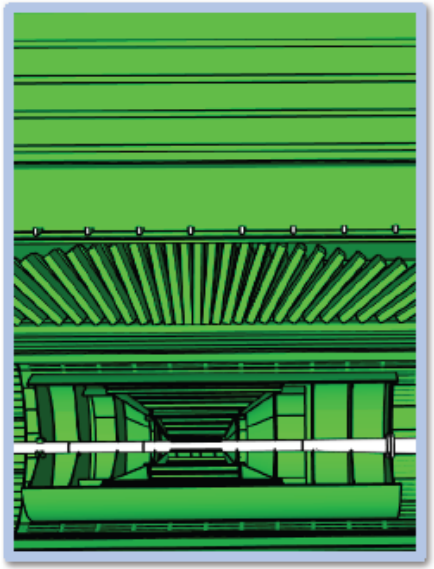

Barrel

Tracking:
- ITS3 MAPS Si (vertex x3; sagitta x2)
- µRWell outer layer (x2)
- AC-LGAD (before hpDIRC)
- µRWell (after hpDIRC)

h-PID:
- AC-LGAD TOF
- hpDIRC

Electron ID:
- SciGlass EM Cal (BEMC)

Hadron calorimetry:
- Outer Fe/Sc Calorimeter (oHCAL)
- Instrumented frame (iHCAL)

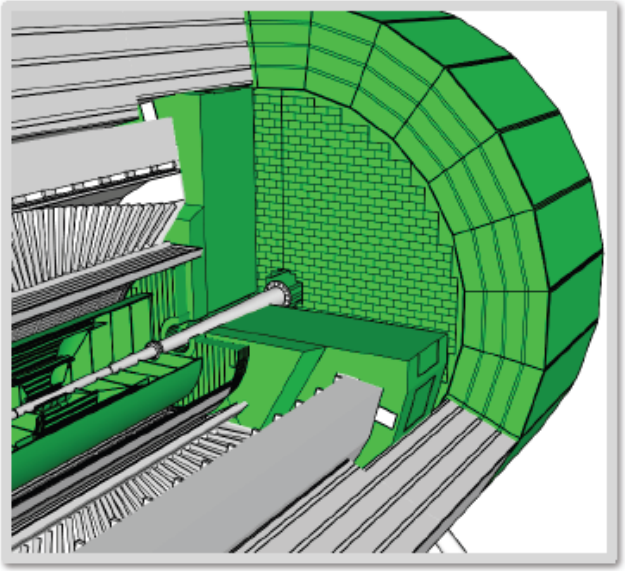

Forward Endcap

Tracking:
- ITS3 MAPS Si discs (x5)
- AC-LGAD

PID:
- dRICH
- AC-LGAD TOF

Calorimetry:
- Pb/ScFi shashlik (FEMC)
- Longitudinally separated hadronic calorimeter (LHFCAL)

Detector description toolkit for HEP (DD4hep):
`https://dd4hep.web.cern.ch/dd4hep/`

- Designed using lessons learned from work on LHC and Linear Collider
- Independent of MC event generators
- Reuses existing software (no need to reinvent the wheel)
  - Works with Geant4 for particle transport
  - Uses ROOT for visualization
- Easy to use and modify

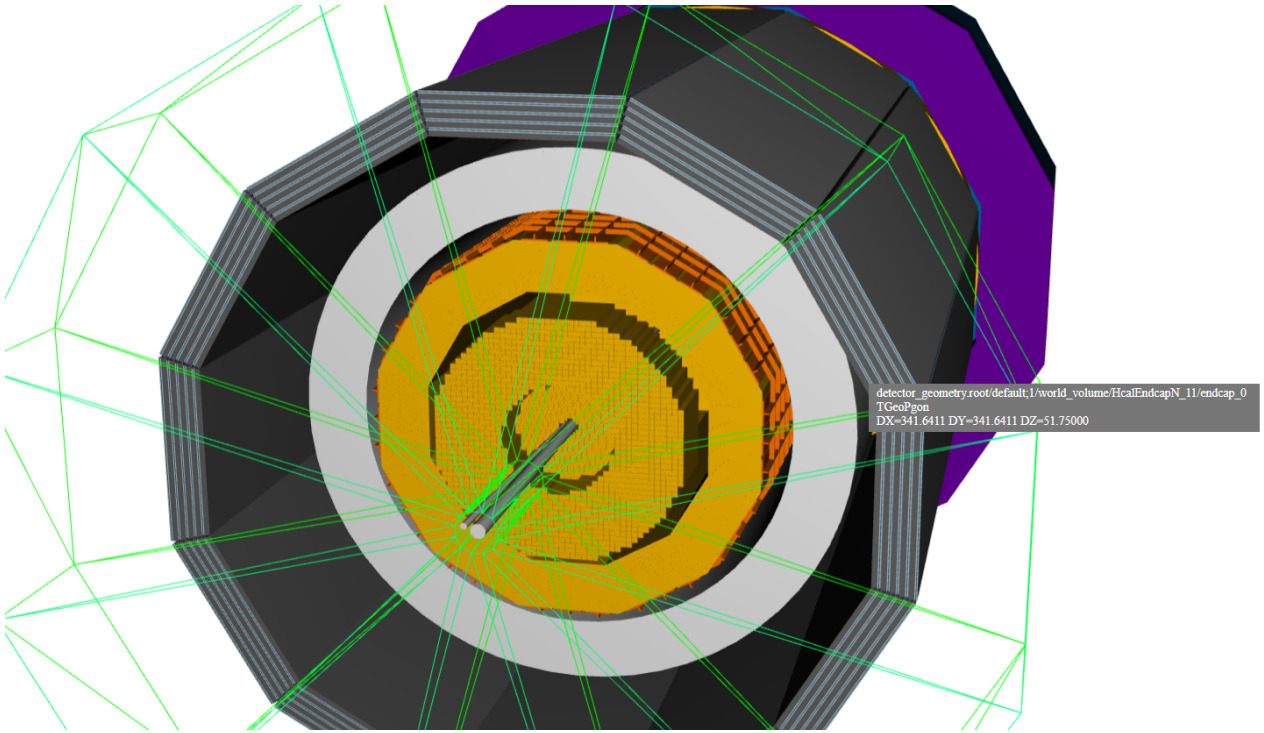

DD4hep - main idea

- Separate detector description from their interpretation
- Compact detector description is contained in .xml file
- Interpretation is done by detector constructors
- Logical detector structure separated from placements
  - Can create one detector element with a given shape
  - Make multiple placements to replicate it

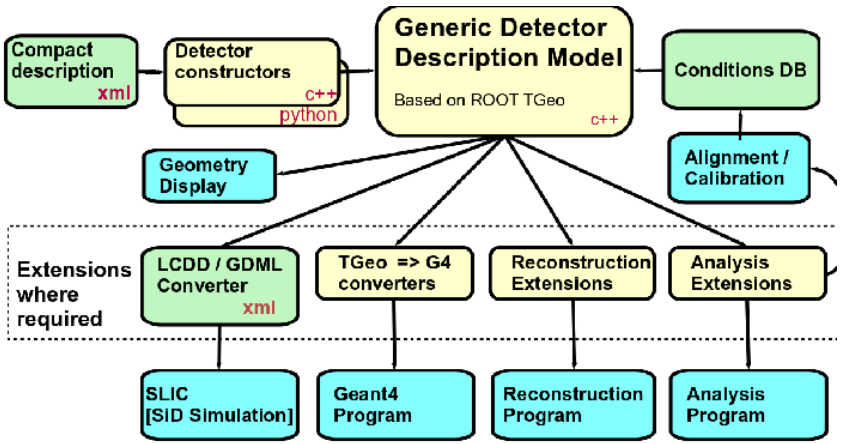

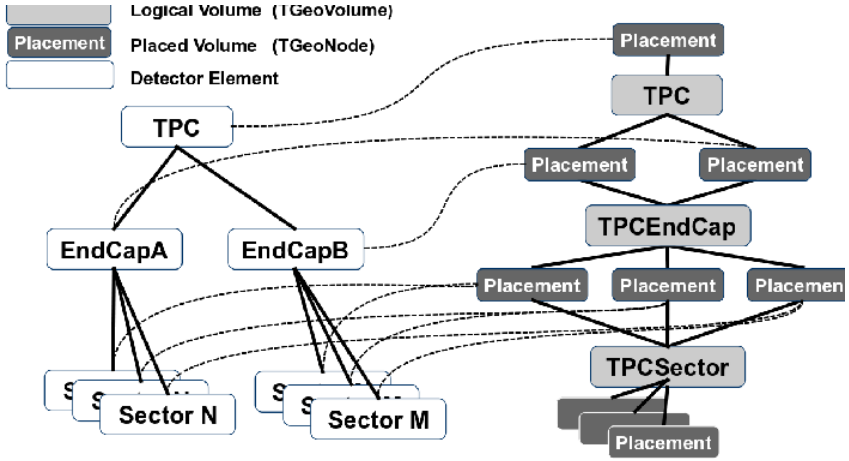

Compact detector description

- Describe and easily adjust the dimensions of detector elements (shapes)
- Set sensitive volumes (also with a fine segmentation)
- Each placed volume is identified by a 64 bit CellID
- Hits are assigned CellID based on the volume and segment in which they are located

Listing: XML compact detector description

```
<detector id="2" name="GEMTracker" vis="RedVis" type="my_GEMTracker" readout="GEMTrackerHits" >
   <layer id="1" z="-100 *cm" inner_r="40*cm" outer_r="120*cm" phi0_offset="0.0*deg" />
   <layer id="2" z="-80 *cm" inner_r="30*cm" outer_r="90*cm" phi0_offset="0.0*deg" />
   <layer id="3" z="-60 *cm" inner_r="20*cm" outer_r="70*cm" phi0_offset="0.0*deg" />
   <layer id="4" z="-40 *cm" inner_r="10*cm" outer_r="20.0*cm" phi0_offset="0.0*deg" />
   <layer id="5" z=" 40 *cm" inner_r="10*cm" outer_r="20.0*cm" phi0_offset="0.0*deg" />
   <layer id="6" z=" 60 *cm" inner_r="25*cm" outer_r="70.0*cm" phi0_offset="0.0*deg" />
   <layer id="7" z=" 80 *cm" inner_r="30*cm" outer_r="90.0*cm" phi0_offset="0.0*deg" />
   <layer id="8" z="100 *cm" inner_r="40*cm" outer_r="100.0*cm" phi0_offset="0.0*deg" />
</detector>

  <readouts>
    <readout name="GEMTrackerHits">
      <segmentation type="CartesianGridXY" grid_size_x="1*cm" grid_size_y="3*cm" />
      <id>system:8,barrel:2,layer:4,module:12,sensor:2,x:32:-16,y:-16</id>
      <!--
      <segmentation type="PolarGridRPhi" grid_size_phi="3.0*degree" grid_size_r="5.0*cm"/>
      <id>system:5,barrel:3,layer:4,module:5,r:32:-16,phi:-16</id>
      -->
    </readout>
  </readouts>
```

Detector constructor

- Interprets the geometry description from .xml file and constructs the detector

Listing: Detector constructor

```
sens.setType("tracker");
  string module_name = "GEM";

  double thickness = 0.01*dd4hep::cm;

  int N_layers = 0;

  for(xml_coll_t lay( x_det, _U(layer) ); lay; ++lay, ++N_layers) {

    xml_comp_t x_layer = lay;
    double inner_r = x_layer.attr<double>( _Unicode(inner_r) ) ;
    double outer_r = x_layer.attr<double>( _Unicode(outer_r) ) ;
    double phi0_offset = x_layer.attr<double>( _Unicode(phi0_offset) ) ;
    double z = x_layer.attr<double>( _Unicode(z) ) ;
    int layer_id = x_layer.id();//attr<double>( _Unicode(z) ) ;

    string layer_name = std::string("gem_layer") + std::to_string(layer_id) ;

    Tube gem_layer(inner_r, outer_r, thickness/2.0);
    Volume gem_layer_vol("gem_layer_vol", gem_layer, carbon);

    gem_layer_vol.setSensitiveDetector(sens);
    DetElement layer_DE( sdet, _toString(layer_id,"layer%d"), layer_id );

    pv = assembly.placeVolume( gem_layer_vol, Transform3D(RotationZ(phi0_offset),Position
          (0.0,0.0,z)) );
    pv.addPhysVolID( "layer", layer_id );
    layer_DE.setPlacement(pv);
```

GEM tracker - example tutorial

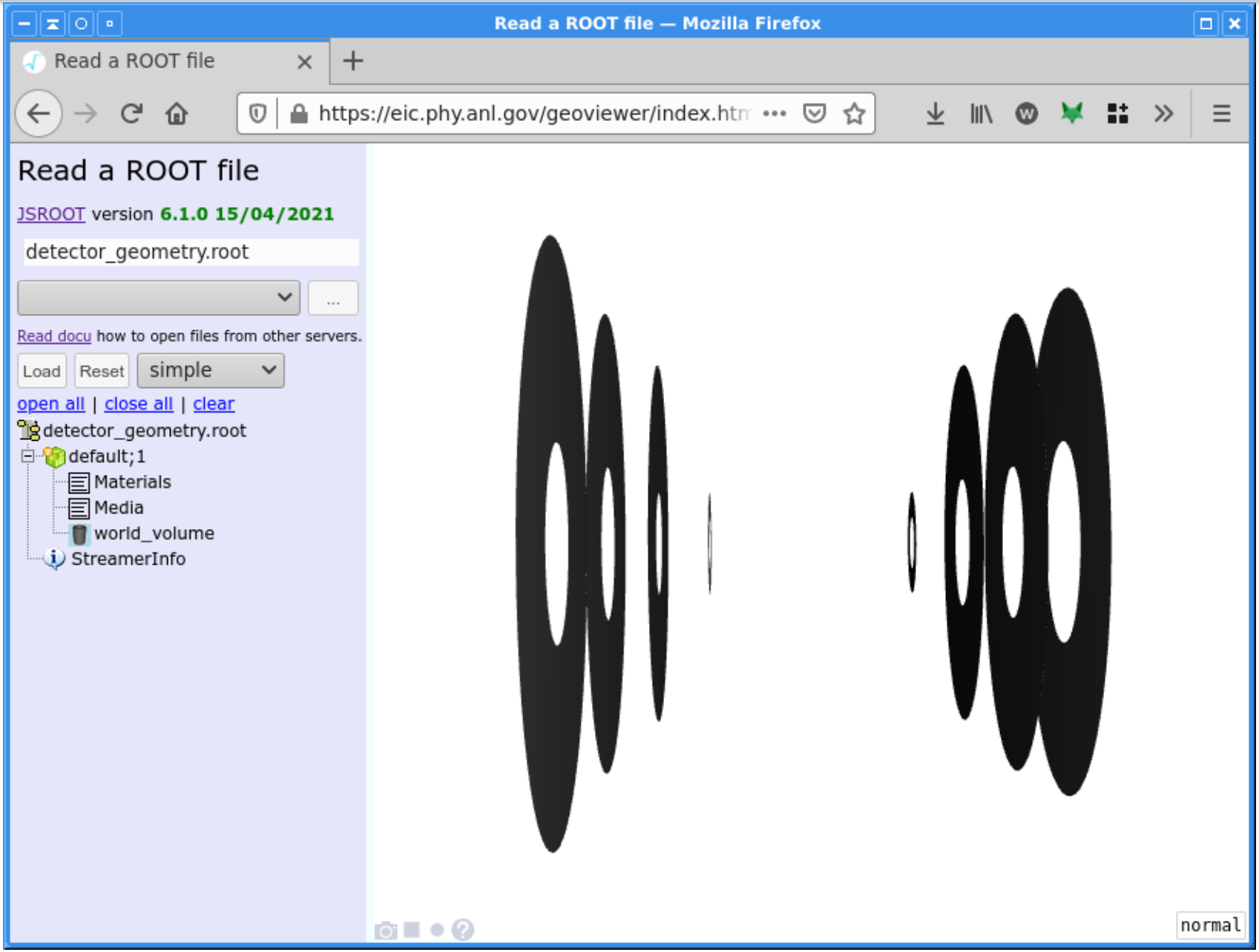

https://eic.phy.anl.gov/tutorials/eic_tutorial/

Reconstruction in ATHENA

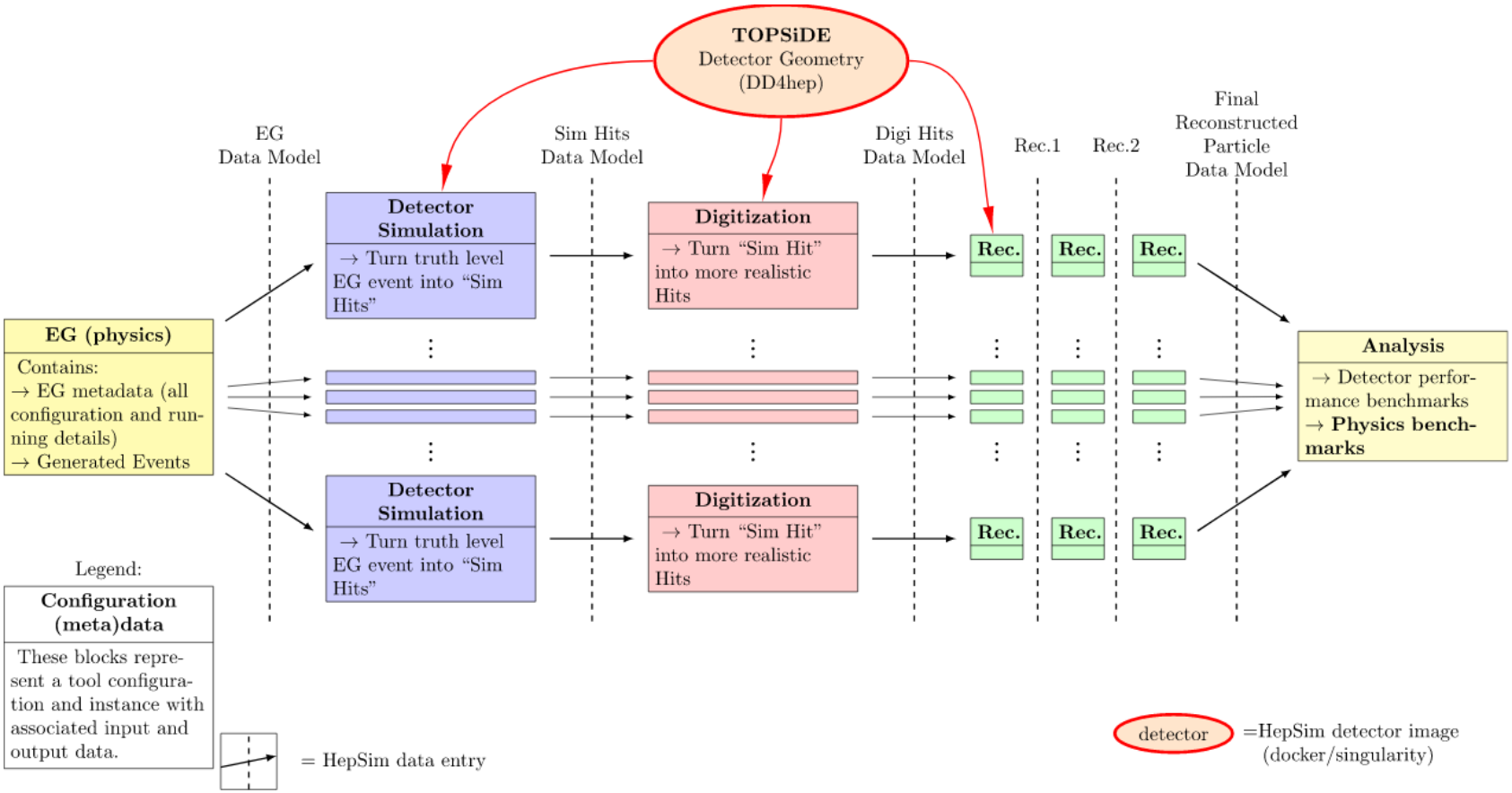

Reconstruction in ATHENA

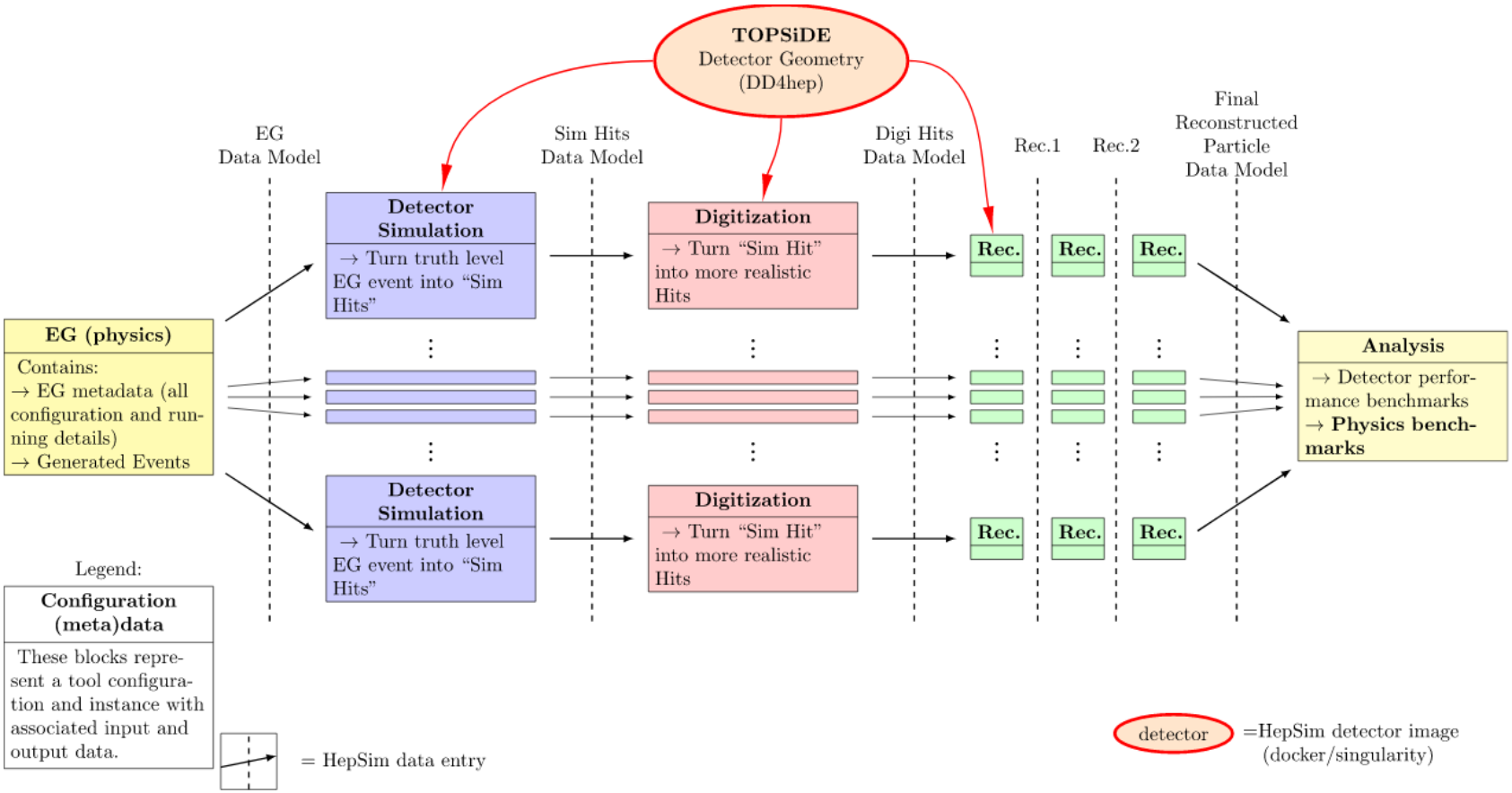

Hadronic showers

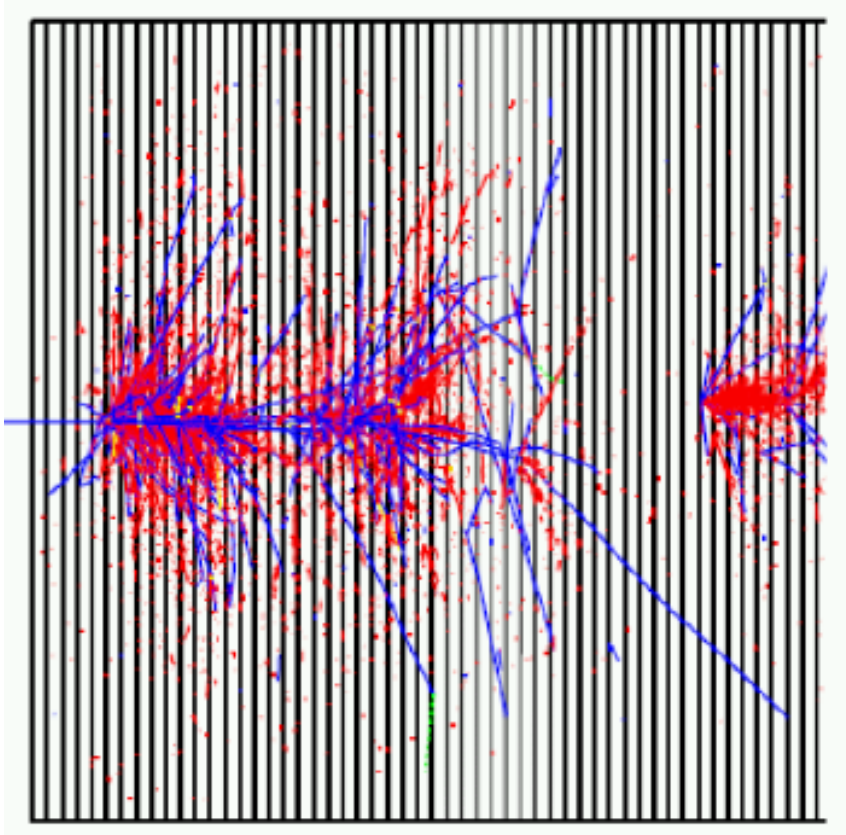

blue = hadronic component

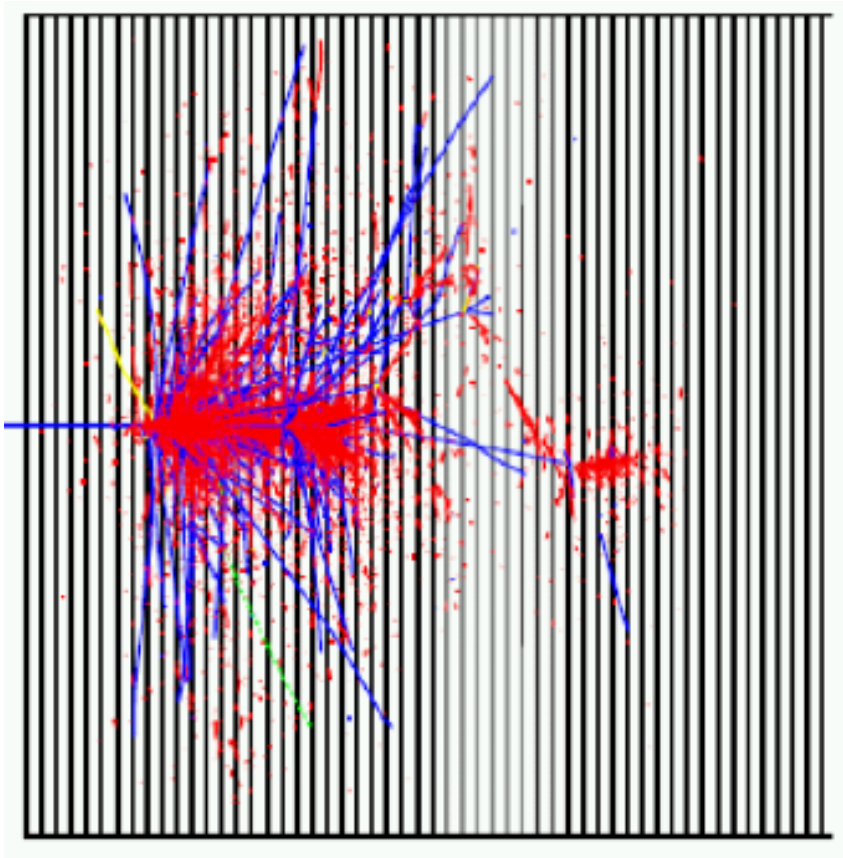

red = electromagnetic component

Energy is converted partially into hadronic component and partially into electromagnetic

$\lambda_{int} \propto A^{1/3}$ - nuclear interaction length
$X_o \propto \frac{A}{Z^2}$ - radiation length

Hadronic showers

Hadronic interaction:

Elastic:

$$p + \text{Nucleus} \rightarrow p + \text{Nucleus}$$

Inelastic:

$$p + \text{Nucleus} \rightarrow \pi^+ + \pi^- + \pi^0 + \ldots + \text{Nucleus}^*$$

$$\left[\begin{array}{l} \text{Nucleus}^* \rightarrow \text{Nucleus A} + n, p, \alpha, \ldots \\ \qquad\quad \rightarrow \text{Nucleus B} + 5p, n, \pi, \ldots \\ \qquad\quad \rightarrow \text{Nuclear fission} \end{array}\right.$$

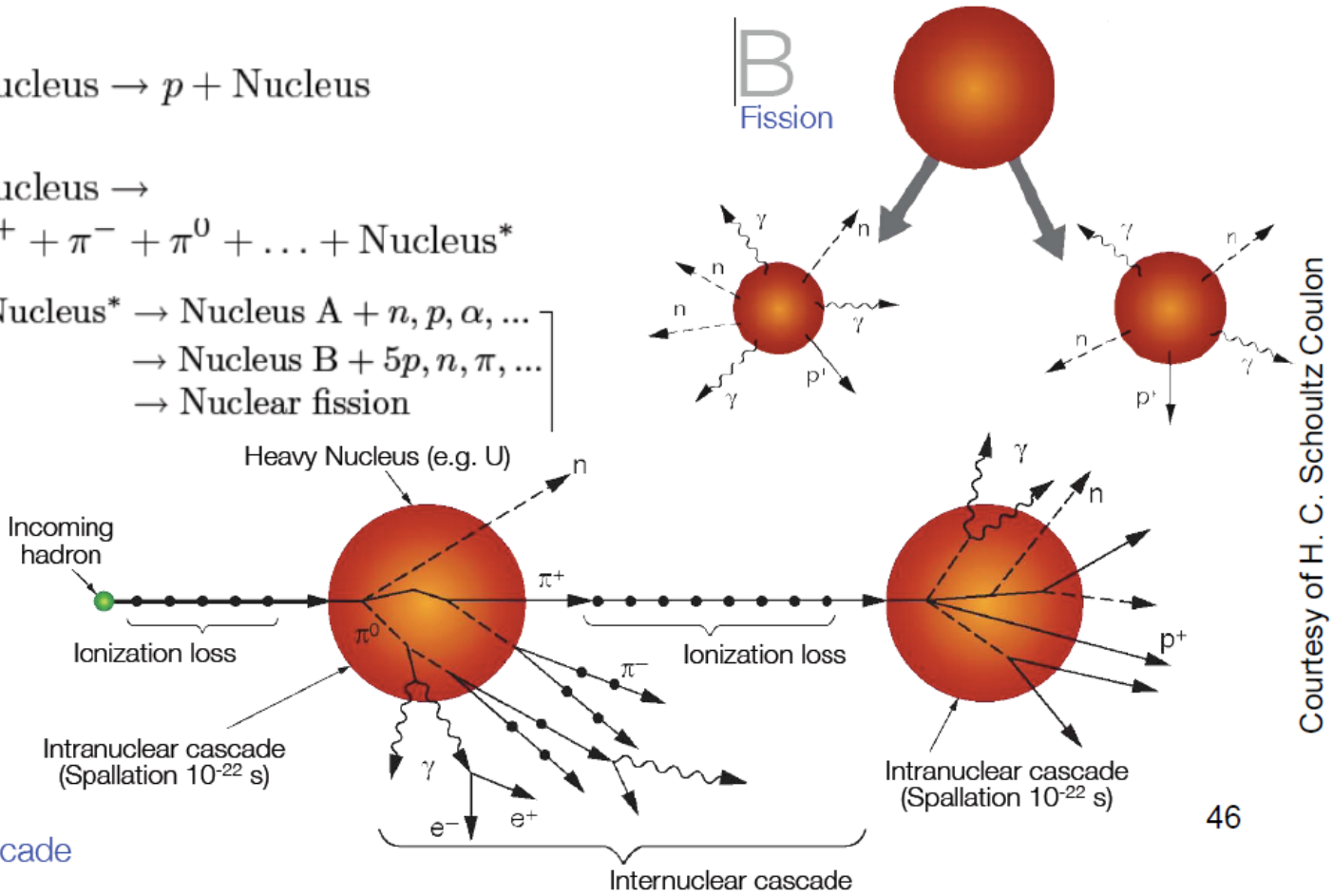

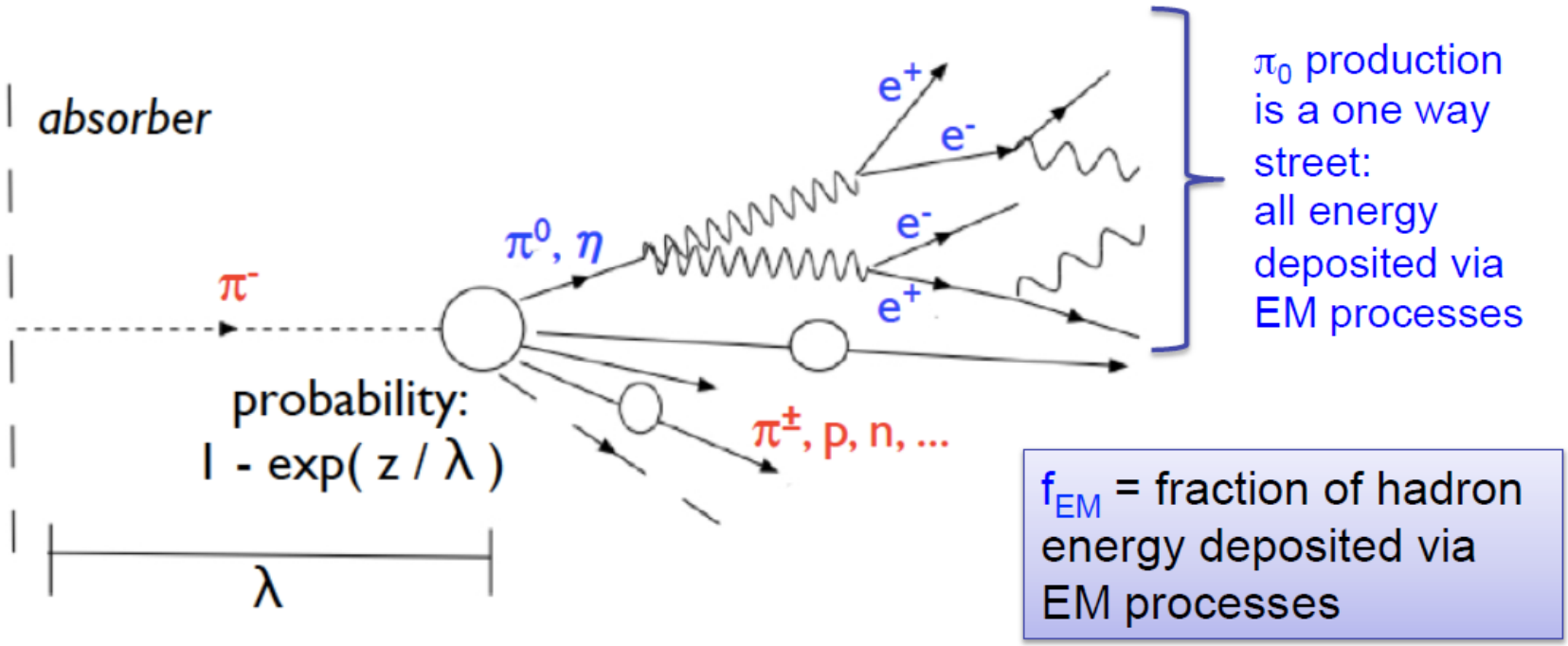

- Electromagnetic:
  - ionization, excitation: $e^{+/-}$
  - photo effect, scattering: γ
- Hadronic:
  - ionization: $\pi^{+/-}$, p
  - invisible energy: binding, recoil

Response to a pion shower:

$$\pi = f_{em}e + (1 - f_{em})h$$

e - response to the electromagnetic component
h - response to the hadronic component

$\frac{e}{h}$: not directly measurable, gives the degree of non-compensation $\frac{e}{\pi}$: ratio of response between electron-induced and pion-induced shower

$$\frac{e}{\pi} = \frac{e}{f_{em}e+(1-f_{em})h} = \frac{e}{h}\frac{1}{1+f_{em}(e/h-1)h}$$

$\frac{e}{h}$ is energy independent $\frac{e}{\pi}$ depends on E via $f_{em}(E)$ - non-linearity

Approaches to achieve compensation:

- $\frac{e}{h} \to 1$ right choice of materials
- $f_{em} \to 1$ - high energy limit

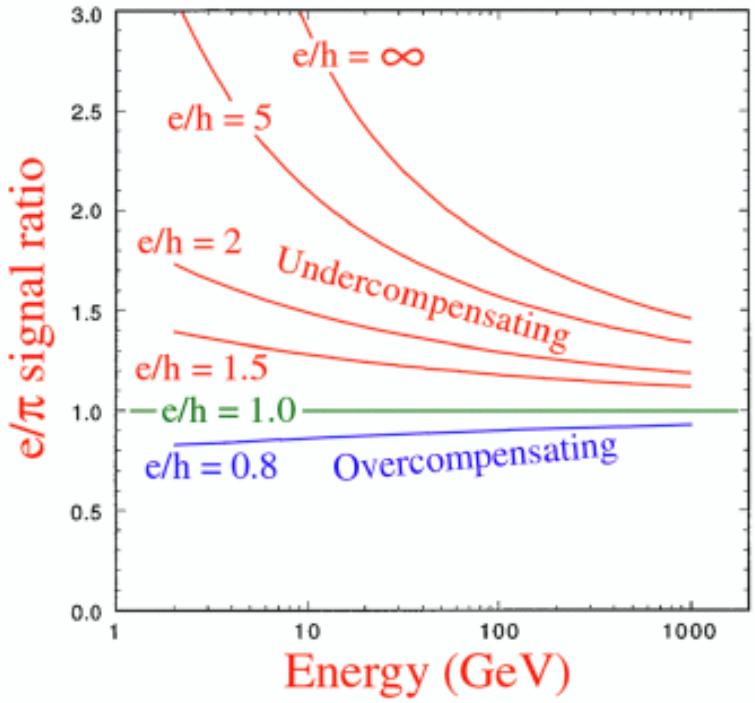

Built a tail-catcher Barrel Hadronic Calorimeter (BHCal) Reuse scintillator tiles from STAR Barrel Electromagnetic Calorimeter (BEMC)

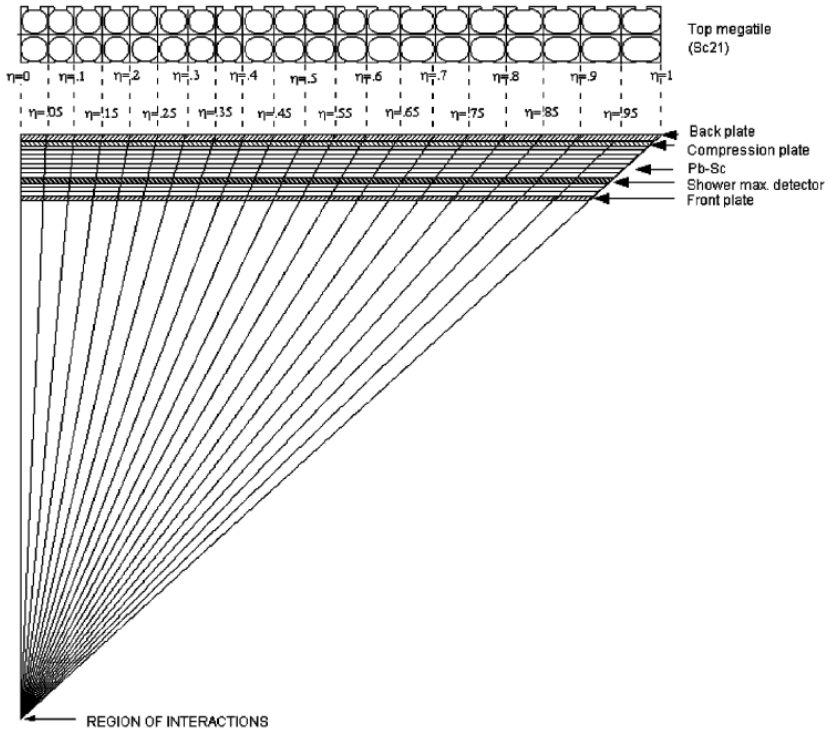

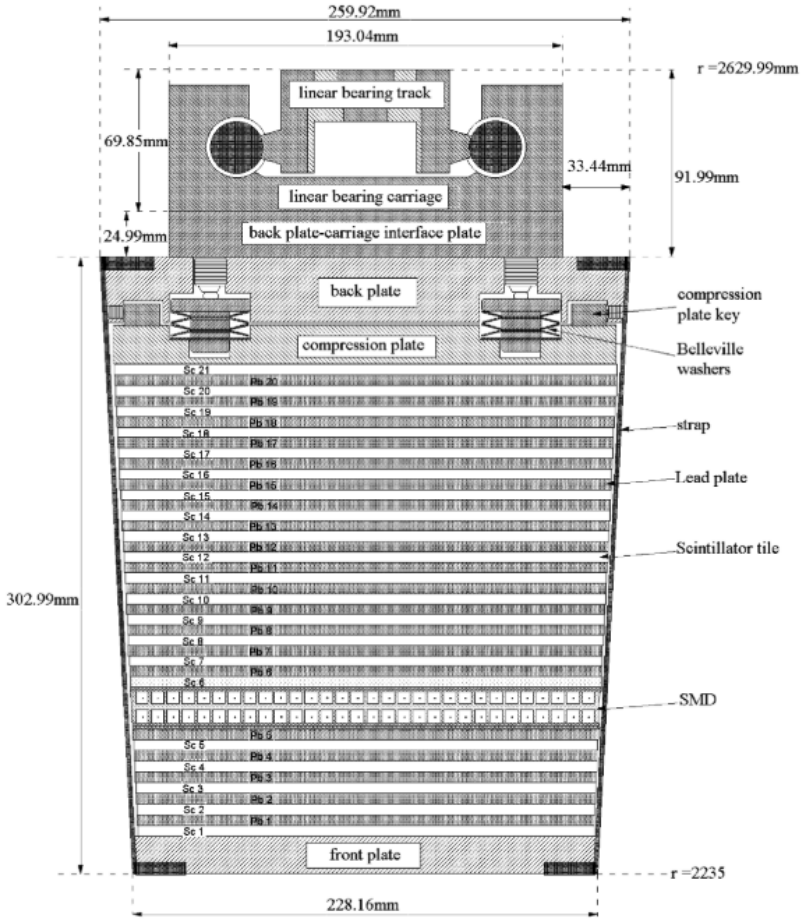

Updated BHCal geometry - 60 modules

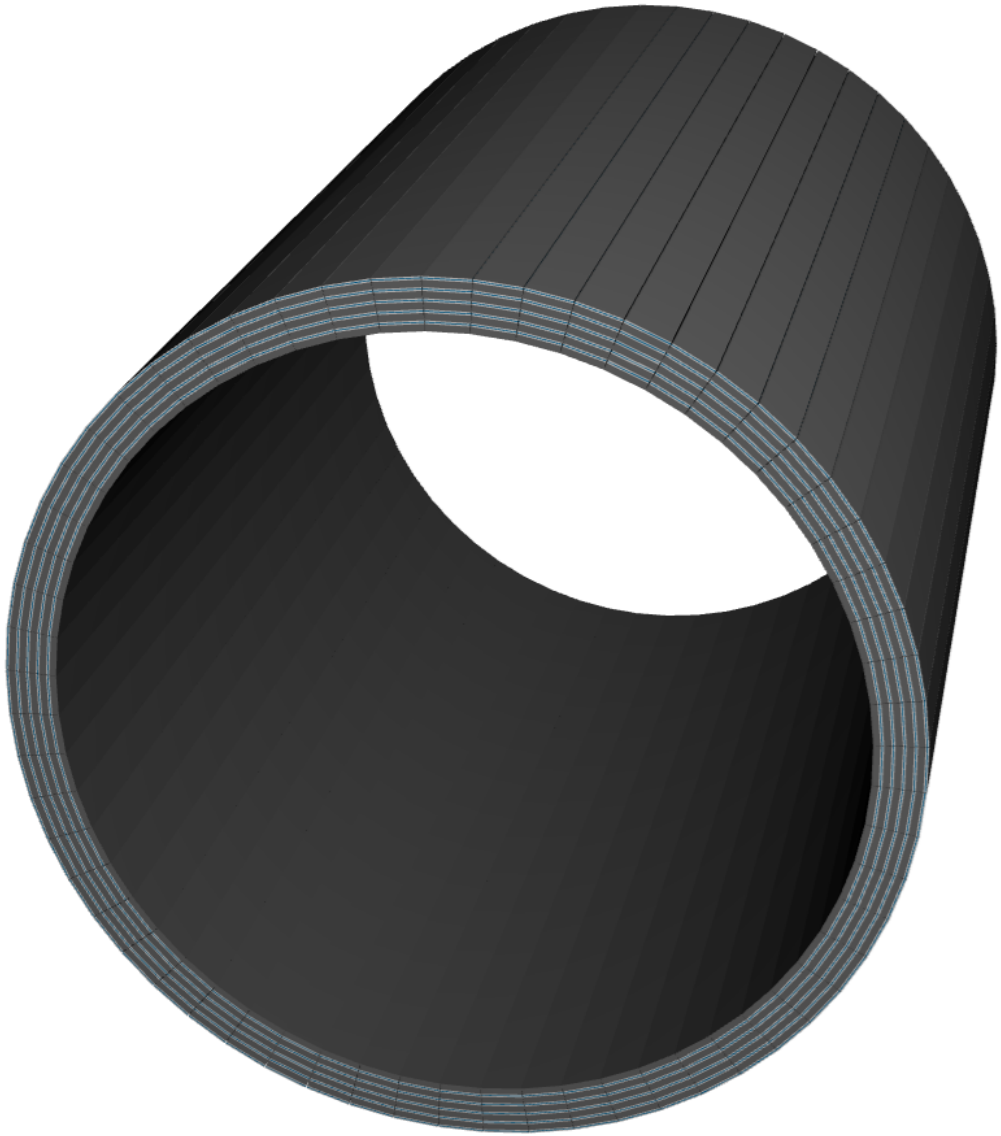

- Updated geometry to 60 modules - to match STAR BEMC modules

Updated BHCal geometry - tiles

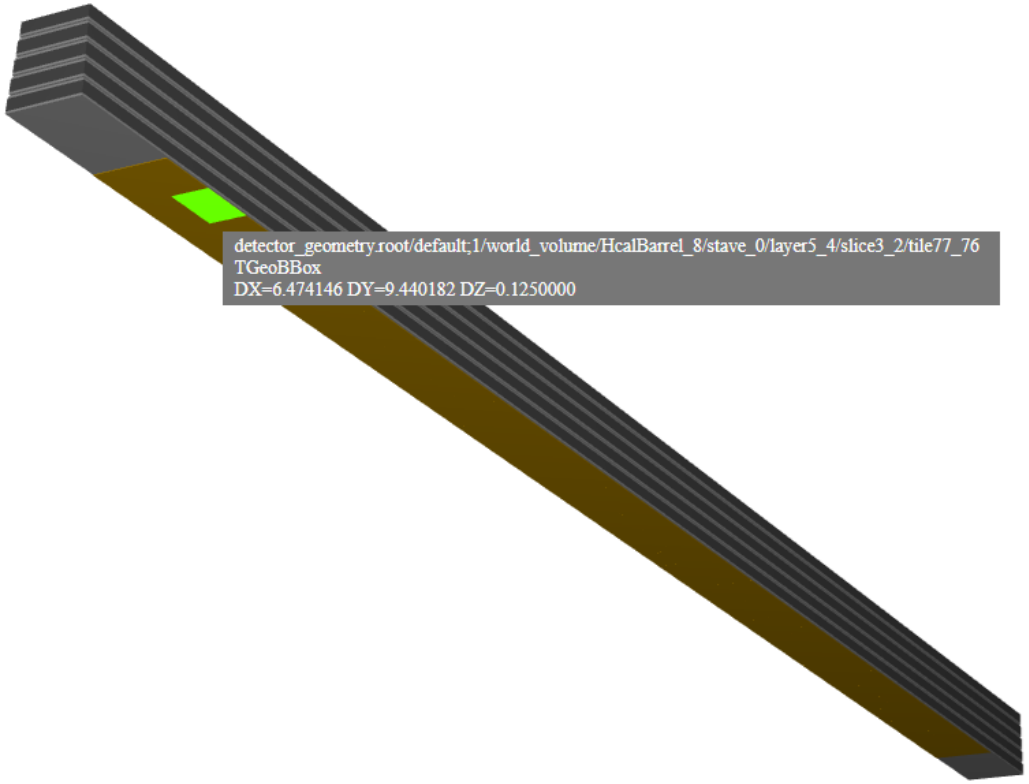

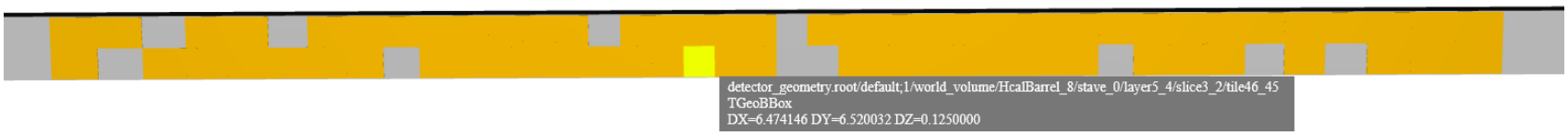

- Implemented 5 layers with:
  - 4 cm steel (dark gray)
  - 0.75 cm air (light gray)
  - 0.5 cm polystyrene tiles 0.05×0.05 $\eta \times \phi$ (dark gold)
  - 0.75 cm air (light gray)

MC particles: neutrons eta,phi

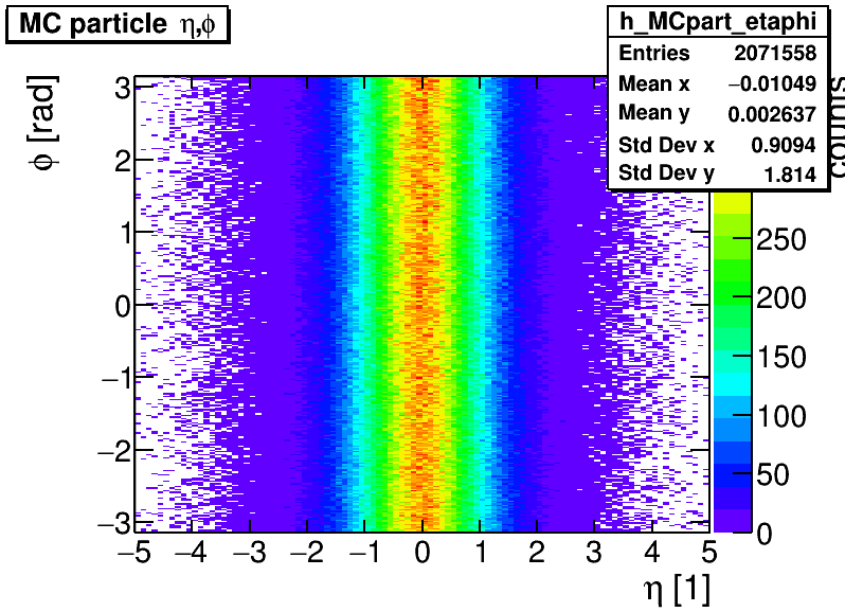

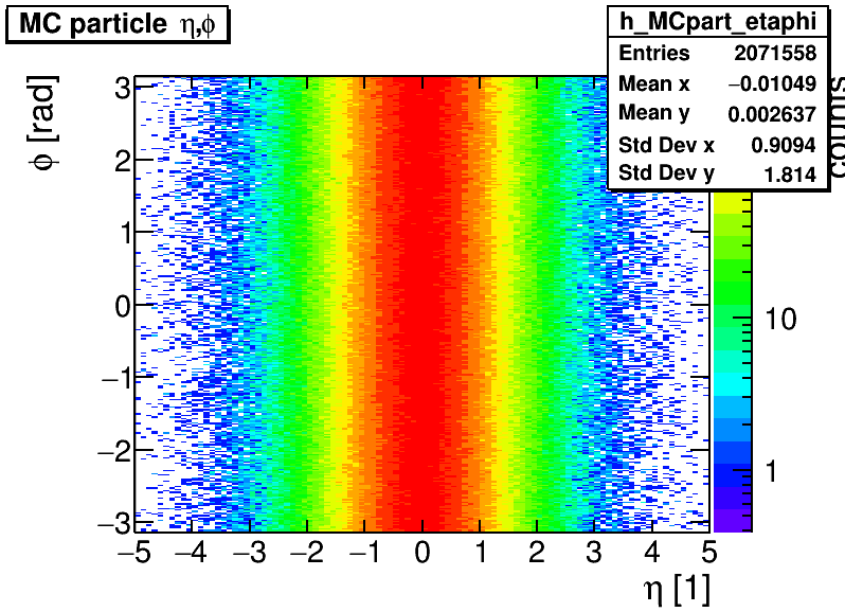

MC particles: protons eta,phi

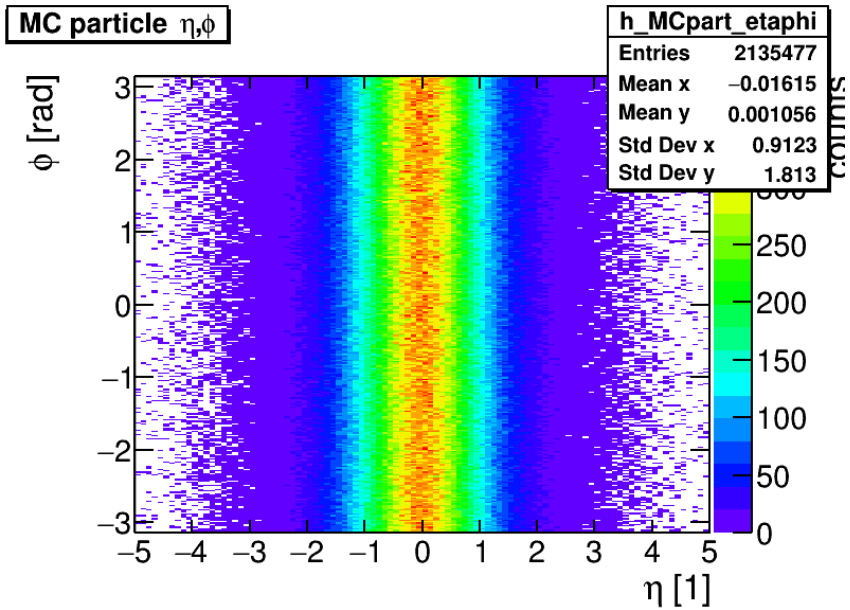

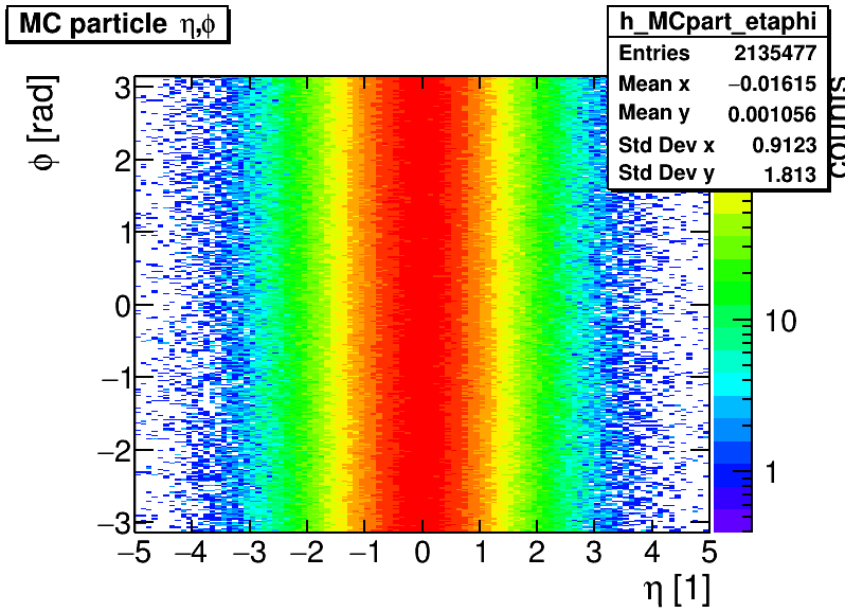

MC particles: pions eta,phi

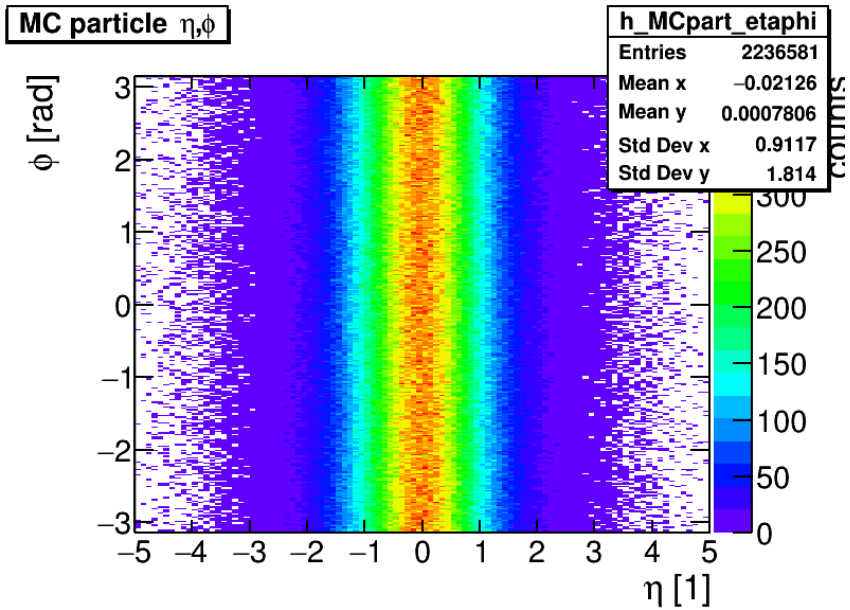

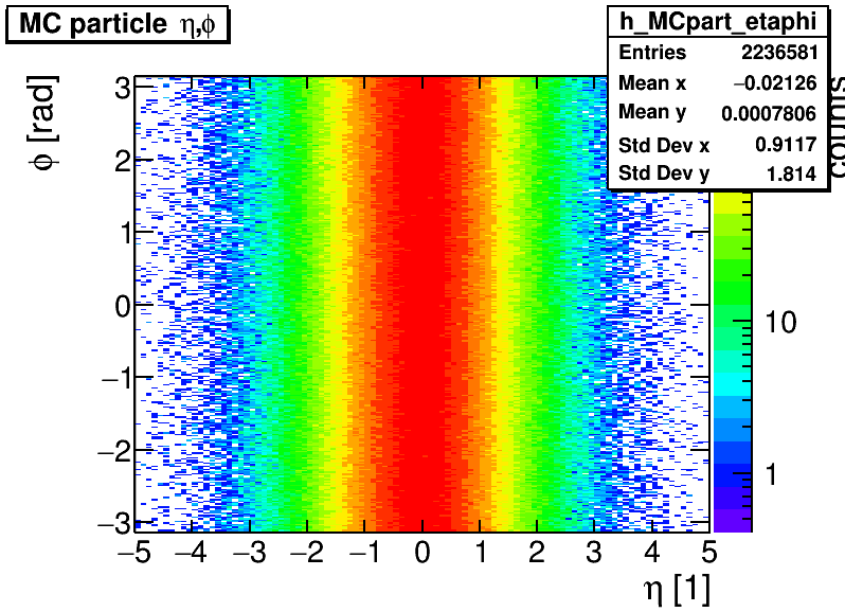

Generated MC particles: neutrons eta,phi

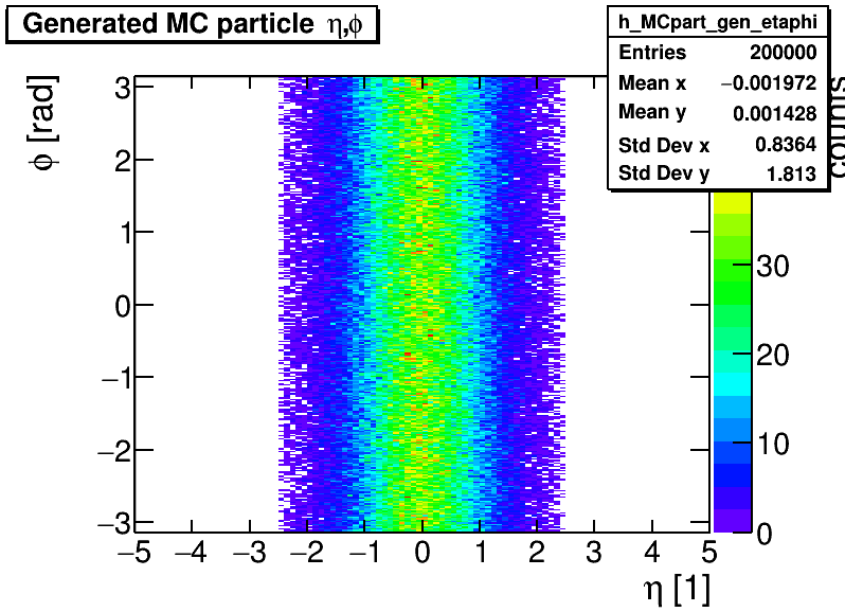

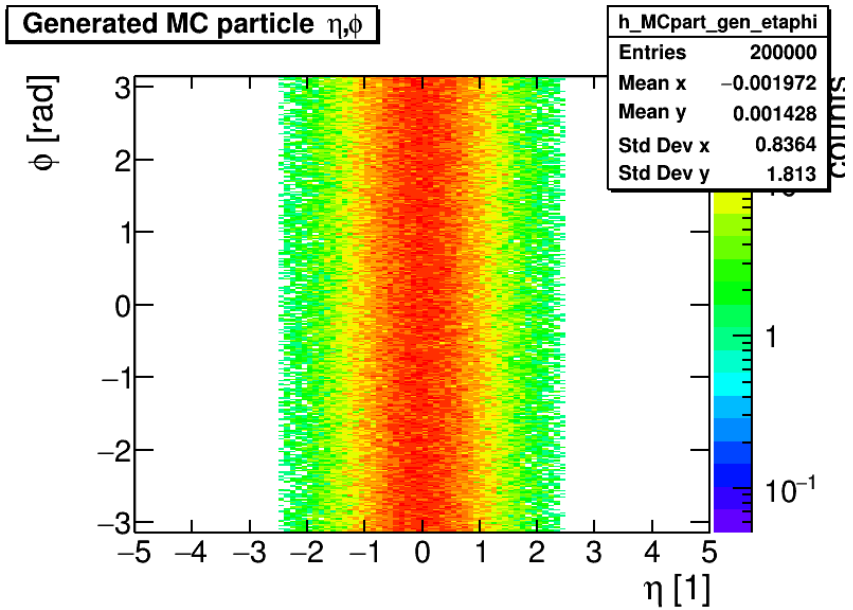

- Generated particles are the original neutrons

Generated MC particles: protons eta,phi

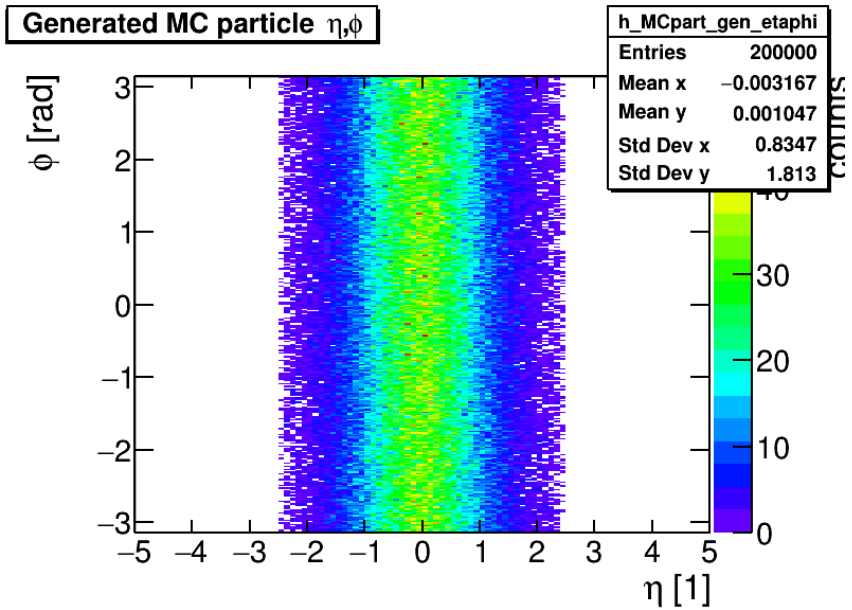

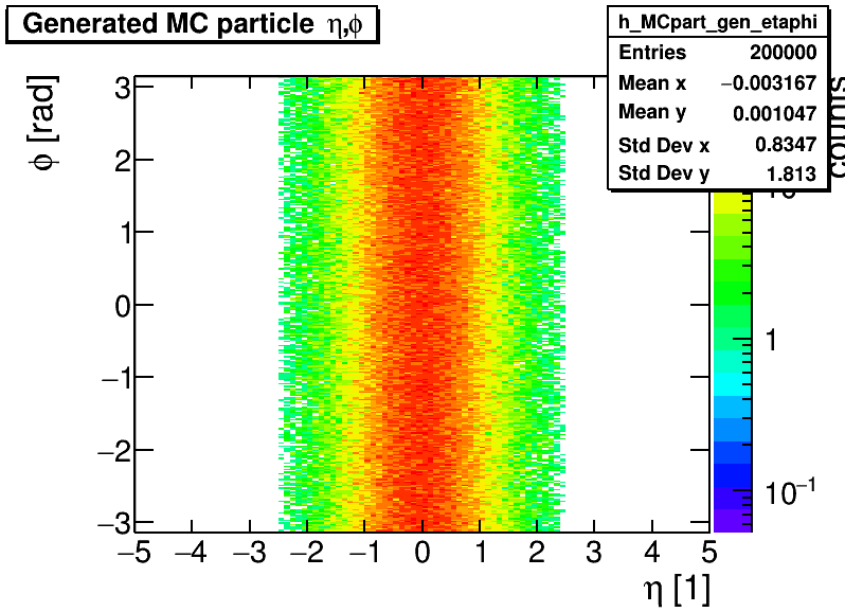

- Generated particles are the original protons

Generated MC particles: pions eta,phi

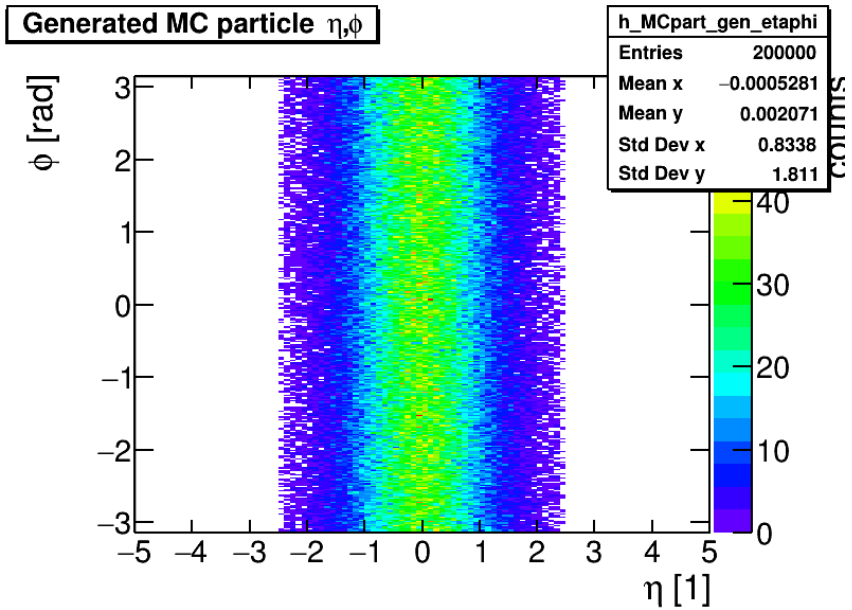

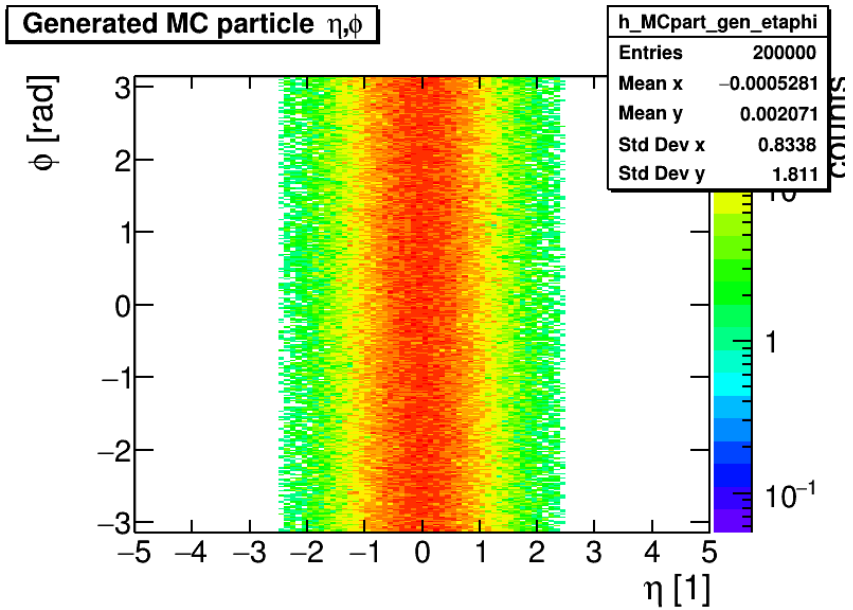

- Generated particles are the original pions

MC particles: neutrons momentum

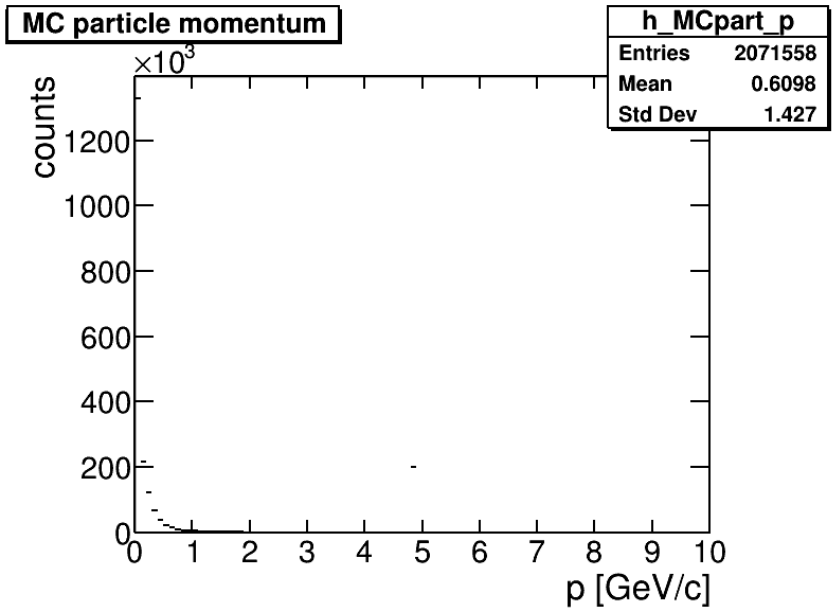

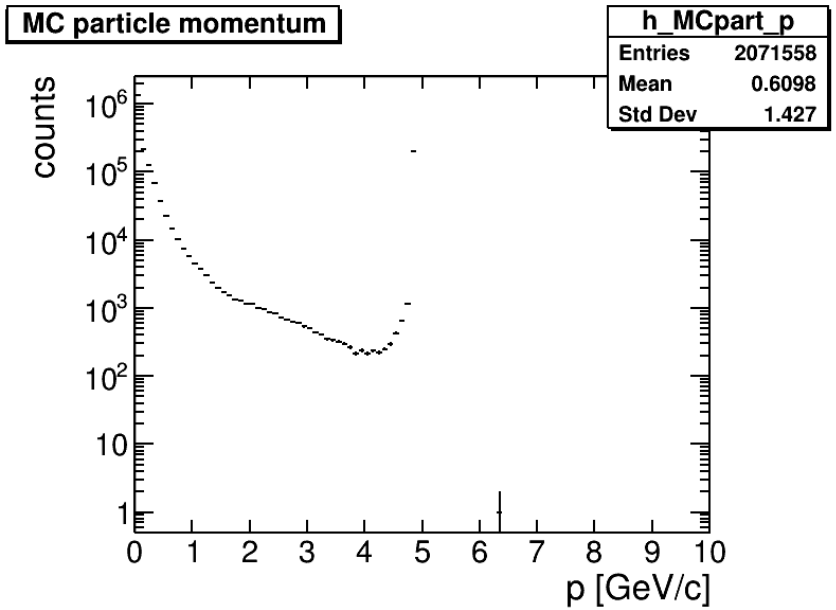

- Peak for monoenergetic generated particles+secondaries

MC particles: protons momentum

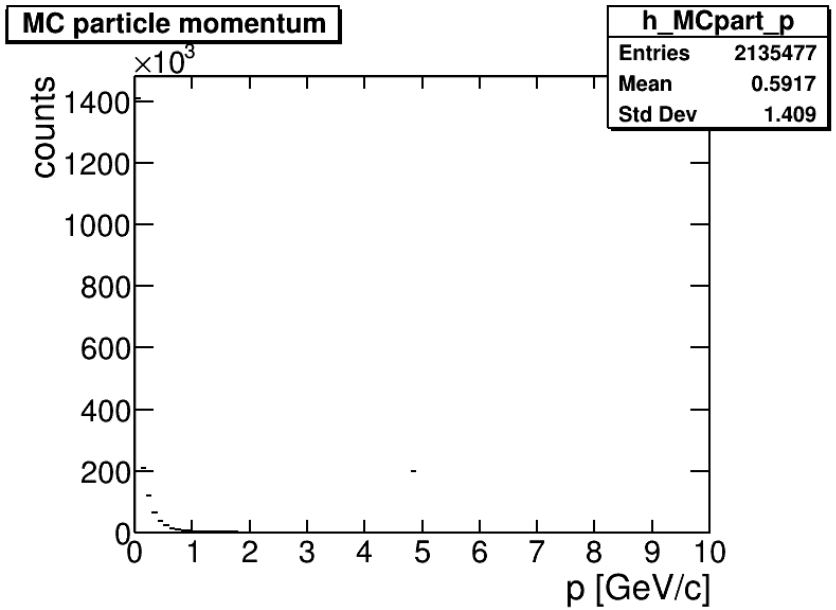

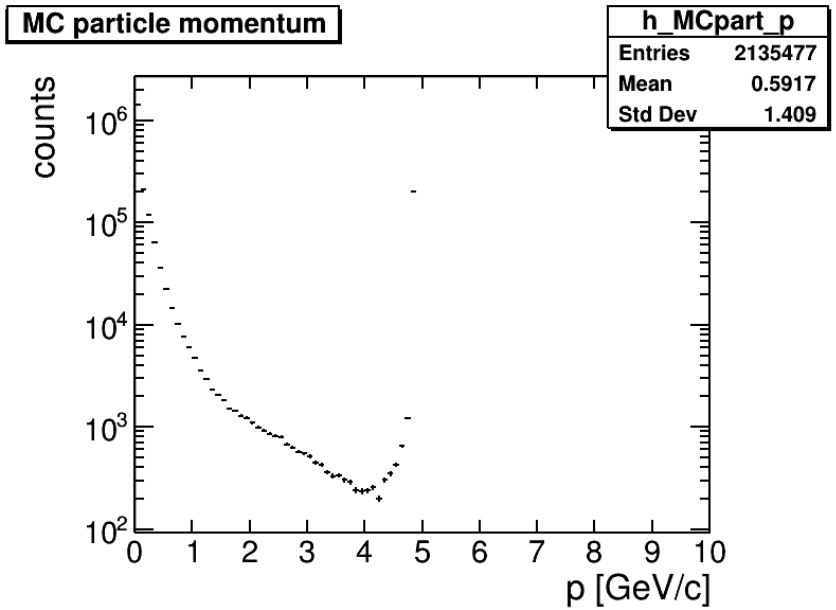

- Peak for monoenergetic generated particles+secondaries

MC particles: pions momentum

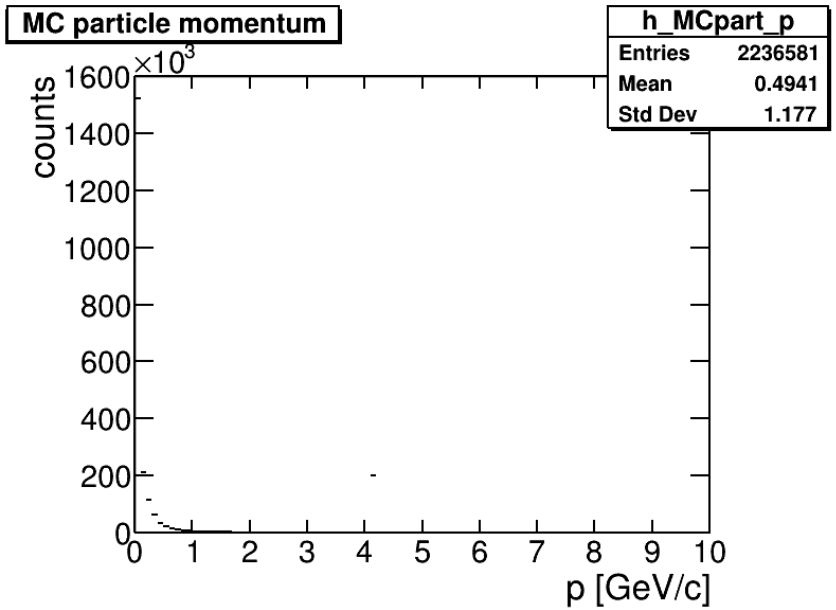

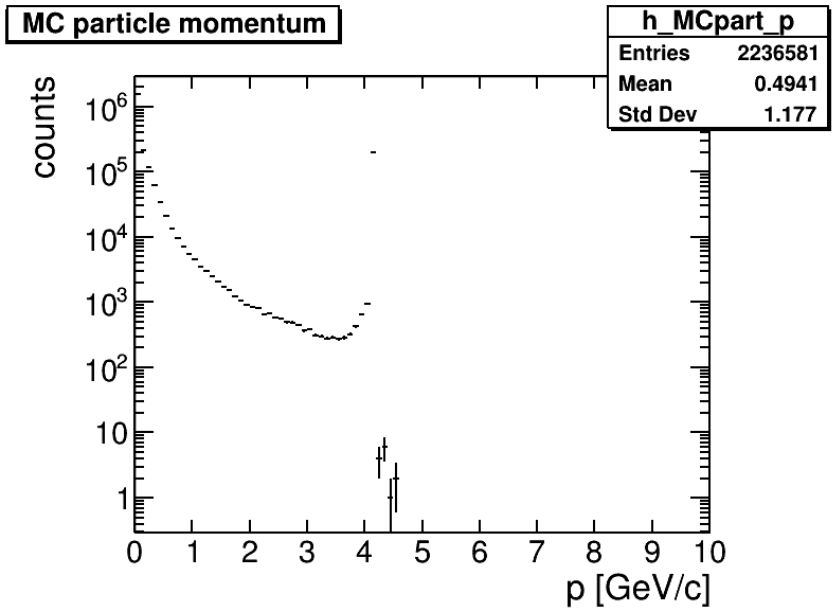

- Peak for monoenergetic generated particles+secondaries

Generated MC particles: neutrons endpoint

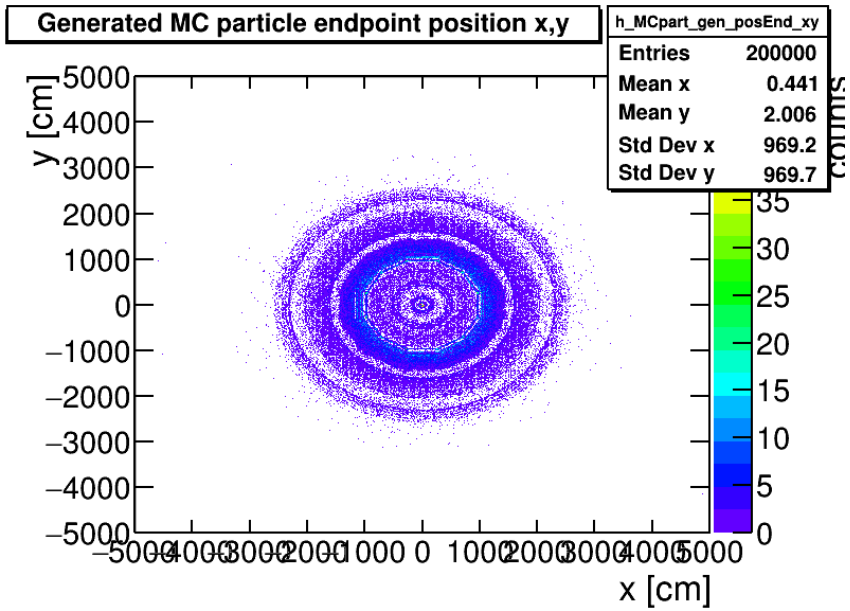

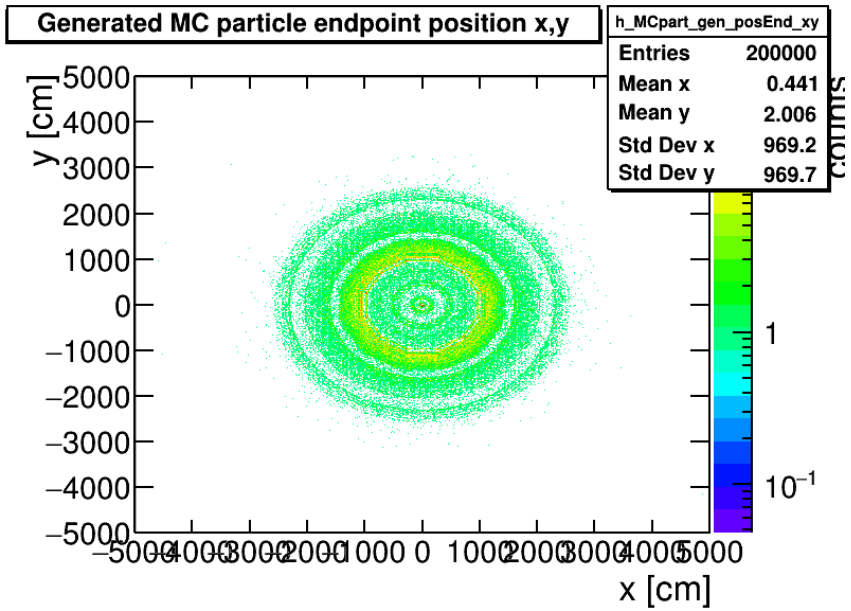

Generated MC particles: protons endpoint

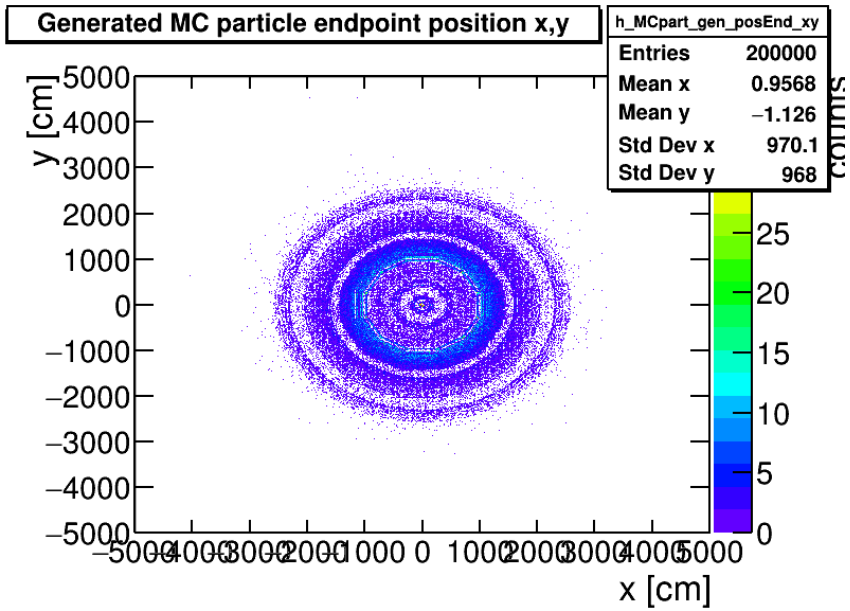

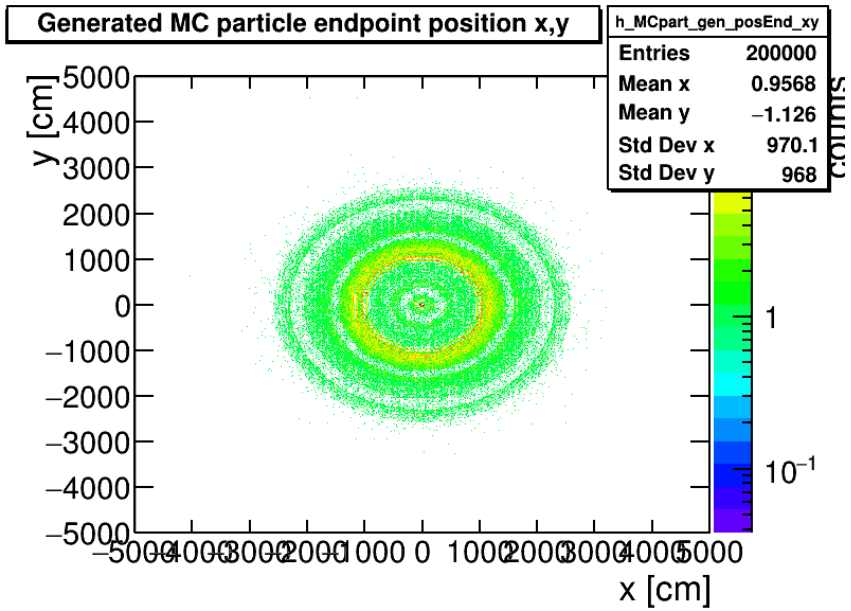

Generated MC particles: pions endpoint

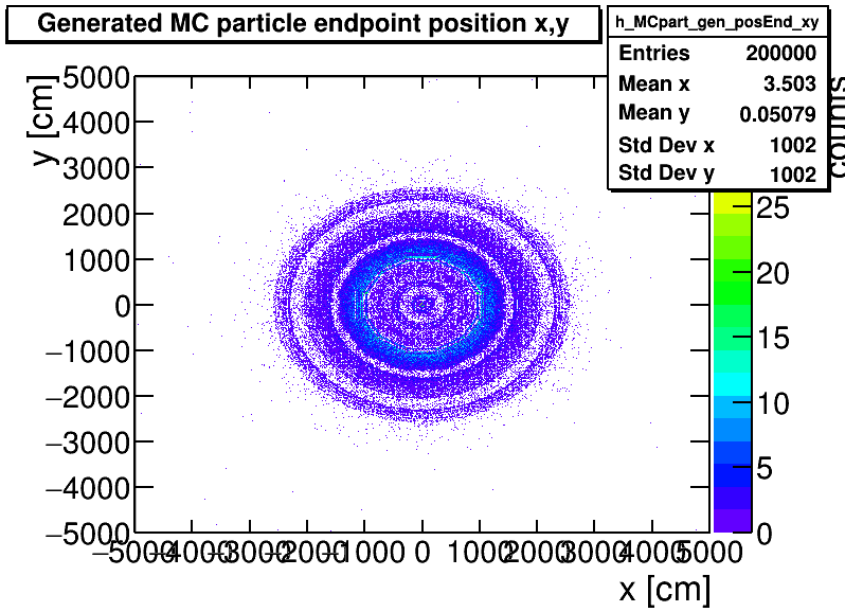

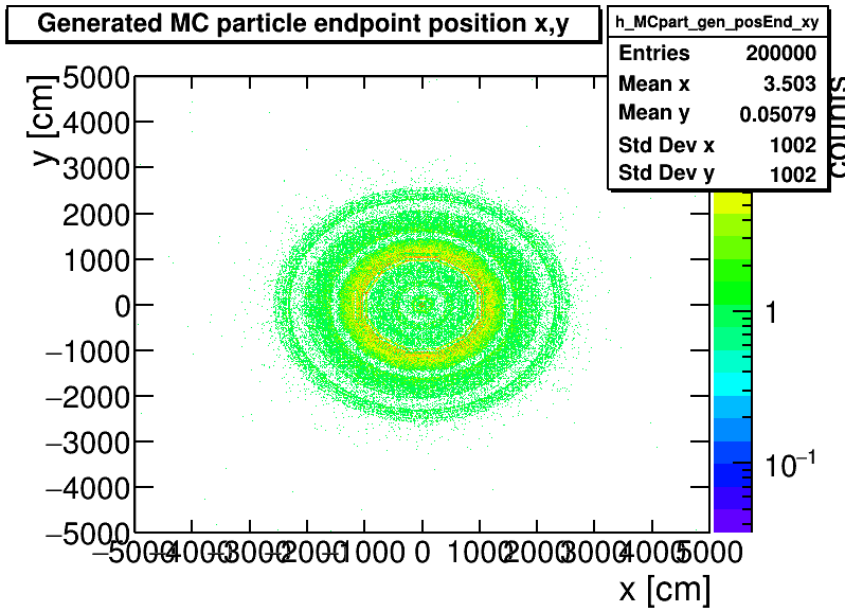

Generated MC particles daughters: neutrons endpoint

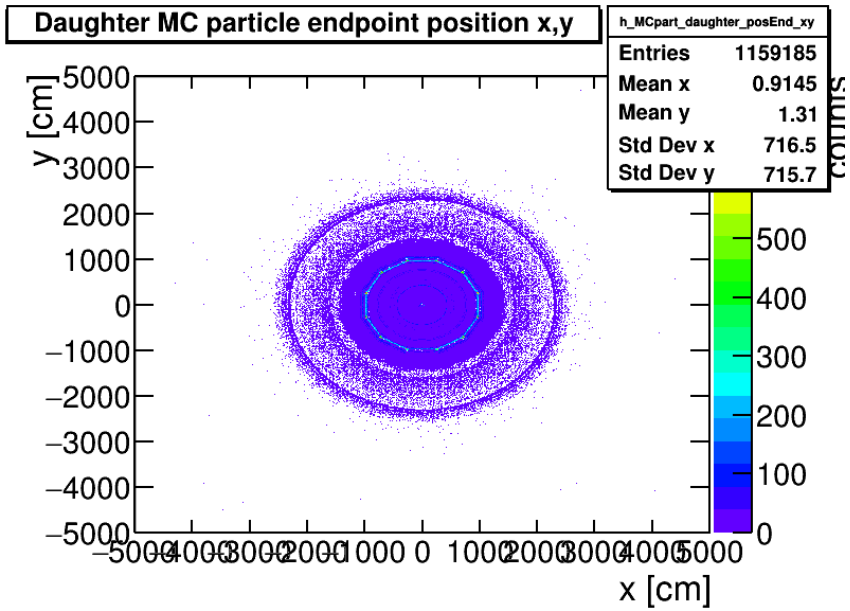

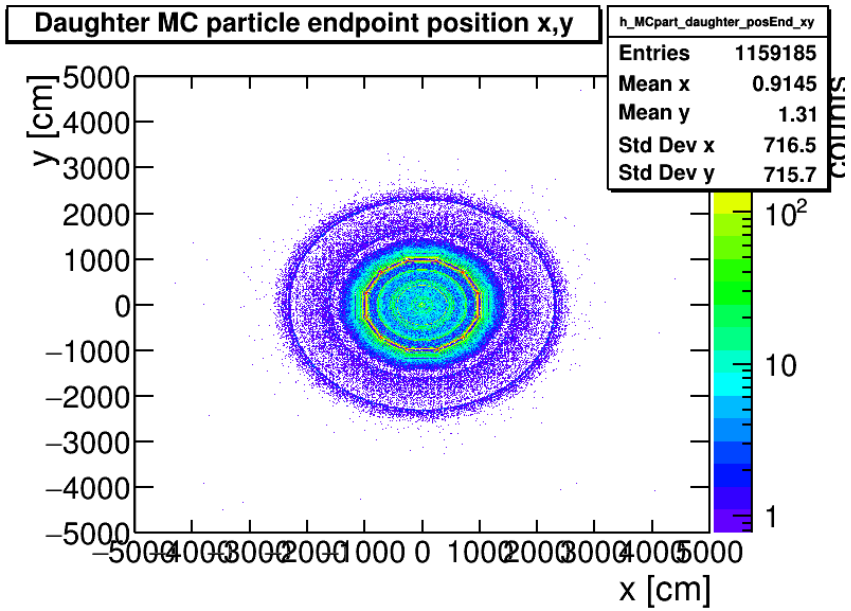

Generated MC particles daughters: protons endpoint

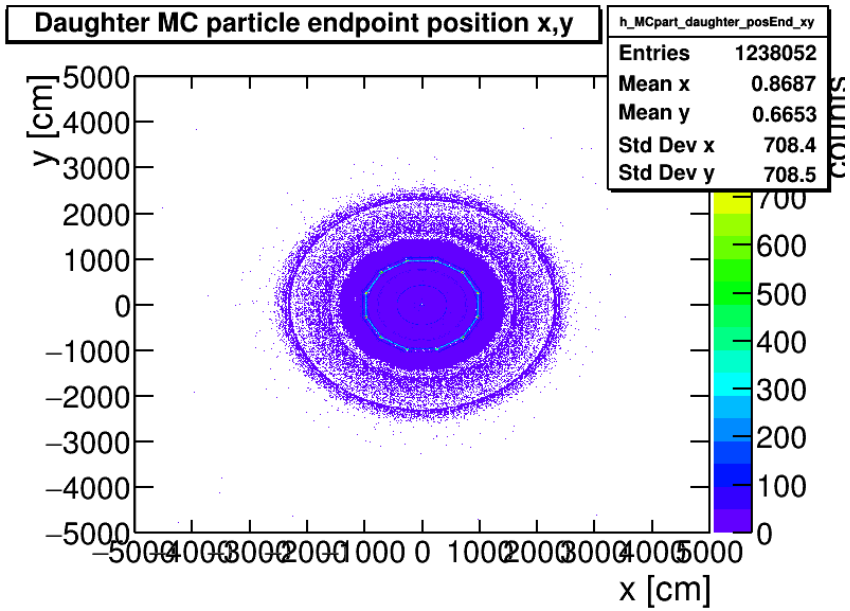

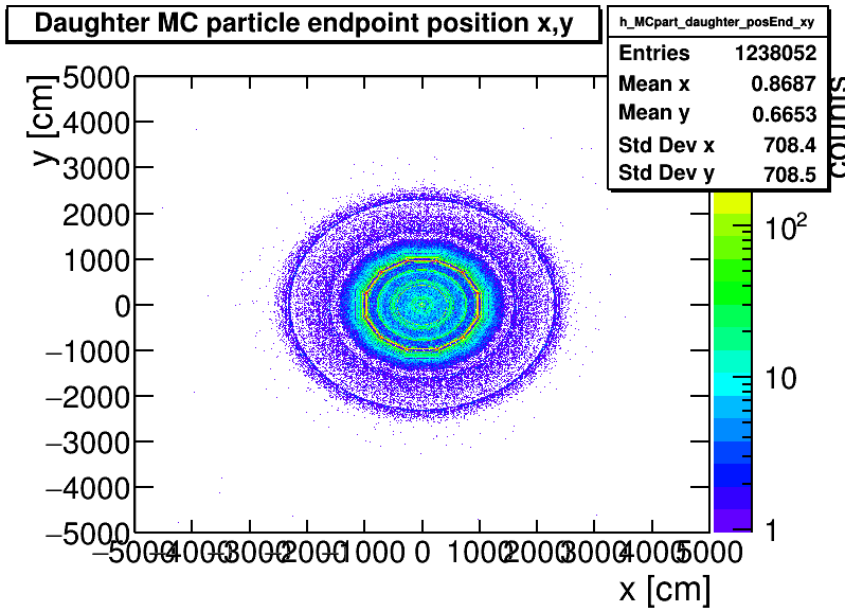

Generated MC particles daughters: pions endpoint

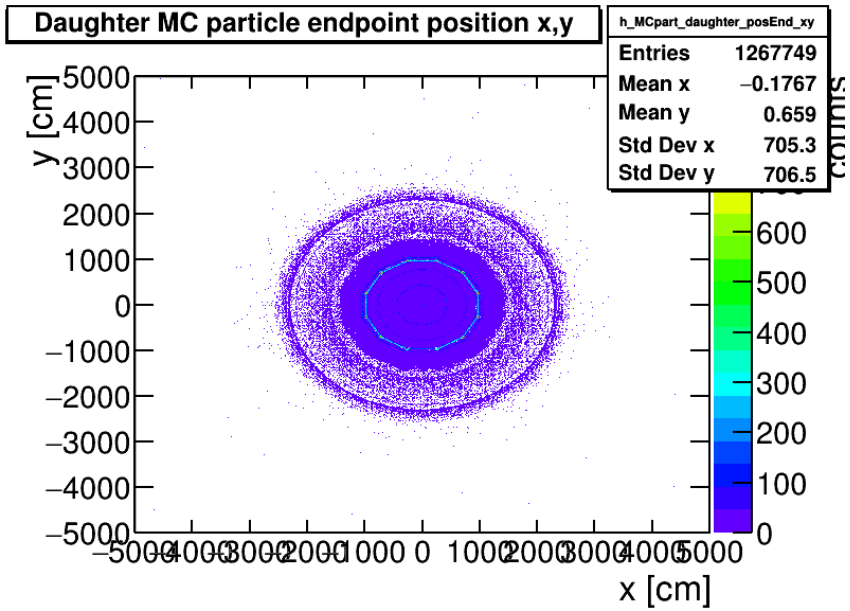

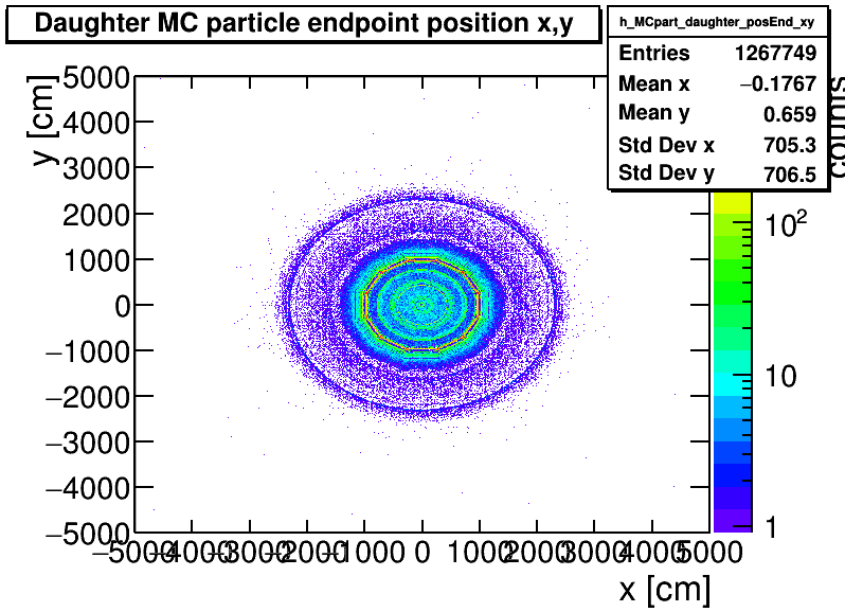

Generated MC particles: daughters

neutrons

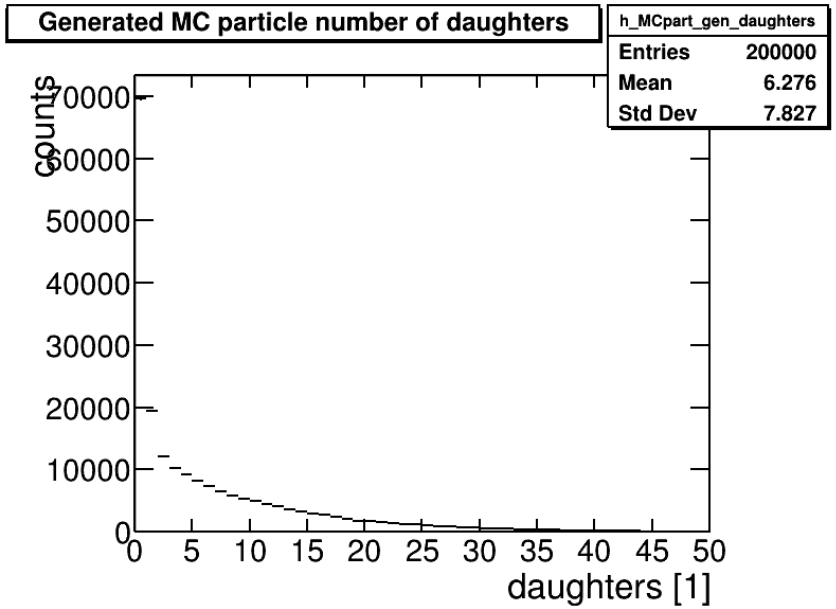

pions

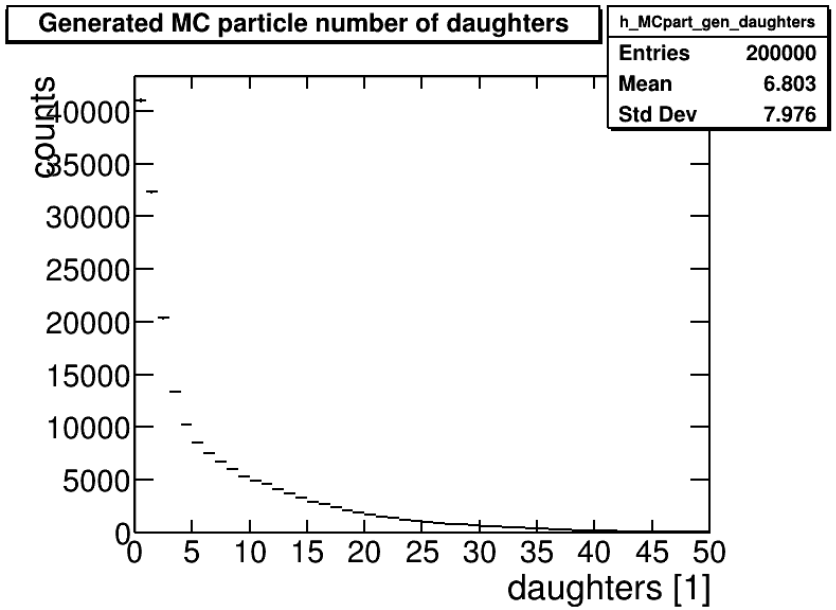

protons

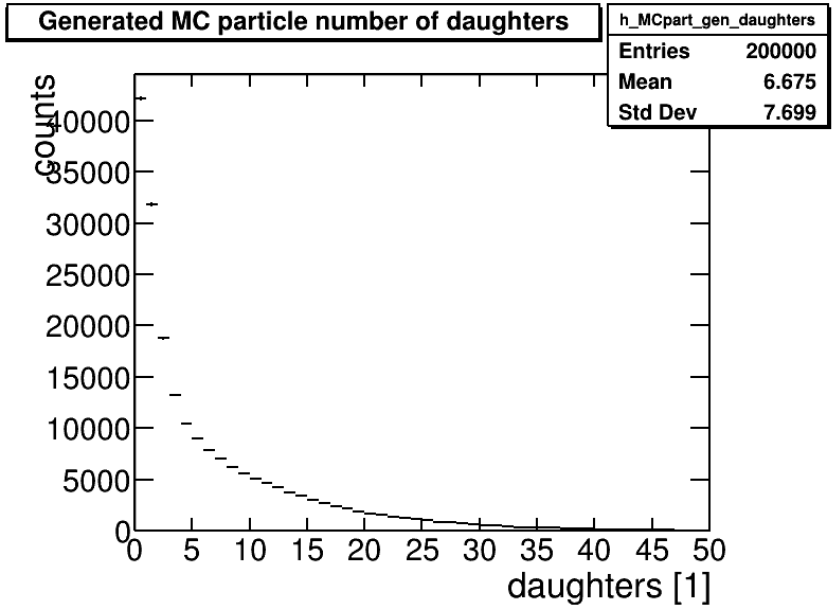

Generated MC particles: daughters

neutrons

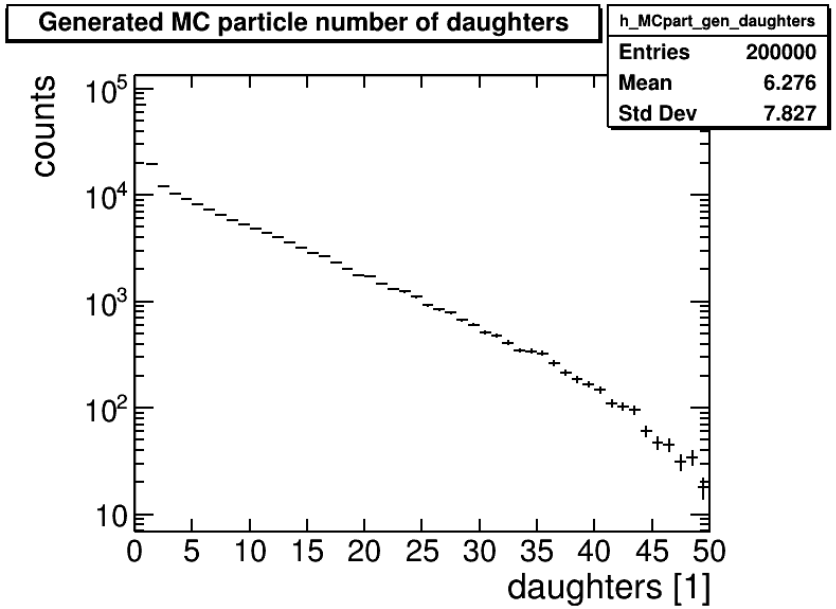

pions

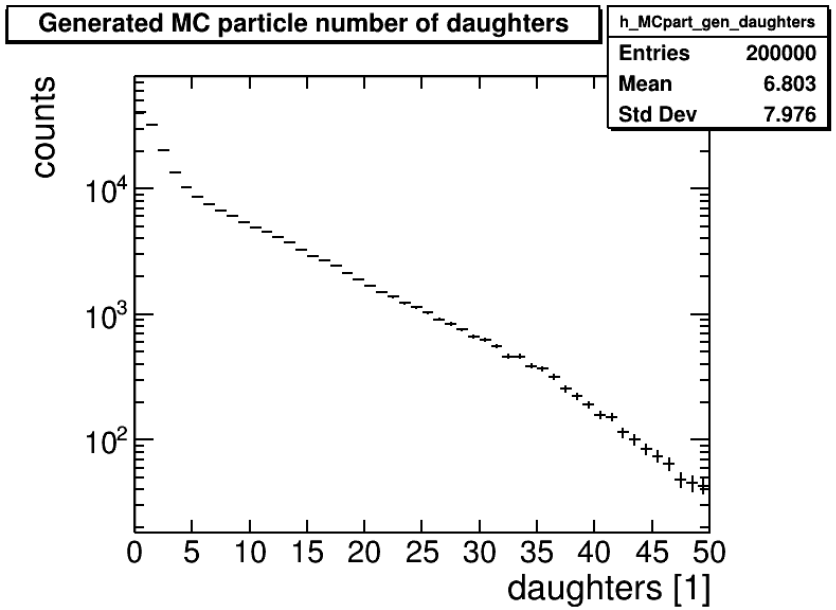

protons

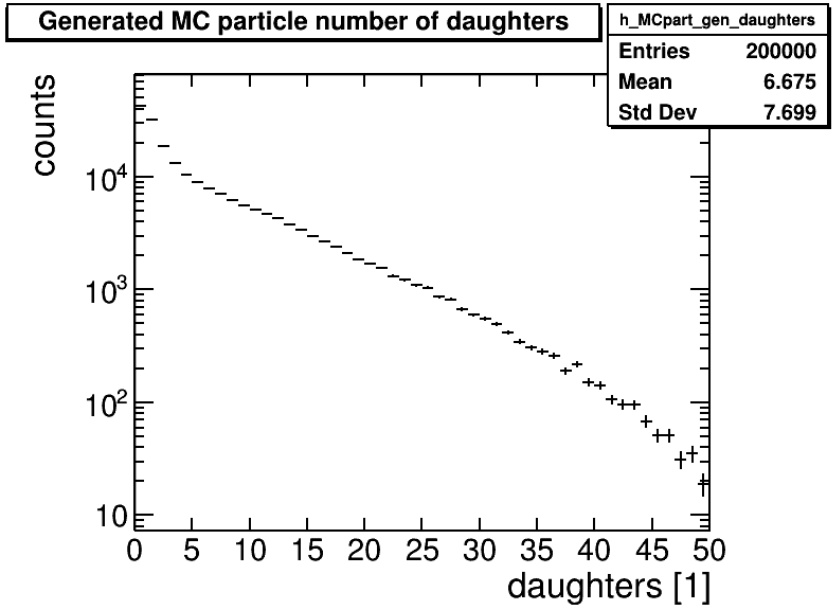

BHCal cluster reconstruction

- Disabled hit merger (no merging of hits between layers and tiles before running clustering algorithm)
  - I'm not sure if this is correct since multiple hits in the same tile may be treated independently
- Clustering done using island algorithm (default) `https://www.jlab.org/primex/weekly_meetings/primexII/slides_2012_01_20/island_algorithm.pdf`
- Hits most likely clustered across layers and tiles
  - This means a single shower will produce a single cluster (I assume)
- Problems:
  - No raw hits info stored in cluster
  - No info on hits in different layers, just the cluster global position
  - No association between MC particles
  - No track-hit association for neutrons (as expected)
- Perhaps some of the above can be enabled in reconstruction and stored

Reconstructed BHCal clusters: energy

neutrons

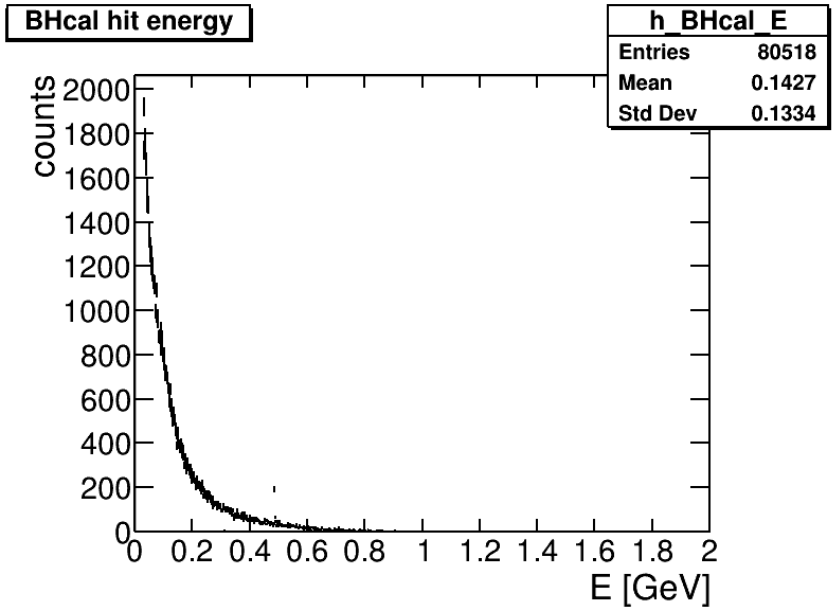

pions

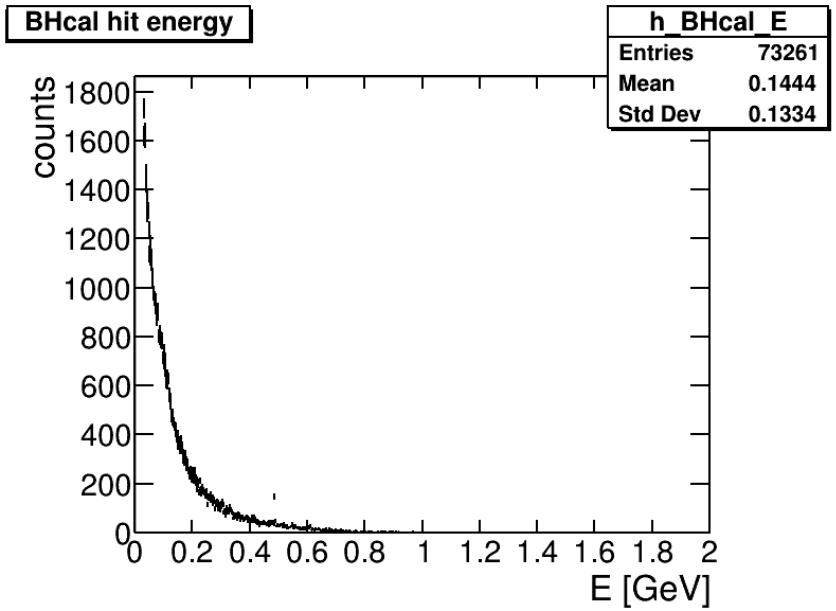

protons

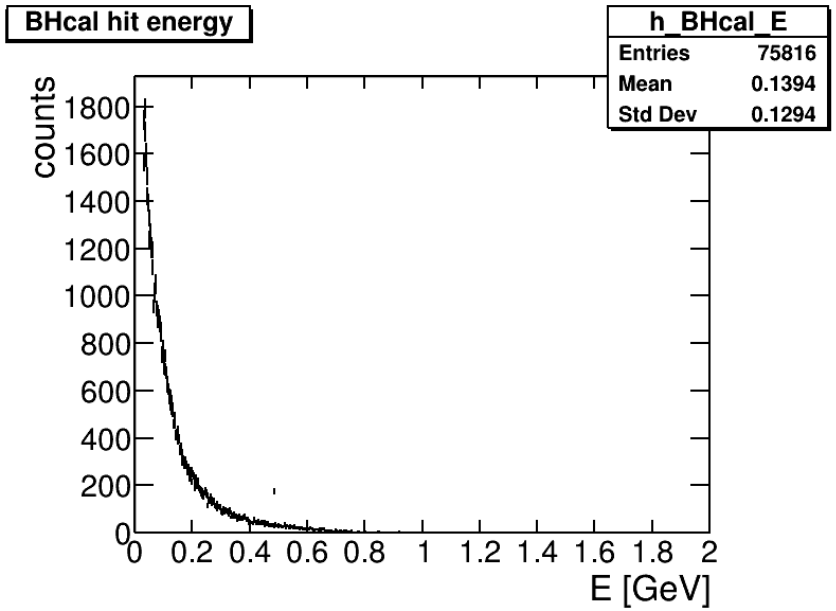

- $\sim$ 40% of neutrons have hits in BHcal

Reconstructed BHCal clusters: energy

neutrons

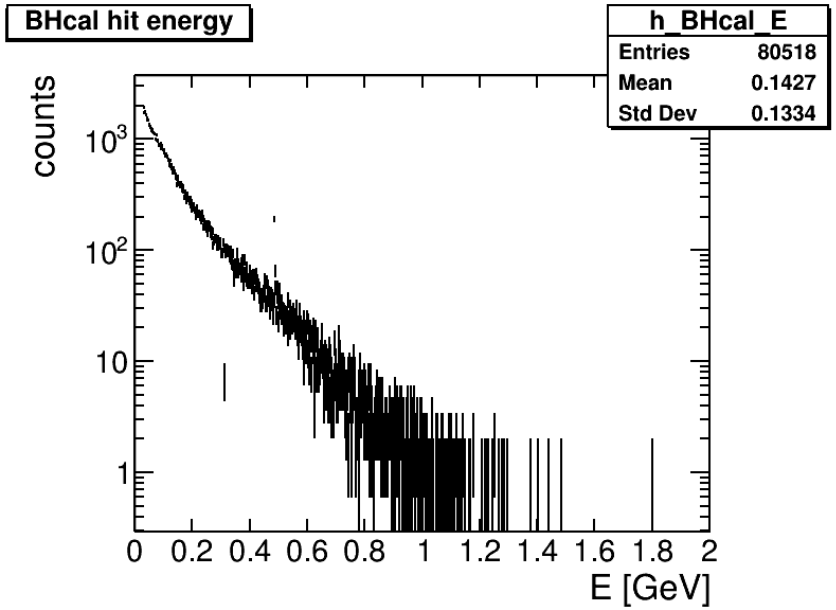

pions

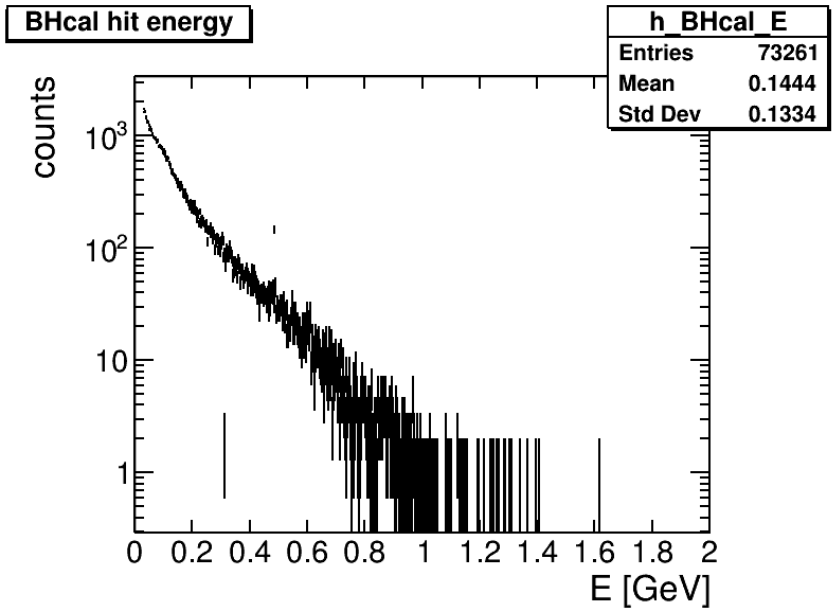

protons

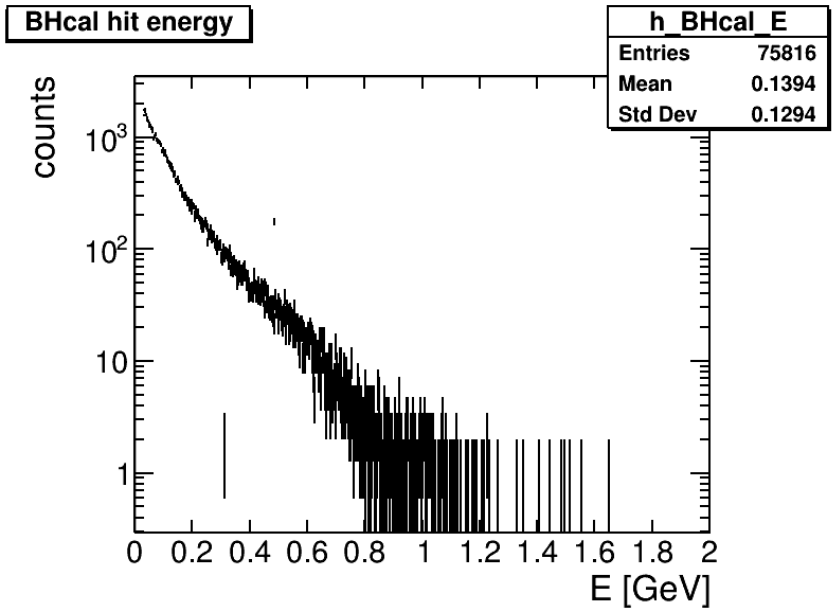

Reconstructed BHCal clusters: energy comparison

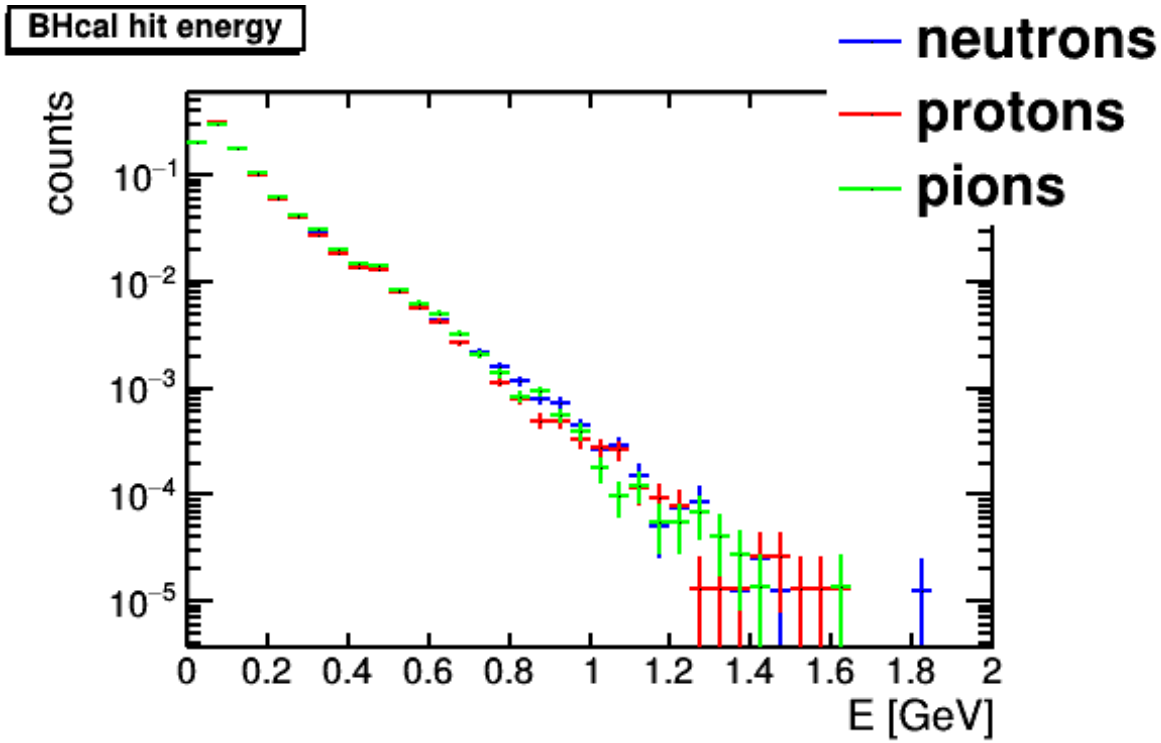

- No significant difference

Raw BHCal hits: energy distribution in layers μ vs. neutrons

muons

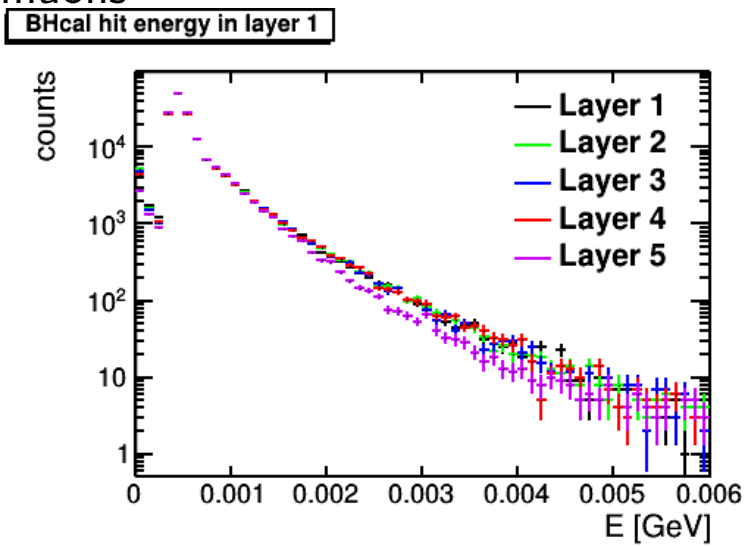

neutrons

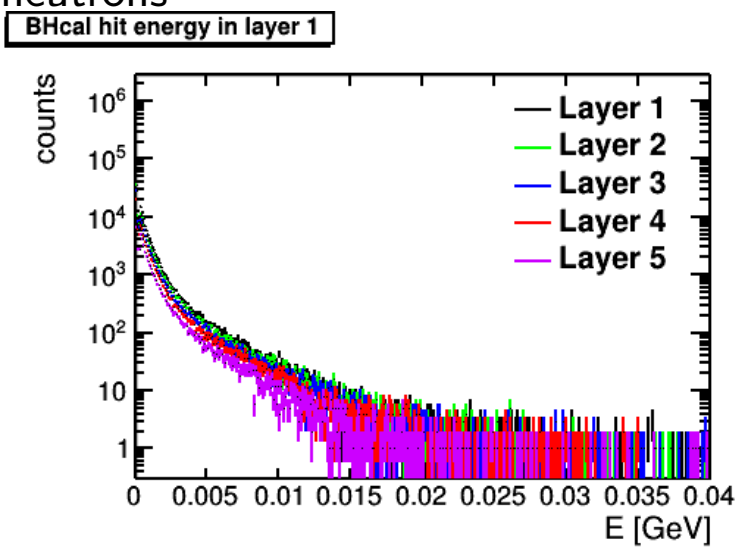

- Raw hits - no clustering
- Muons deposit less energy per layer than neutrons (as expected)
- Less energy in outer layers (as expected)

Reconstructed BHCal clusters: nHits

neutrons

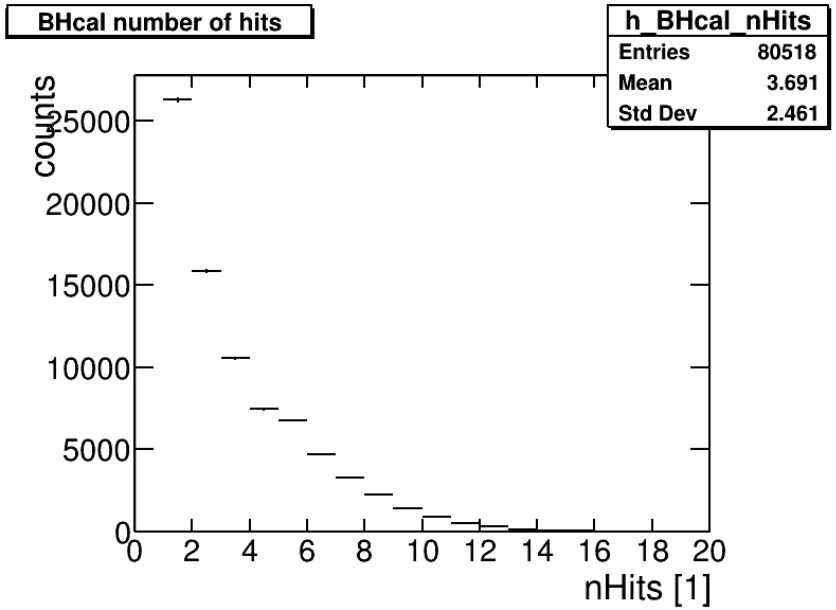

protons

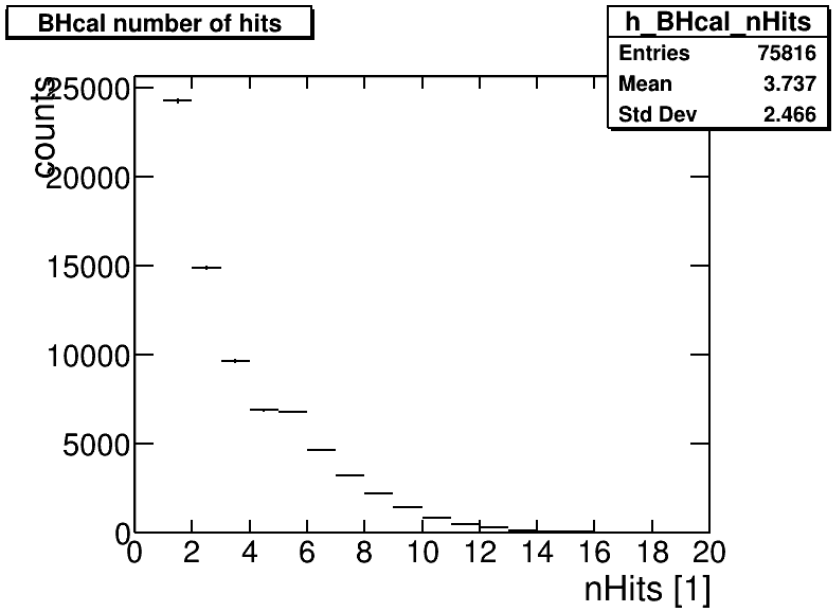

pions

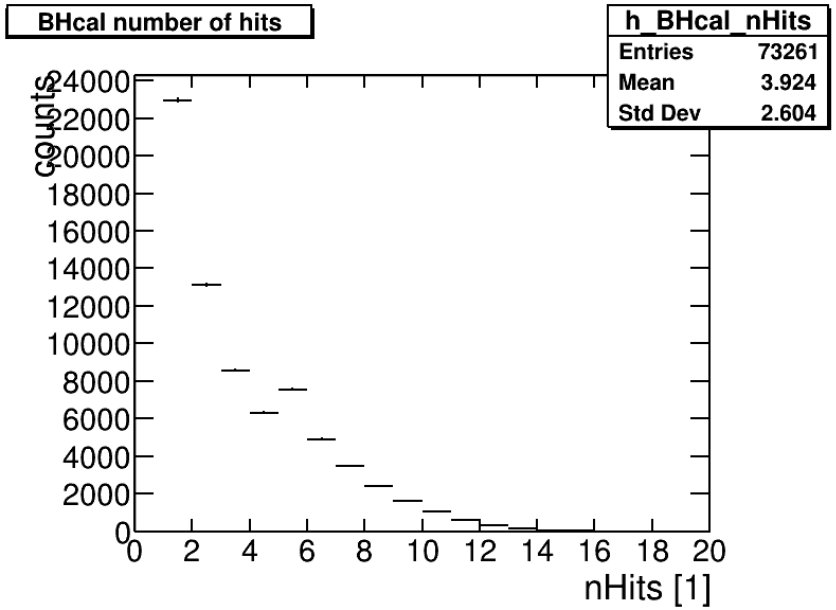

- Large fraction of clusters at low energy have just 1-2 hits

Reconstructed BHCal clusters: nHits vs. energy

neutrons

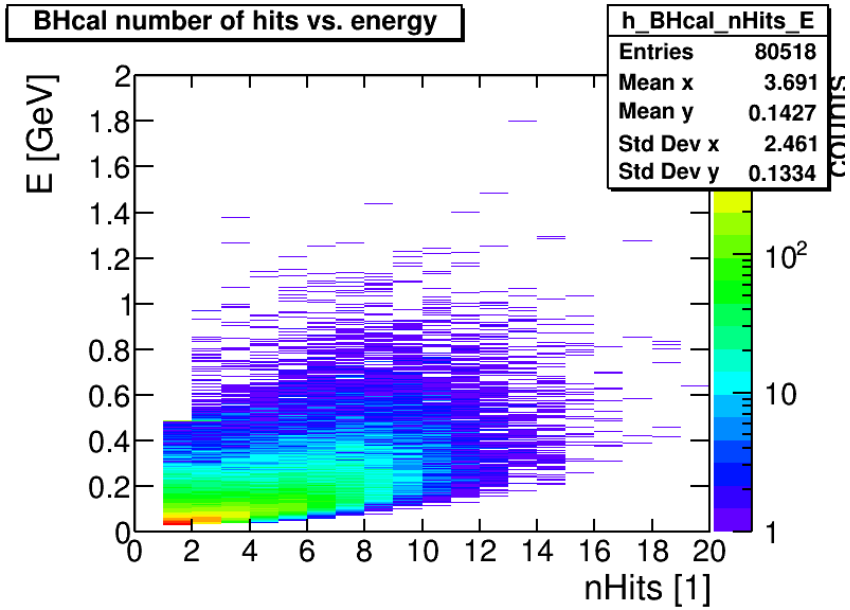

pions

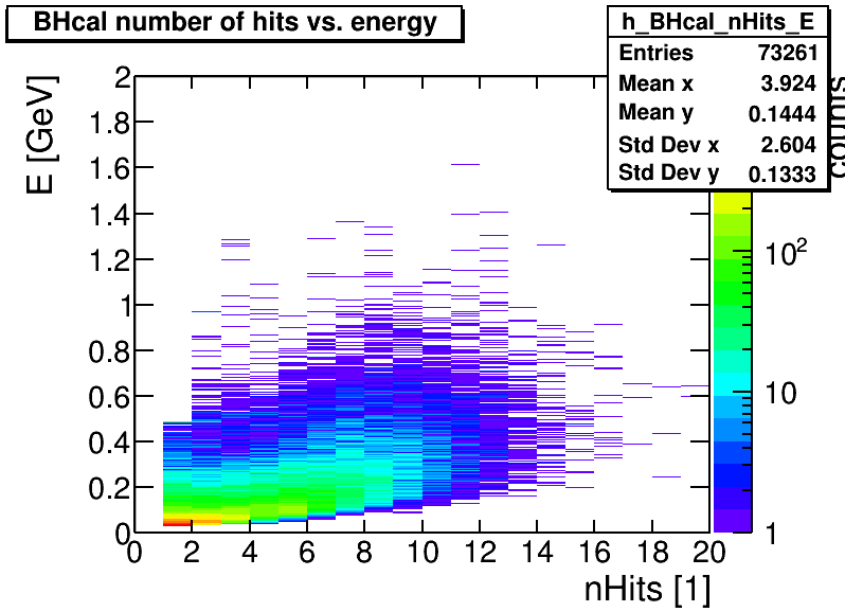

protons

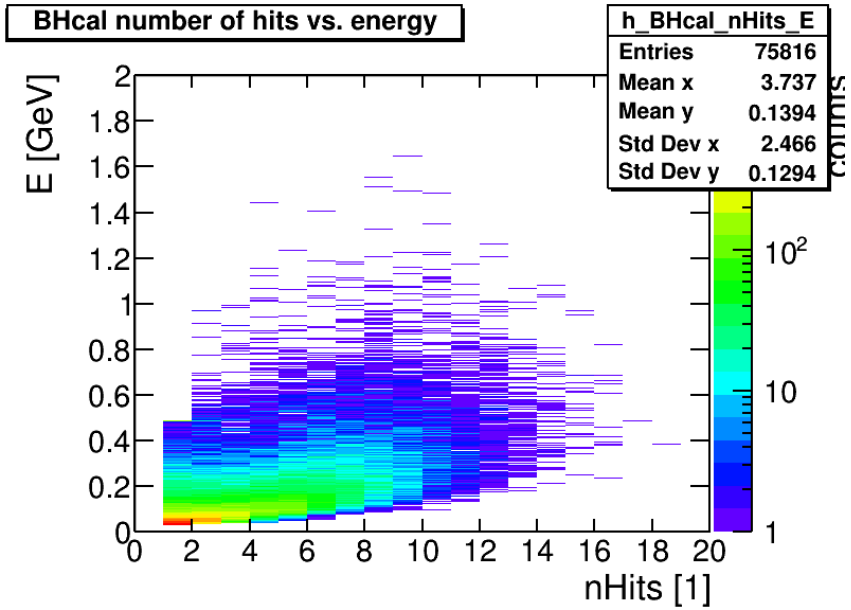

- Large fraction of clusters at low energy have just 1-2 hits

Reconstructed BHCal clusters: eta, phi

neutrons

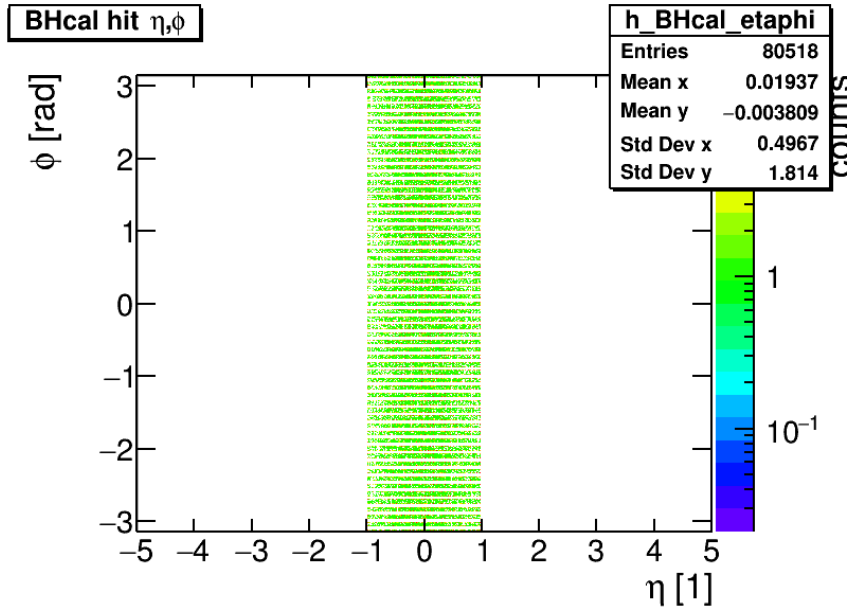

pions

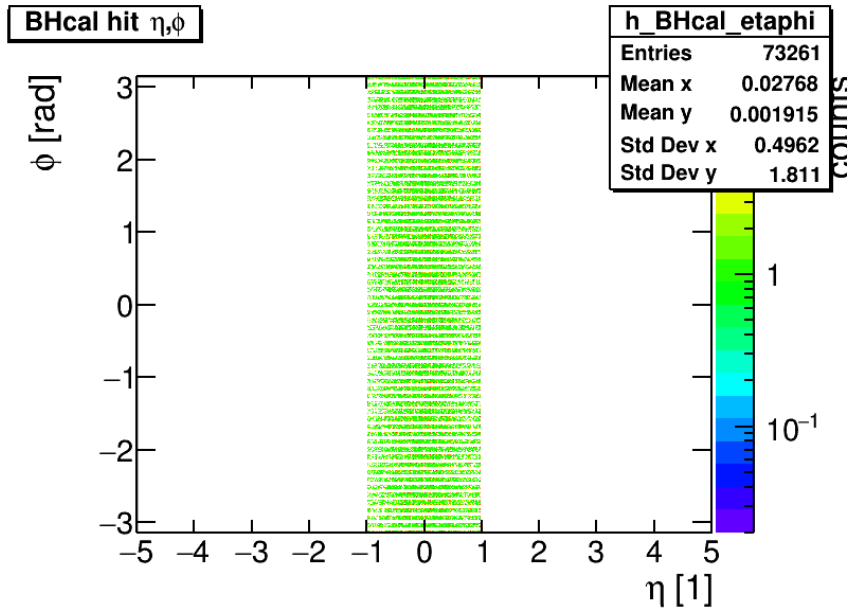

protons

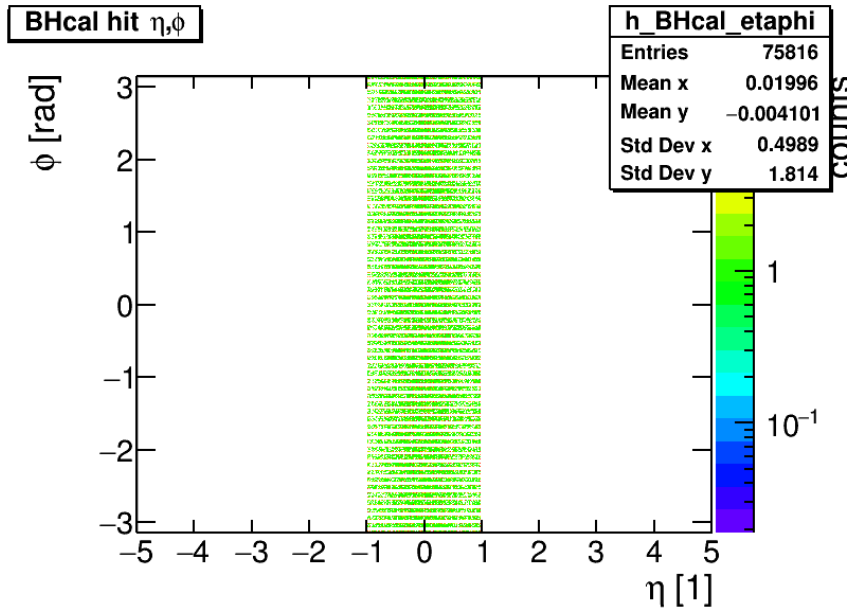

Reconstructed BHCal clusters: x, y

neutrons

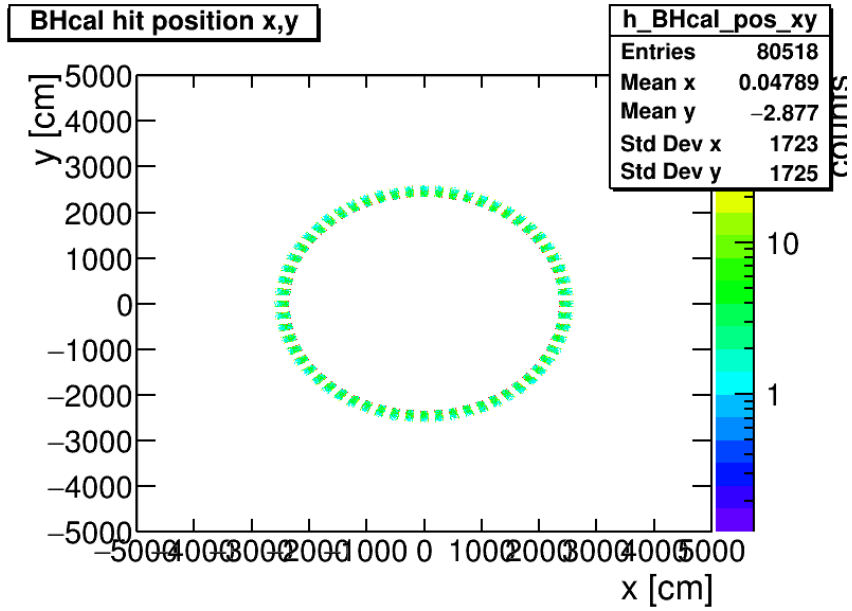

pions

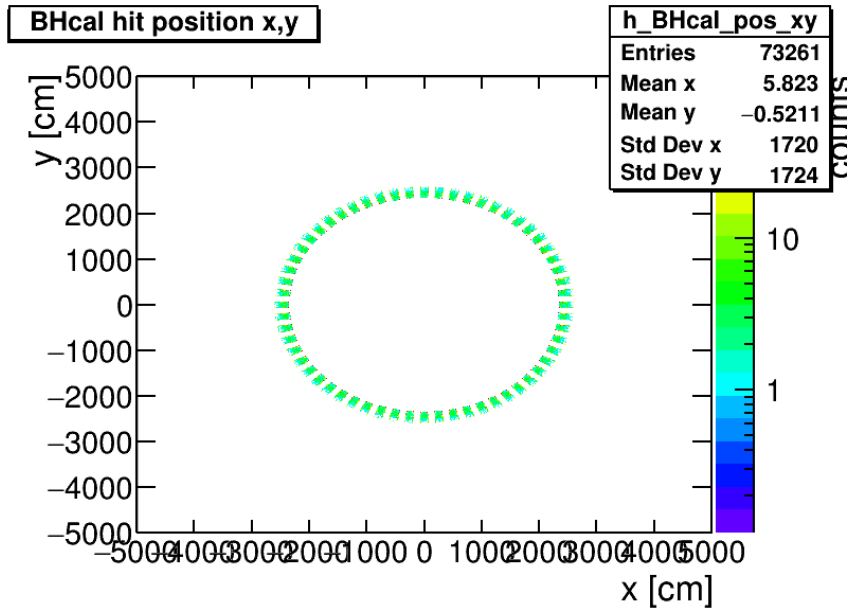

protons

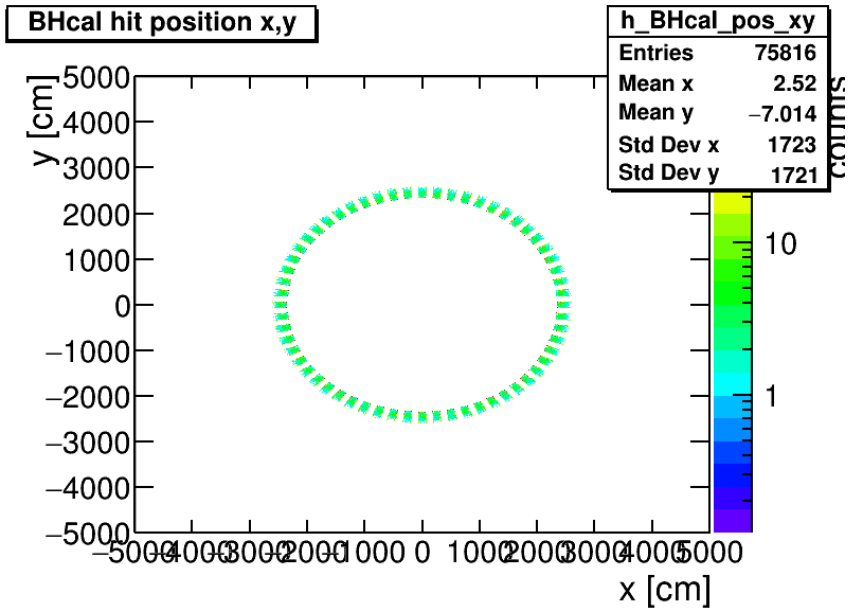

Reconstructed BHCal clusters: intrinsic theta, phi

neutrons

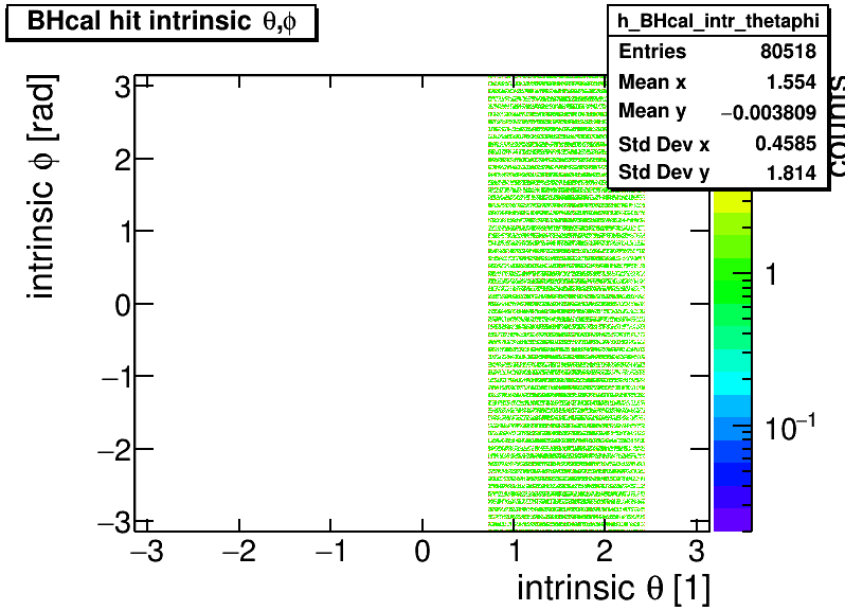

pions

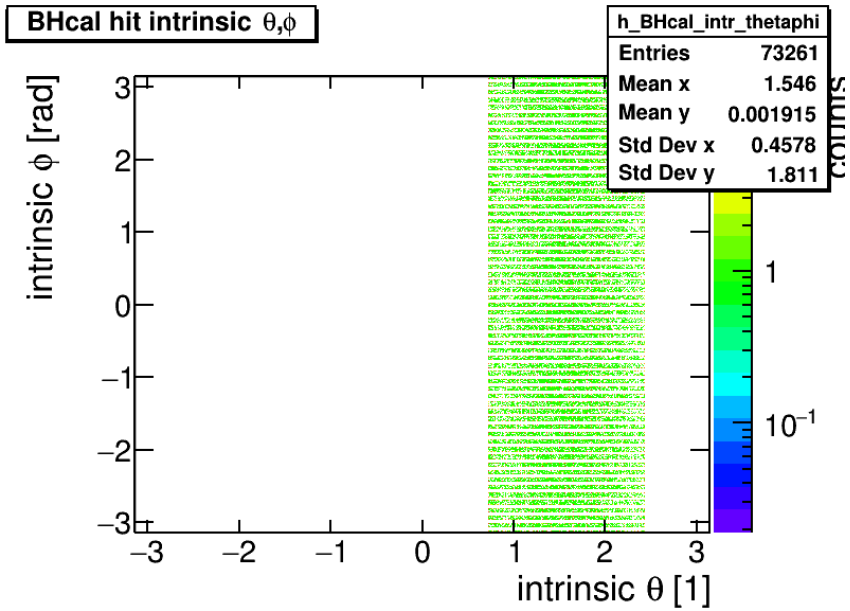

protons

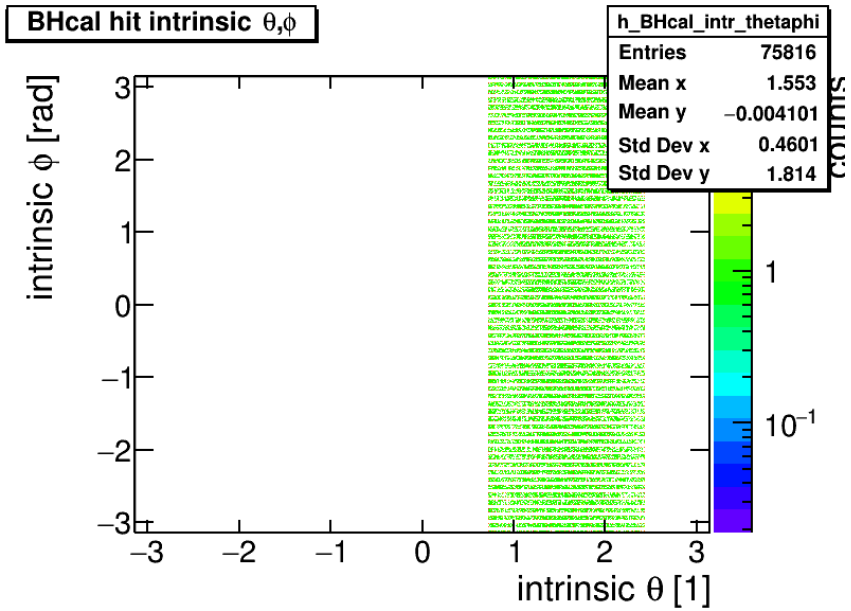

Summary

EIC

- Detectors in preparation - ECCE design favored for Detector-1
- Development underway
- Start of construction of EIC in 2024

BHcal for ATHENA

- Implemented BHCal geometry with scintillator tiles from STAR BEMC
- Tests performed for simulated and reconstructed data
- Further steps: determine method for neutral hadron shower identification
- Gained experience with software most likely to be used for Detector-1

Thank you for your attention!

BACKUP

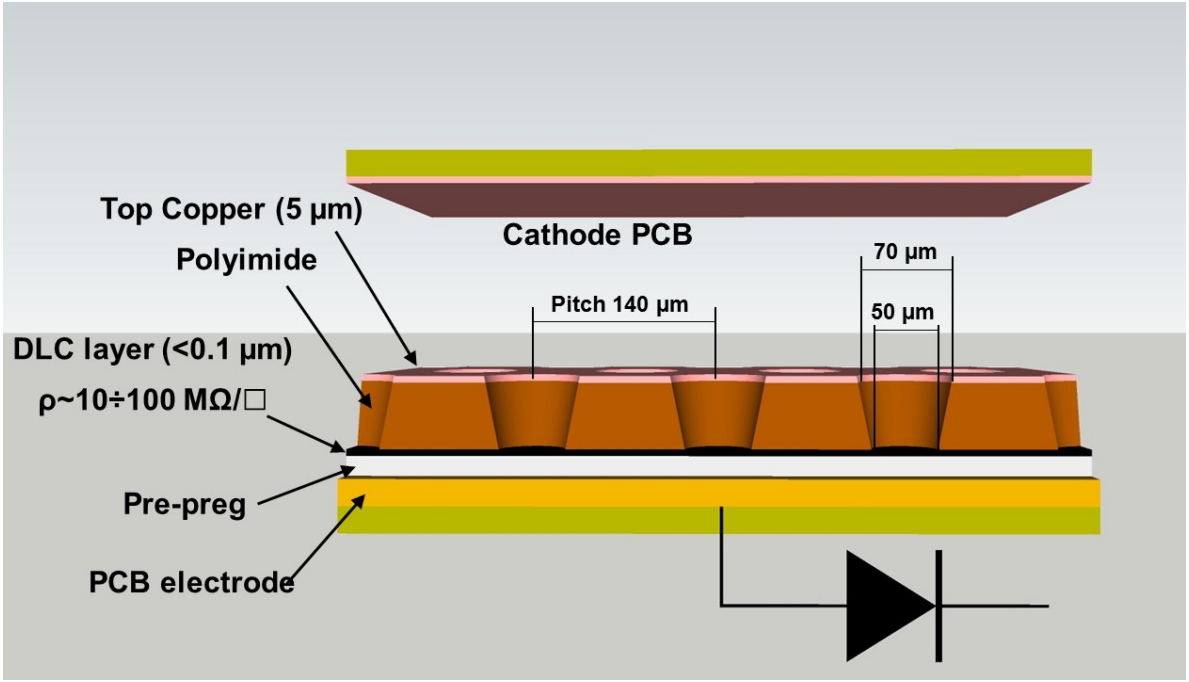

The micro-Resistive WELL (μ-RWELL) is a compact, simple and robust Micro-Pattern Gaseous Detector (MPGD) developed for large area HEP applications requiring the operation in harsh environment. The detector amplification stage, similar to a GEM foil, is realized with a polyimide structure micro-patterned with a blind-hole matrix, embedded through a thin Diamond-Like-Carbon (DLC) resistive layer with the readout PCB. The introduction of a resistive layer ($\rho = 50\%20 M\Omega m$) mitigating the transition from streamer to spark gives the possibility to achieve large gains ($> 10^4$), while affecting the detector performance in terms of rate capability.
G. Bencivenni et. al. 2020 JINST 15 C09034

AC-coupled Low-gain avalanche diodes

- Provides good spatial and timing resolution

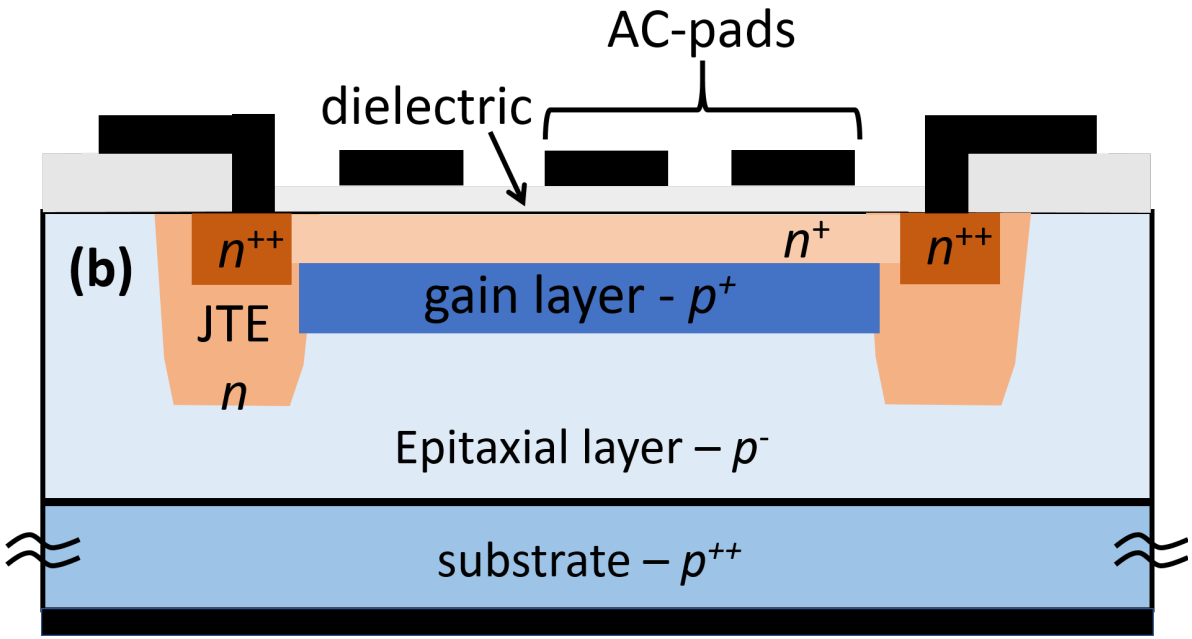

JINST 15 P09038 (2020)